

TRABAJO ESPECIAL DE GRADO

**DISEÑO, PRODUCCIÓN Y VALIDACIÓN DE UN CHASIS EN
MATERIALES COMPUESTOS PARA UN AUTO DE FORMULA
STUDENT.**

**DESIGN, MANUFACTURING AND TESTING A
SANDWICH MONOCOQUE FOR A FORMULA
STUDENT RACE CAR**

Presentado ante la Ilustre
Universidad Central de Venezuela
Por el Br. Brivio G, Jonathan D.
Para optar al Título
de Ingeniero Mecánico

Caracas, 2015

TRABAJO ESPECIAL DE GRADO

DISEÑO, PRODUCCIÓN Y VALIDACIÓN DE UN CHASIS EN MATERIALES COMPUESTOS PARA UN AUTO DE FORMULA STUDENT.

DESIGN, MANUFACTURING AND TESTING A SANDWICH MONOCOQUE FOR A FORMULA STUDENT RACE CAR

TUTOR ACADÉMICO: Prof. Ugo Icardi
Politécnico de Torino, Italia

Presentado ante la Ilustre
Universidad Central de Venezuela
Por el Br. Brivio G, Jonathan D.
Para optar al Título
de Ingeniero Mecánico

Caracas, 2015

Acknowledgements

This Master thesis project could not have been taken into conclusion without the help and support of several people.

First of all, I would like to thank my mom, Rossana Gaspero that without her sacrifice my experience here in Italy could not have been possible. Her faith and guidance was invaluable during the development of this thesis. She kept me focused and motivated during the entire course of my life, finally now is time to thank you for all these efforts, that's why this thesis is dedicated to you. Mom, thank you for giving the chance to fulfill my dreams!

I am also grateful to my younger brother Erick Brivio who always brings joy to our family and assists my mother as much as he can while I'm away. Also, I'm deeply grateful to the rest of my family for the support they provided me through my entire life.

I would like to thank my second family, The amazing people of the Squadracorse Polito team, after a year together, I just want to thank you for making this experience possible.

Thanks to all my Venezuelan friends, that made me feel like home from far.

Last but not least, I would like to thank the Owners of ERRE TI, without them this project could not have been possible. Also I would like to thank all the Polito staff that provided support during this project.

Agradecimientos

En primer lugar, quisiera agradecer a mi madre, Rossana Gaspero, que sin su sacrificio y dedicación mi experiencia aquí en Italia no podría haber sido posible. Su fe y su orientación fueron invaluable durante el desarrollo de esta tesis. Ella me mantuvo enfocado y motivado durante todo el curso de mi vida. Finalmente llegó el momento de darte las gracias por todos tus esfuerzos, es por eso que esta tesis la dedico a ti. ¡Mamá, gracias por dar la oportunidad de cumplir mis sueños!

Brivio, Jonathan¹.

DISEÑO, PRODUCCIÓN Y VALIDACIÓN DE UN CHASIS EN MATERIALES COMPUESTOS PARA UN AUTO DE FORMULA STUDENT.

Tutores Académicos: Prof. Ugo Icardi. Politecnico de Torino, Italia.

Facultad de Ingeniería. Escuela de Ingeniería Mecánica. Año 2015, 94p.

¹jonathanbrivio@gmail.com

Resumen

El proyecto que se presenta a continuación se describen cuáles han sido los pasos dados cubrir todas las fases necesarias para realizar de un chasis en materiales compuestos para un vehículo de Formula Student/SAE del grupo estudiantil “squadra corse” del Politécnico de Torino, partiendo desde el concepto hasta la producción, se presentando los resultados obtenidos experimentalmente.

La Formula Student/SAE es una competición universitaria a nivel mundial que consta de varias pruebas y consiste en el diseño y fabricación por parte de los estudiantes de un monoplaza que será evaluado tanto en el apartado de diseño como en el de comportamiento en circuito. En este proyecto se describen los distintos pasos que se han ido dando para la obtención de un cuerpo aerodinámico para un monoplaza de fórmula SAE, así como las conclusiones y el resultado final obtenido.

En primer lugar, se realizó un estudio del estado del arte, se determinaron los aspectos fundamentales a tener en cuenta en el diseño y se estudiaron las distintas tecnologías de producción de los chasis actuales. Al mismo tiempo se realizó un estudio profundo de las normas de la formula SAE 2013. La seguridad es uno de los principales requisitos ya que se trata de una competición estudiantil, y por lo tanto son muchas las restricciones a las que el chasis está sometido por parte de la organización para garantizar la seguridad de los participantes.

Para realizar el diseño del chasis se partió de un modelo base formado por las partes de la estructura de seguridad que se encontraban normalizadas y los diferentes componentes que el chasis debe sostener. Una vez cumplida la normativa se introdujeron los cambios en el diseño, probando nuevas ideas y analizando los resultados obtenidos.

La normativa impone que todos los materiales utilizados en la producción del chasis del vehículo sean probados experimentalmente para determinar sus características mecánicas, utilizando la teoría clásica de laminados para materiales compuestos se seleccionaron los materiales con la mayor proporción de rigidez / densidad que estuvieran comercialmente disponibles. Siguiendo los requisitos de la normativa, se realizaron las pruebas experimentales para determinar las características de rigidez, resistencia y deformación de un laminado con los materiales seleccionados.

Los primeros resultados de las pruebas permitieron utilizar datos experimentales en el modelo de cálculo a elemento finito de tipo estático lineal que se realizó con el paquete de software de ALTAIR, permitiendo un dimensionamiento de los materiales a utilizar para producir el chasis teniendo como objetivo minimizar el peso y satisfacer todos los requisitos de resistencia mecánica

a las fuerzas dinámicas y estáticas que el vehículo puede sostener durante su uso, así como los requisitos mínimos de rigidez para garantizar el correcto funcionamiento de la suspensión.

Una vez determinadas las características de los materiales a utilizar, espesores, zonas, etc. mediante el cálculo numérico para satisfacer los objetivos del proyecto, se procedió a probar experimentalmente los diferentes laminados resultantes del análisis para validar el modelo y tener los datos necesarios para demostrarle a la organización de la competencia la seguridad del chasis.

Para concluir la fase de diseño, se finalizó el modelo CAD del chasis y se realizaron todos los diseños técnicos necesarios para la producción de los moldes necesarios para realizar el chasis.

Por otra parte, se procedió con el uso del software Laminate Tools para determinar la forma “plana” de las pieles de fibra de carbono y permitir preparar la materia prima necesaria para la producción. Sucesivamente, se realizó el proceso de laminación de todas las capas y el proceso de curado en autoclave.

Para finalizar el proceso de producción, una vez retirado el chasis del molde, se procedió a realizar el mecanizado de los agujeros y diversos puntos de interés bajo una fresa a control numérico.

Una vez que el modelo estuvo totalmente ensamblado, se realizó una prueba de rigidez torsional para validar de manera definitiva la rigidez total de la estructura y establecer si se lograron satisfacer los objetivos de rigidez del proyecto.

METODOLOGÍA

1. Planteamiento del problema

El objetivo de la competencia de Formula Student/SAE es el de construir un vehículo de carreras ligero, competitivo y seguro siguiendo buenas prácticas de ingeniería y manteniendo los costos en un rango aceptable. Generalmente estos equipos estudiantiles buscan mejorar el vehículo anualmente, tomando como punto de partida el vehículo de la temporada precedente y aplicando pequeñas modificaciones buscando mejorar las prestaciones del prototipo y los resultados en las competencias.

De la experiencia acumulada desde el 2005 de la “squadracorse” las especificaciones técnicas del prototipo del 2013 denominado “SCR” son las siguientes:

- Chasis realizado en materiales compuestos de tipo “sándwich”
- Batería de 400 V
- Sistema de frenado regenerativo
- alta eficiencia de transmisión a engranajes helicoidales
- Dos motores eléctricos Magneti Marelli TMG LOW 60KW
- Implementación de un paquete aerodinámico
- Potencia máxima limitada a 85 kW

En específico, este proyecto se concentra en el chasis, todas las especificaciones técnicas fueron determinadas mediante un proceso de benchmarking con el precedente vehículo de la “Squadracorse”, denominado SC12e que tenía las características presentes en la **tabla 1**.

Tabla 1. Especificaciones técnicas del chasis del SC12e

| Características | Valor |
|-------------------------------------------|-------|
| Masa [kg] | 44.51 |
| Rigidez Torsional [N*m/rad] | 72404 |
| Proporción rigidez / masa [[N*m/(rad*kg)] | 1509 |
| Tiempo de producción | 1 mes |

2. Objetivos del proyecto

Con el fin de desarrollar el chasis en materiales compuestos se definieron los siguientes objetivos del proyecto:

- Garantizar la seguridad del conductor en caso de accidente
- Rigidez suficiente para garantizar el correcto funcionamiento de la suspensión
- Bajo peso
- Diseño que permita un fácil acceso a los componentes internos del auto
- Facilidad de producción

3. Especificaciones técnicas del chasis

- Satisfacer todas las normativas “Formula SAE 2013 rules”
- La rigidez torsional superior o igual a 72404 [N*m/rad]
- Variación de los ángulos característicos de la suspensión menor a 0,1 grados en condiciones de operación
- Peso menor de 25 kg
- Tiempo manufactura inferior a 1 mes

4. Proceso de diseño, construcción y desarrollo

Para desarrollar el proyecto se siguieron las fases ilustradas en la **Figura 1**

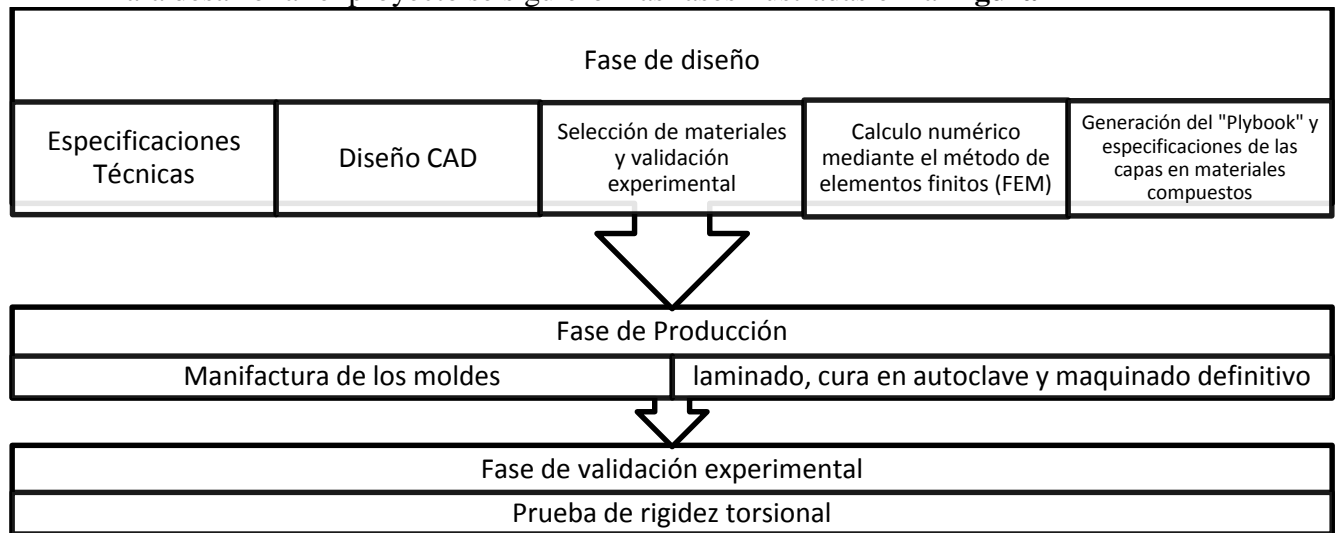


Figura 1. Diagrama de flujo del proceso de diseño, construcción y desarrollo

5. Especificaciones de los programas utilizados
 - a. Programa de diseño asistido por computadora CAD
 - i. **Catia V5 r19**
 - b. Programa de análisis estructural:
 - i. Pre-procesador: **Altair Hypermesh**
 - ii. Solver: **Altair Optistruct v12**
 - iii. Post-procesador: **Altair Hyperview**
 - c. Programa generador de las capas de materiales compuestos
 - i. **Anaglyph Laminate tolos**
6. Casos de estudio analizados mediante el método de elementos finitos (FEM).

El análisis utilizando el método de elementos finitos consideraron tres casos de estudio, derivados de las simulaciones realizadas por el equipo de Dinámica vehicular de la Squadrace, estos resultados determinaron el input de aceleraciones a las cuales el chasis viene sometido durante la operación del vehículo.

Para evaluar la resistencia estructural del chasis realizado en materiales compuestos se utilizó el criterio de fallas de Tsai-wu, el cual es utilizado para predecir el fallo en materiales compuestos anisótropos.

Casos de estudio - eventos dinámicos

- Frenada a 2g de deceleración
- Máxima aceleración lateral a 1.5g
- Combinado: Frenada a 2g con 1.5g de aceleración lateral

Caso de estudio - rigidez

- Prueba de rigidez torsional

7. Selección de Materiales

Se utilizó una matriz de evaluación para ponderar las características de rigidez a flexión, a torsión y resistencia, normalizadas con la densidad de los materiales comercialmente disponibles en el mercado.

8. Caracterización experimental de los materiales

Una vez seleccionados los materiales, se realizaron las muestras y se realizaron las diferentes pruebas experimentales definidas en el reglamento de la Formula SAE 2013.

Las pruebas experimentales aplicadas a las muestras de materiales compuestos son las siguientes:

- Pruebas de flexión a 3 puntos: dicha prueba se utilizó para determinar el módulo elástico y el esfuerzo máximo a tracción de la capa externa del sándwich.
- Prueba de intrusión con un penetrador cilíndrico de 25mm de diámetro, de la cual

se determinó el esfuerzo cortante máximo de las capas del sándwich.

9. Validación experimental del modelo de calculo

Para validar el resultado final del proyecto, se realizó una prueba de rigidez torsional del prototipo completo. La prueba consiste en ejercer un par torsor en una de las extremidades de la suspensión mientras que se fijan los desplazamientos de la otra, midiendo el ángulo de deformación respecto al plano horizontal.

RESULTADOS Y DISCUSIÓN

Una vez concluida la fase de diseño el modelo CAD definitivo cumple con las normas establecidas por la Formula SAE, además de satisfacer todas las necesidades de accesibilidad requeridas por los componentes internos del vehículo.

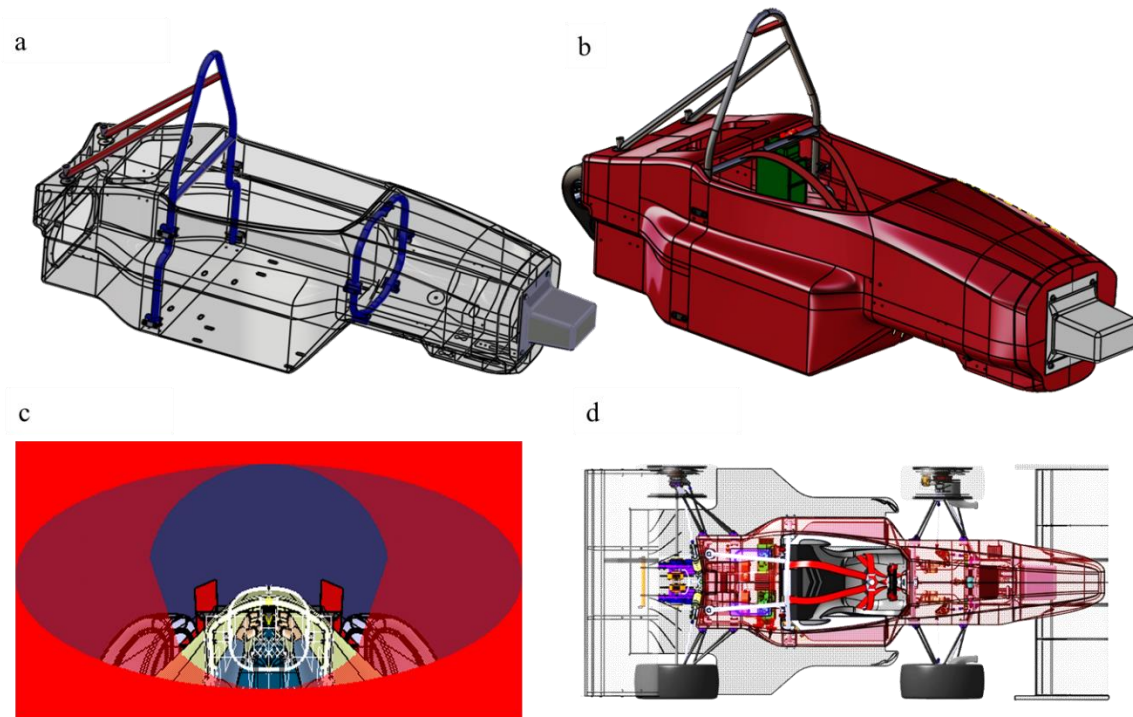


Figura 2. (a,b) Modelo CAD definitivo del chasis del prototipo SCR, (c) Ergonomía desde el punto de vista del piloto, (d) Vista superior en transparencia con todos los componentes internos.

Los materiales seleccionados utilizando la matriz de evaluación para realizar las muestras a probar experimentalmente fueron los siguientes:

- **Hexply M49 200T2x2 CHS- 3k**, para ser utilizado como las capas más externas de la estructura tipo sándwich, consiste en un tejido de fibra de carbono tipo CHS- 3K de alta resistencia, pre-empañado con una matriz de resina epoxi M49, comercialmente disponible con un 42% de contenido de resina en peso y fabricada por Hexcel.

- **Hexweb 5052 3/16 0.0178.** fue seleccionado como material del núcleo de la estructura, este material tiene forma de nido de abeja, cuenta con un tamaño de celda de con 3/16 pulgadas, y espesores de pared de 0.0178 mm, como resultado de los cálculos analíticos debe utilizarse con un espesor mínimo de 22 mm.
- **Película adhesiva Redux 312.** Una película de adhesivo epoxi fue sugerido por nuestro proveedor, siendo el más rendimiento disponible para enlace carbono con el núcleo de nido de abeja.

Los resultados de la caracterización experimental de las muestras realizadas con los materiales descritos anteriormente se presentan en la **tabla 2 y 3**, cabe destacar que el valor de resistencia de la capa en fibra de carbono es notablemente inferior al calculado teóricamente, esta diferencia es debida al modo de fallo dominante del laminado fue el del colapso del núcleo por inestabilidad.

Detalles de la muestra del laminado:

- 4x capas de T200T2 Hexcel M49 42%, espesor de cada capa=0,25mm, orientadas a [0/90/0/90 grados]
- Núcleo de aluminio en forma de nido de abeja, 5052 Hexcel, espesor = 22mm

Tabla 2. Resultados de la prueba de flexión a 3 puntos

| Propiedades de las capas externas (FCRP) | Valor mínimo requerido por la FSAE | Valor experimental | Valor calculado |
|------------------------------------------|------------------------------------|--------------------|-----------------|
| Máxima fuerza | 7100 N | 13179 N | 12000 N |
| Módulo de Young [Ex] | 32.4 GPa | 67.7 GPa | 63GPa |
| Resistencia a la tracción [Sy] | 201 MPa | 296 MPa | 905 MPa |

Tabla 3. Resultados de la prueba de penetración

| Propiedades de las capas externas (FCRP) | Valor mínimo requerido por la FSAE | Valor experimental |
|------------------------------------------|------------------------------------|--------------------|
| Máxima fuerza | 9108 N | 12830 N |
| Máximo esfuerzo cortante [S12] | 116 MPa | 163.4 MPa |

Sucesivamente, ya que se caracterizaron correctamente los materiales, se extrapolaron los resultados del laminado a todas las zonas de seguridad definidas por la normativa.

Los resultados de los cálculos estructurales definitivos lograron satisfacer los requisitos de seguridad establecidos por la normativa, asimismo, cumplen también con los requisitos de resistencia y rigidez establecidos al inicio del proyecto. Las **tablas 4 y 5** presentan un resumen de los resultados.

Tabla 4. Resultados de los cálculos FEM – pruebas de rigidez

| Variable medida | Suspensión anterior | | | Suspensión posterior | | |
|------------------------------|---------------------|---------------------|-----------|----------------------|---------------------|-----------|
| | Frenada | Aceleración lateral | combinado | Frenada | Aceleración lateral | combinado |
| Variación de caster [grados] | 0.076 | 0.048 | 0.074 | - | 0.052 | 0.073 |
| Variación de camber [grados] | 0.084 | 0.085 | 0.092 | - | 0.064 | 0.080 |
| Variación de toe [grados] | 0.052 | 0.073 | 0.071 | - | 0.071 | 0.058 |
| Rigidez torsional | 116320 [N*m/rad] | | | | | |

Tabla 5. Resultados de los cálculos FEM – Factor de seguridad derivado del criterio de Tsai-wu

| | Frenada | Máxima aceleración lateral | Combinado |
|----------------------------|---------|----------------------------|-----------|
| Criterio de Tsai-wu (TW) | 0.308 | 0.649 | 0.513 |
| Factor de seguridad = 1/TW | 3.247 | 1.541 | 1.949 |

El “plybook” o distribución de todas las capas de los diferentes materiales necesarios para la construcción del chasis, separado por zonas, se pueden observar en la **figura 3**.

| | Material | Zone 1 - Sideimpact | Zone 2 - FBS | Zone 3 - TSS | Zone 4 - Rear Structural | Zone 5 Rear Design | Zone 6 SI design | Zone 7 Front Design | Zone 8 - Floor pedalbox | Zone 9 Floor FBS | Zone 10 Floor SI | Zone 11 Floor Rear | CFRP Inserts |
|-------------|------------------|---------------------|-----------------|-----------------|--------------------------|--------------------|------------------|---------------------|-------------------------|------------------|------------------|--------------------|------------------|
| Outer Layer | CFRP M49 T200T 2 | Ply 10 - 45 deg | Ply 10 - 45 deg | Ply 10 - 45 deg | Ply 10 - 45 deg | | | | | | | | |
| | CFRP M49 T200T 2 | | Ply 9 - 0 deg | Ply 9 - 0 deg | Ply 9 - 0 deg | | | | | | | | |
| | CFRP M49 T200T 2 | | Ply 8 - 45deg | Ply 8 - 45deg | Ply 8 - 45deg | | | | | | | | |
| | CFRP M49 T200T 2 | Ply 7 - 0deg | | | | | | | | | | | |
| | CFRP M49 T200T 2 | Ply 6 - 0deg | | | | | | | | | | | |
| | CFRP M49 T200T 2 | Ply 5 - 0deg | Ply 5 - 0deg | Ply 5 - 0deg | Ply 5 - 0deg | | | | | | | | |
| | CFRP M49 T200T 2 | | Ply 4 - 45deg | Ply 4 - 45deg | Ply 4 - 45deg | Ply 4 - 45deg | Ply 4 - 45deg | Ply 4 - 45deg | Ply 4 - 45deg | Ply 4 - 45deg | Ply 4 - 45deg | Ply 4 - 45deg | Ply 4 - 45deg |
| | CFRP M49 T200T 2 | | Ply 3 - 0deg | Ply 3 - 0deg | Ply 3 - 0deg | Ply 3 - 0deg | Ply 3 - 0deg | Ply 3 - 0deg | Ply 3 - 0deg | Ply 3 - 0deg | Ply 3 - 0deg | Ply 3 - 0deg | Ply 3 - 0deg |
| CORE | 5052 Hexcel | Ply1 - 22mm | Ply1 - 22mm | Ply1 - 22mm | Ply1 - 22mm | Ply2 - 10mm | Ply2 - 10mm | Ply2 - 10mm | Ply2 - 10mm | Ply2 - 10mm | Ply2 - 10mm | Ply2 - 10mm | Ply 1000 Hextool |
| Inner Layer | Symmetrical | Symmetrical | Symmetrical | Symmetrical | Symmetrical | Symmetrical | Symmetrical | Symmetrical | Symmetrical | Symmetrical | Symmetrical | Symmetrical | Symmetrical |

Figura 3. "plybook" - Matriz de distribución de capas de materiales separada por zona.

Una vez definido el plybook se procedió con el corte de todas las capas de fibra de carbono y el núcleo en honeycomb de aluminio, se fabricaron los moldes y se procedió con la laminación y la cura en autoclave del componente, una vez terminado el resultado final se puede observar en la **figura 4**. Seguidamente, la figura 5 presenta el vehículo ensamblado totalmente.



Figura 4. Chasis fabricado con materiales compuestos para el prototipo SCR.



Figura 5. Prototipo SCR completo presentado en el Museo del auto de Torino.

Aunque el resultado final fue satisfactorio, el know-how de ERRETI compositi, la empresa que patrocinó la producción del chasis, aun teniendo años de experiencia en la producción de piezas de CFRP, no fue suficiente para predecir varios problemas que retrasaron la producción del chasis de 1 mes a 3 meses.

Los siguientes factores fueron los que más impactaron el tiempo de producción:

- Los retrasos para utilizar la autoclave debido a la propia producción de los componentes de la compañía.
- Durante el proceso de laminación, las capas externas tenían problemas de adhesión al molde, se perdieron un par de semanas para procurar un adhesivo especial a base epoxi para utilizar solo con las primeras capas.

- El chasis se decidió de hacerlo en una sola pieza para obtener las mayores ventajas estructurales, permitiendo que sólo una persona pueda trabajar durante la laminación, por lo tanto, no se pudo reducir el tiempo de esta fase, cosa que se puede evitar en futuro dividiendo el molde a la mitad y pegando los dos componentes al final del proceso.

Seguidamente, los resultados de la prueba de rigidez torsional efectuada al prototipo se presentan en la **tabla 6**. Comparados con los resultados del prototipo del año 2012, como se puede observar, los valores no solo satisfacen los requisitos iniciales, sino que superan ampliamente la proporción de rigidez respecto al peso.

Tabla 6. Resultados de la prueba de rigidez torsional de la SCR, comparación con la SC12e

| | SC12e | SCR | Delta |
|--------------------------------------|-------|-------|-------|
| Rigidez Torsional [Nm/rad] | 72404 | 84008 | 16% |
| Peso del chasis [kg] | 37 | 25 | -32% |
| Rigidez Torsional / Peso [Nm/rad/kg] | 1956 | 3360 | 72% |

Comparando los resultados de la prueba de rigidez torsional y con el resultado de la simulación a elementos finitos, presentados en la tabla 7, se observa que el modelo FEM sobreestima la rigidez en un 28% respecto al resultado obtenido experimentalmente

Tabla 7. Comparación entre los resultados experimentales y el cálculo FEM de la rigidez torsional del chasis de la SCR

| | Elementos Finitos | Experimental | Delta |
|----------------------------|-------------------|--------------|-------|
| Rigidez Torsional [Nm/rad] | 116320 | 84008 | -28% |

Las causas de esta diferencia entre el resultado experimental y el calculado numéricamente pueden ser:

- Los defectos durante la laminación respecto a la condición ideal suceden siempre, sobre todo porque es un proceso manual poco reproducible.
- La rigidez propia de los componentes de la suspensión puede ser menor a la estimada, se necesita realizar una prueba de rigidez teniendo en cuenta solo estos componentes.
- El modelo FEM, utiliza elementos de tipo Shell, con una formulación de placas de Timoshenko, utilizadas en la industria para simular los materiales compuestos, pero dicha formulación fue ideada para calcular placas cuyo espesor sea mucho menor al de las otras dos direcciones. En este caso, se requeriría modelar en 3D el núcleo del sándwich, y modelar con elementos Shell solo las paredes externas del sándwich. Para componentes con esta complejidad, es un trabajo largo, sino, imposible. La consecuencia es que se sobreestima la rigidez, pero actualmente la industria resuelve esta problemática agregando un factor de amplificación entre 1.4-1.5 a los requisitos de rigidez.

Para finalizar, durante las pruebas en la pista, el chasis no mostró ningún tipo de problemas estructurales, el nivel de confort y estabilidad durante el manejo fueron descritas como óptimas, de consecuencia se puede esperar que todos los sistemas funcionan dentro el rango de valores esperados.

CONCLUSIONES

Se logró construir un chasis realizado con materiales compuestos para el equipo de Formula Student del Politécnico de Torino. Cuyas especificaciones técnicas finales satisfacen casi todos los requisitos establecidos al inicio del proyecto:

- Cumple con la normativa de la Formula SAE 2013
- La rigidez torsional es 16% superior a la requerida
- La variación de los ángulos característicos de la suspensión durante la operación no genera problemas perceptibles.
- Peso igual a 25 kg.

Debido a la falta de experiencia del equipo en la producción de componentes con esta tecnología, el objetivo de tiempo de producción inferior a 1 mes, no se pudo alcanzar, y como consecuencia el proyecto sufrió fuertes retrasos en el programa. En el futuro se recomienda preparar los moldes para ser laminados en dos partes separadas y programar con la empresa de producción el flujo de trabajo para que los recursos materiales y humanos estén disponibles cuando se necesite.

POLITECNICO DI TORINO
I FACOLTÀ DI INGEGNERIA
Corso di LAUREA MAGISTRALE in INGEGNERIA DELL'AUTOVEICOLO
(AUTOMOTIVE ENGINEERING).

MASTER THESIS



*DESIGN, MANUFACTURING AND TESTING A SANDWICH MONOCOQUE
FOR A FORMULA STUDENT RACE CAR*

Author: Jonathan Brivio

Tutor: Icardi, Ugo.

July, 2014

IMPOSTA DI BOLLO ASSORTA IN MODO VIRTUALE
AUTORIZZAZIONE DELL'AGENZIA DELLE ENTRATE UFFICIO
TERRITORIALI DI TORINO I N. 5 - DAL 01/01/2013, PROT. N. 167008/2012

POLITECNICO DI TORINO

REPUBBLICA ITALIANA
IN NOME DELLA LEGGE

IL RETTORE
PROF. MARCO GILLI

VISTI GLI ATTESTATI DEGLI STUDI COMPIUTI
VISTA LA VALUTAZIONE FINALE ESPRESSA
IL GIORNO 25 LUGLIO 2014

CONFERISCE A

JONATHAN BRIVIO

NATO A CARACAS (VENEZUELA) IL 25 MAGGIO 1990

LA LAUREA MAGISTRALE

IN

INGEGNERIA DELL'AUTOVEICOLO (AUTOMOTIVE ENGINEERING)

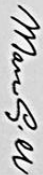
CLASSE N. LM-53 - D.M. 270/2004

IL PRESENTE DIPLOMA VIENE RILASCIATO A TUTTI GLI EFFETTI DI LEGGE
DATA TORINO IL 25 LUGLIO 2014

IL DIRETTORE GENERALE
(DAVIDE BERGAMINI)



IL RETTORE
(MARCO GILLI)



Via 1° Mayo, Torino

MATR. 182447

Summary

Acknowledgements

Chapter 1: Introduction

| | |
|------------------------------------------------------------------------|----|
| 1.1 - Formula SAE / Formula Student Competitions..... | 16 |
| 1.2 – The History of the Team Squadracorse Politecnico di Torino | 18 |
| 1.3 – The Vehicle chassis | 22 |
| 1.4 – Formula SAE Rules 2013 – Driver Cell | 22 |

Chapter 2: Introduction to composite materials and structures and their analysis

| | |
|--------------------------------|----|
| 2.1 – Composite Materials..... | 25 |
| 2.2 – Sandwich structures..... | 34 |

Chapter 3: Monocoque specifications

| | |
|-----------------------------------------------|----|
| 3.1 – Problem statement | 36 |
| 3.2 – Project Schedule | 36 |
| 3.3 – Requirement discussion..... | 36 |
| 3.4 – Benchmarking..... | 38 |
| 3.5 – SCR Monocoque Specific objectives | 38 |

Chapter 4: Monocoque Design

| | |
|---------------------------------------------------------------------------------|----|
| 4.1 – Design Process | 39 |
| 4.2 – Vehicle Package | 39 |
| 4.3 – Ergonomics..... | 42 |
| 4.4 – Final Monocoque CAD Model | 44 |
| 4.5 – Vehicle loads | 44 |
| 4.6 – Process followed to define the monocoque materials and safety zones | 50 |

| | |
|------------------------------------------------------------------------------|----|
| 4.7 – Material Selection | 50 |
| 4.8 – Safety zones defined by the rules..... | 50 |
| 4.9 - Composite Sandwich Equivalence | 52 |
| 4.10 – CFRP skins and Core details | 57 |
| <u>Chapter 5: Finite Element Analysis</u> | |
| 5.1 – FEA process | 60 |
| 5.2 - FEM model details | 60 |
| 5.3 – Final layup stacking sequence | 61 |
| 5.4 – FEA Static Linear Simulation results | |
| 5.4.1 – Torsional Stiffness Results | 63 |
| 5.4.2 - Static loadcase results – Braking condition..... | 64 |
| 5.4.3 - Static loadcase results – Max lateral Acceleration..... | 66 |
| 5.4.4 - Static loadcase results – Maximum Combined accelerations | 67 |
| 5.5 - Summary of the result of the FEA linear static simulations | 68 |
| 5.6 – Different Layup experimental validation..... | 69 |
| 5.7 - Safety Attachments verification according to the FSAE Rules 2013 | 70 |
| 5.8 - Perimeter shear testing..... | 70 |
| 5.9 - Summary of the perimeter shear test results..... | 72 |
| 5.10 - Safety attachments and suspension inserts calculation results..... | 73 |
| 5.11- ENSAT Pullout Test | 76 |
| 5.12 - Safety Harness Attachments Pullout Tests..... | 77 |

Chapter 6: Manufacturing

6.1 - Manufacturing Process.....79

6.2 - Carbon Fiber and draping analysis and plybook generation.....80

6.3 - Manufacturing Images.....83

Chapter 7 – Testing

7.1 – Torsional stiffness test bench.....90

7.2 - Torsional Stiffness Test Results and comparison.....92

7.3 - Track Testing.....93

7.4 - Presentation of the SCR at the “Museo Nazionale dell'Automobile di Torino” the
16th of July 2013.....94

7.5 - Crash Test Event.....94

Chapter 8: Conclusions96

Bibliography

Chapter 1 - INTRODUCTION

1.1 - Formula SAE / Formula Student Competitions

Formula SAE [1] is a student design competition organized by SAE International (SAE, previously known as the Society of Automotive Engineers). The competition was started in 1978 and was originally called SAE Mini Indy.

The concept behind Formula SAE is that a fictional manufacturing company has contracted a student design team to develop a small Formula-style race car. The prototype race car is to be evaluated for its potential as a production item. The target marketing group for the race car is the non-professional weekend autocross racer. Each student team designs, builds and tests a prototype based on a series of rules, whose purpose is both ensuring on-track safety (the cars are driven by the students themselves) and promoting clever problem solving.

During a Formula SAE event, the cars are evaluated by judges in a series of static and dynamic events, which include technical inspections, evaluations on the design of the car and its performance in the race, aimed to evaluate how well the vehicle behaves and goodness of its design and production. The maximum score assigned during a SAE event is 1000 points, 675 are made available by the dynamic events and 325 from the static ones.

- **Static Events (325 points)**

- Technical Inspection (no points)

The objective of technical inspection is to determine if the vehicle meets the FSAE Rules requirements and restrictions and if, considered as a whole, satisfies the intent of the Rules.

- Cost Report (100 points)

This event involves in creating a report of all part costs for the entire car. This is used to determine the cost of the car and manufacturability. Depending of the competition there is a 'Real Case Scenario' which is used to test the student's ability to deal with cost and manufacturing challenges.

- Business Presentation (75 points)

The objective of the presentation event is to evaluate the team's ability to develop and deliver a comprehensive business case that will convince the executives of a corporation that the teams design best meets the demands of the amateur, weekend competition market, and that it can be profitably manufactured and marketed.

- Design (150 points)

Engineering Design is one of the more prestigious events during the competition. During this event the students defend their knowledge of the car and engineering concepts to a panel of judges. The students should explain to the judges the entire design process of their car, from the concept to the manufacturing and discuss with the judges all the pros and cons of their choices.

- **Dynamic Events (675 points)**

- Acceleration (75 points)

The acceleration event evaluates the cars acceleration in a straight line over a distance of 75m.

- Skid Pad (50 points)

The objective of the skid-pad event is to measure the cars cornering ability on a closed circuit with two constant radius corners of 8m to the right and left. The faster car gets the highest score.

- Autocross (150 points)

Autocross is a one lap sprint usually 1-2km long. The objective of the autocross event is to evaluate the car's maneuverability and handling qualities on a tight course without the hindrance of competing cars. The autocross course will combine the performance features of acceleration, braking, and cornering into one event.

- Endurance (300 points)

The Endurance Event is a closed circuit race of 22km long. There are two drivers, each driving half of the distance.

- Fuel Economy (100 points)

The cars fuel economy will be measured in conjunction with the Endurance Event. The fuel economy shows how well the car has been tuned for the competition. This is a compromise event because the fuel economy score and endurance score will be calculated from the same heat. No refueling is allowed during an endurance heat.

In addition to these events, various sponsors of the competition provide awards for superior design accomplishments. For example, best use of E-85 ethanol fuel, innovative use of electronics,

recyclability, crash worthiness, analytical approach to design, and overall dynamic performance are some of the awards available.

Formula SAE encompasses all aspects of a business including research, design, manufacturing, testing, developing, marketing, management, and fund raising. Formula SAE takes students out of the class room and puts them in the real world.

Today, the competition has expanded and includes a number of spinoff events. Formula Student is a similar SAE-sanctioned event in the UK, as well as Formula SAE Australasia (Formula SAE-A) taking place in Australia. Formula ATA is the formula student event organized in Italy by the “Associazione Tecnica dell'Automobile”.

1.2 - The history of the Team “Squadra Corse Politecnico di Torino” [2]

Founded in 2005 by ten automotive students from Politecnico di Torino united by their passion for motorsports and wiliness to learn, Squadra Corse took part to its first competition the same year with the SC05 that opened a new path for the biggest and most successful formula SAE team of Italy. Many years of experience and development, combined with the desire to improve, have yielded to excellent results.

In 2011 the team choose to design the first full electric prototype ever built in Italy, the SC12e to participate on the formula student competitions of 2012, reaching outstanding results, positioning itself 7th on the worldwide standings.

Today, the team it is composed of 72 students coming from 12 different countries and representing large number of engineering fields.

After building eight prototypes and participating in several competitions, in 2012, Squadra Corse started the design its second full electric car. After the excellent results obtained in previous editions, the main goal was to increase the performance with respect the SC12e.

Squadra Corse Politecnico di Torino Prototypes

SC05



SC06



SC07



SC08



SC08H



SC09



SCX



SCXX



SC12e



1.3 - The Vehicle Chassis

The chassis is a fundamental part of a vehicle, the task of the chassis structure is to bear the forces and payloads of the vehicle, all of the vehicle components are fasten to it. Therefore, it affects the performance, safety of reliability.

The chassis has also the task of connecting the front and rear suspensions of the car, this feature gives rise to one of the main aspects to consider when designing a vehicle's chassis, when a load is applied to a wheel is transferred by means of the suspensions and it will eventually produce a deformation of the chassis, it behaves as a large torsion bar, cancelling the suspension effect shifting the roll centers. It is therefore obvious that greater the rigidity, the suspension will work better and the handling and safety of the vehicle will be improved.

In motorsports, for open wheeled formula type vehicles several types of chassis have been developed on the past years. In formula student, typically, the chassis features a tubular frame construction. But on recent years, aluminum honeycomb structures and CFRP (carbon fiber reinforced plastic) structures have been developed and implemented.

1.4 - Formula SAE 2013 Rules – Driver's Cell

The Formula SAE/Student Competitors must follow a series of specific rules that will constraint the vehicle performance specifications and safety features, these rules can be found at the web site of the Formula SAE series [3].

For 2013, the rules that impact the design of the chassis are extensive, and as almost every component is directly fastened to it several rules impacting these components might impact in consequence the frame. In any case, a set of the main rules that will define the specifications of the SCR are the following:

- Wheelbase (T2.3): at least 1525 mm
- Track (T2.4): The smaller track of the vehicle (front or rear) must be no less than 75% of the larger track.
- General conditions (T3.1, T3.2): Among other requirements, the vehicle's structure must include two roll hoops that are braced, a front bulkhead with support system and Impact Attenuator, and side impact structures.
- Minimum material requirements (T3.3): The minimum dimensions of the steel tubes used for the frame should be at least the following:

| ITEM or APPLICATION | OUTSIDE DIMENSION X WALL THICKNESS |
|--------------------------------------------------------------------------------------------------------------------------------------------------------------------------|--------------------------------------------------------------------------------------------------------------------------------------------------------------------------------------------------------------------------------------------------------------------------|
| Main & Front Hoops, Shoulder Harness Mounting Bar | Round 1.0 inch (25.4 mm) x 0.095 inch (2.4 mm) or Round 25.0 mm x 2.50 mm metric |
| Side Impact Structure, Front Bulkhead, Roll Hoop Bracing, Driver's Restraint Harness Attachment (except as noted above) EV: Accumulator Protection Structure | Round 1.0 inch (25.4 mm) x 0.065 inch (1.65 mm) or Round 25.0 mm x 1.75 mm metric or Round 25.4 mm x 1.60 mm metric or Square 1.00 inch x 1.00 inch x 0.049 inch or Square 25.0 mm x 25.0 mm x 1.25 mm metric or Square 26.0 mm x 26.0 mm x 1.2 mm metric |
| Front Bulkhead Support, Main Hoop Bracing Supports EV: Tractive System Components | Round 1.0 inch (25.4 mm) x 0.049 inch (1.25 mm) or Round 25.0 mm x 1.5 mm metric or Round 26.0 mm x 1.2 mm metric |

Table 1– minimum tubing dimensions

- Roll Hoops (T3.9, T3.10, T3.11): Minimum distance between the reference male (95 percentile with helmet) and the main hoop described by Figure 1. Bidimensional template for the pilot posture.

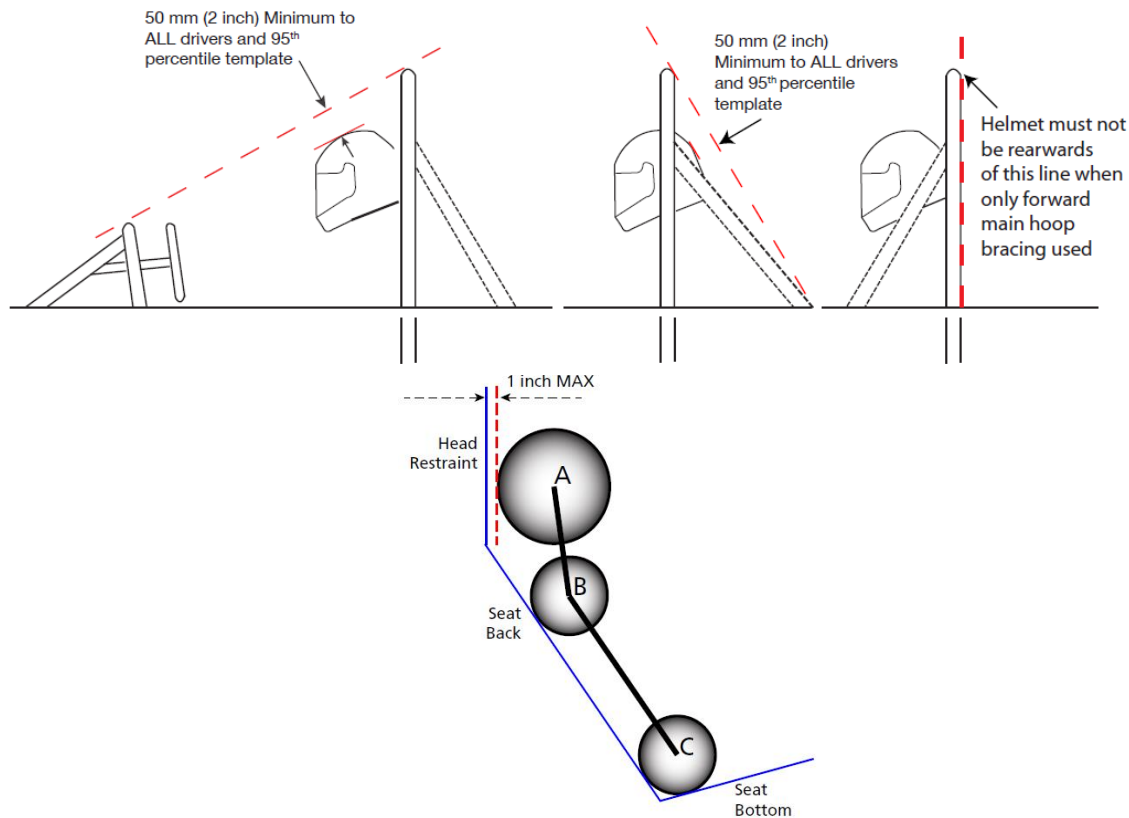


Figure 1 - Helmet – Hoops clearance [top] and pilot position [Bottom]

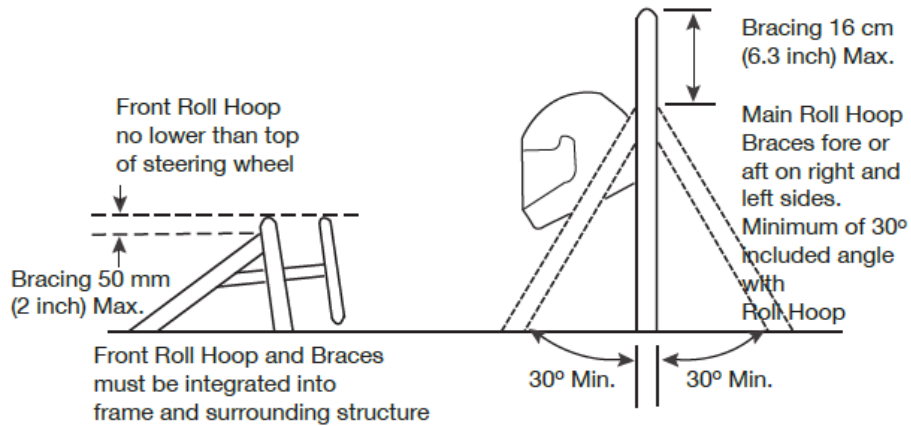


Figure 2 – Main hoop bracing supports constraints

- Roll Hoop Bracing (T3.12, T3.13, and T3.14): the main roll hoop bracings should be attached the nearest possible to the roll hoop tip, this distance cannot exceed 160 mm and the vertical angle between the supports and the roll hoop cannot be smaller than 30 deg. Also, the front roll hoop bracings should be attached the nearest possible to the roll hoop tip, this distance cannot exceed 50 mm.

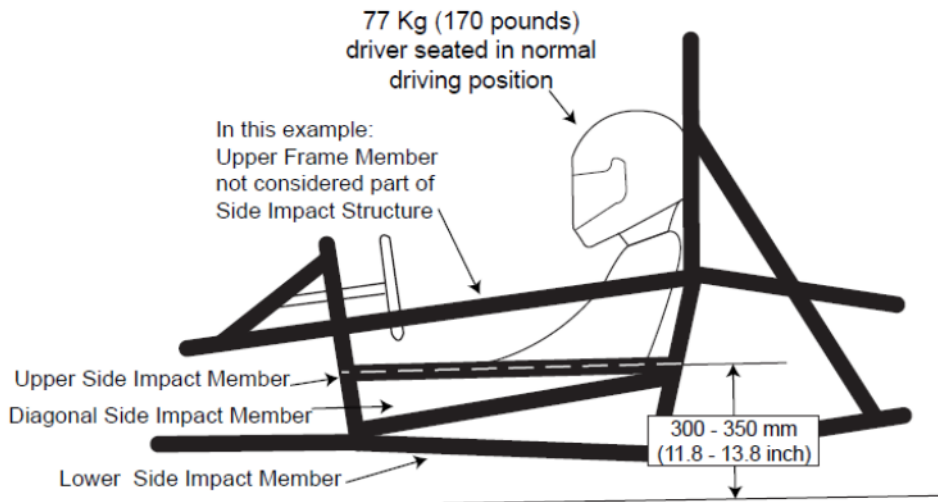


Figure 3 – Side impact structure

- Front Impact Structure (T3.18): The driver's feet and legs must be completely contained within the Major Structure of the Frame. While the driver's feet are touching the pedals, in side and front views no part of the driver's feet or legs can extend above or outside of the Major Structure of the Frame.

Chapter 2 – Introduction to composite materials, structures and their analysis

2.1 - Composite Materials [4]

A composite material is a material usually not present in nature which is derived from a macroscopic combination of two or more distinct materials, with a well-defined interface that separates them. Despite every material have their own mechanical characteristics, the union of the components leads to a new material in which the mechanical and physical properties are overall higher than those of the individual constituents. Although one of the most significant characteristics of composite materials is a high strength-to-weight ratio, which has guided the choice of these materials in fields such as aerospace and automotive, where weight reduction is a fundamental requirement, these materials have excellent resistance to fatigue, corrosion and impacts, as well as special electrical, thermal, environmental.

A composite material is usually constituted by:

1. A matrix, which bonds the reinforcement material, transferring the external loads and protects it from corrosion, and shear forces.
2. The reinforcement material, usually fibers (long, short) or particles with high mechanical properties, that usually adds rigidity and greatly impedes crack propagation.
3. The core, many composite layup designs also include a co-curing or post curing of the prepreg with other mediums, such as honeycomb or foam.

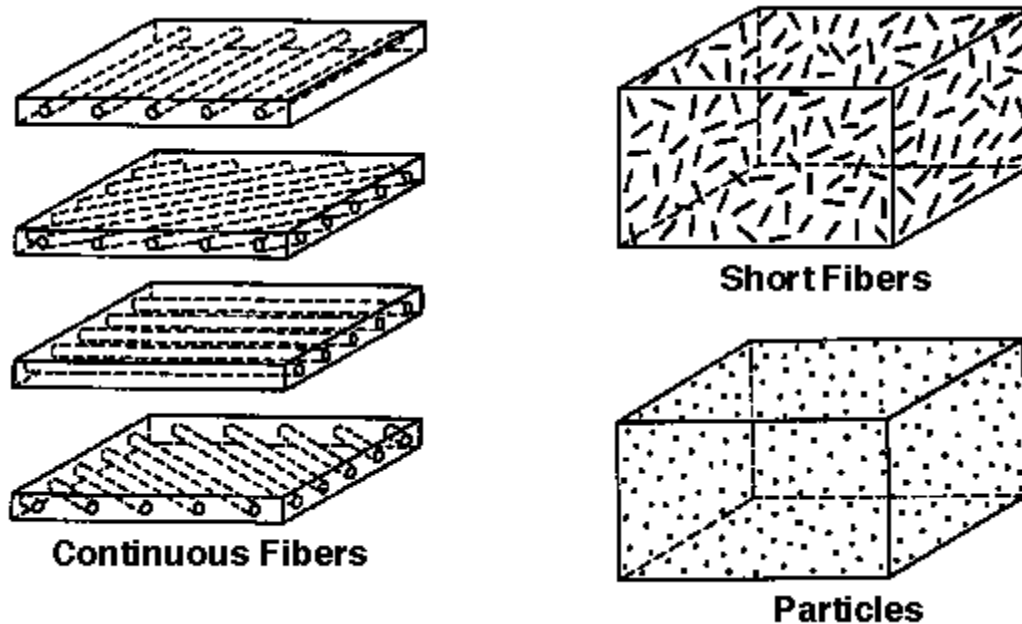


Figure 4 - Types of reinforcement materials

The classification of the composite materials can be made in several ways: the two most common are those depending on the type of matrix and depending on the type of fiber used.

In the first case, it is called ceramic matrix composites (CMC - ceramic matrix composites), metal (MMC - metallic matrix composites) or polymer (PMC - Polymer matrix composites). Among these composites, it is necessary to further distinguish between the thermoset composite, the most widely used in the construction of automotive structures, and thermoplastic matrix composites.

In the second case reference is made to the shape of the reinforcement, which may consist of particles, discontinuous fibers or continuous fibers. The fibers can be arranged along predefined directions, organized in layups with in one or more layers or three-dimensional structures. In particular, three types of reinforcing fibers are well established, thanks to their particular characteristics:

- Glass fibers, which, in the more advanced versions (S-glass) have a relatively high rigidity, a great resistance and a relatively low cost.
- Carbon fibers or graphite, which, are significantly more expensive than glass fibers, however, are considerably lighter and more rigid.
- Aramid fibers (Kevlar), these fibers have a nice tensile strength and specific weight ratio, high stiffness and high toughness characteristics, but are disadvantaged by the lack of compressive strength.

The carbon fibers and graphite are produced from precursors, typically polymeric, which are subjected to a pyrolysis process and partial conversion (carbon fibers) or total (graphite fibers). The precursor materials consist mainly of fibers of polyacrylonitrile (PAN), cellulose (rayon) or pitch obtained from petroleum distillation. Depending on the precursor material the fibers are classified in PAN-based, rayon-based, and pitch-based.

The pitch-based fibers achieved considerable interest because of the low cost of the raw material and the modulus of elasticity they possessed (very high, up to over 900 GPa). The production process starts from polymeric fibers or pitch obtained by melt spinning.

The PAN and Rayon based fibers, are manufactured from its raw material, which is maintained in tension and subjected to a first heat treatment, stabilization and partial oxidation by heating in the presence of air at about 250 ° C. Subsequently, the fibers are pyrolyzed at high temperature, up to 1000°C and subsequently heated up to over 1300 to 1500 °C, in an inert environment (nitrogen), for the carbonization of the material. In the case of high modulus fibers the heat treatment is pushed at temperatures above 1800-2000°C, sometimes more than 3000°C, where graphitization it's almost complete.

The carbon fibers, as the majority of the reinforcing fibers for composites (glass, Kevlar, boron, etc.) Exhibit brittle behavior with a fragile failure after the field of elastic deformation, without evidence of plasticity. Figure 5 shows the typical stress-strain curves of some of the most common reinforcing fibers. The rupture occurs when the stress reaches a critical value for the propagation of a defect in the material. The fiber strength is then governed by the presence of the inevitable defects along it; rupture will occur at the most severe flaw present. The probability of finding a defect also depends on the volume of material considered or by the diameter, in the case of fibers with uniform section. It follows that the resistance will be distributed over a range of values and that, on average, longer fibers present lower resistances due to the scale effect.

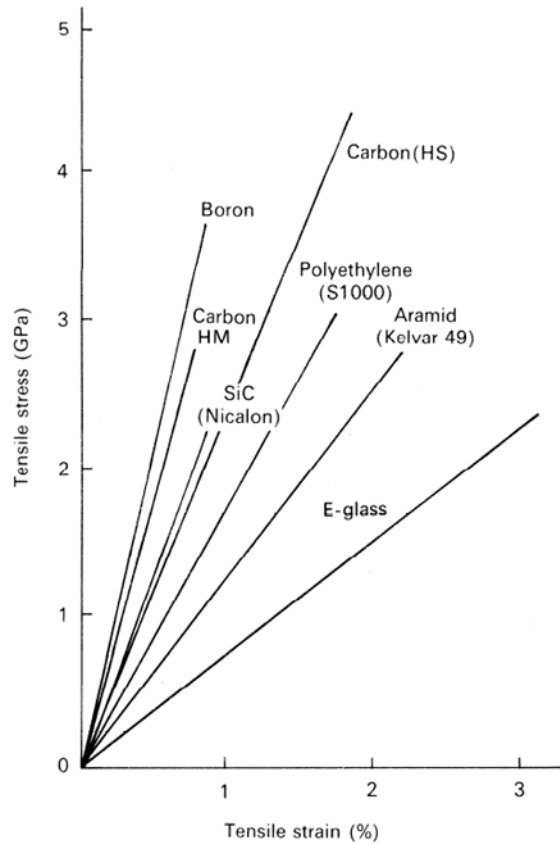


Figure 5- Stress-Strain curves of common reinforcement fibers

The compressive strength of the fibers is considerably lower than the tensile strength, with differences of the order of 20-50%. This difference is related to the inherent instability in compression resulting from the slenderness of the fibers. These behaviors must be taken into account in structural applications. The graphitic carbon has high chemical inertness. The low reactivity of the graphite determines both a low wettability of the fiber, and a reduced ability to create effective links with the polymers that form the continuous matrix of the final composite.

In order to increase the wettability and the possibility of bonds at the interface, the fibers are very often subjected to surface treatments, already in the production phase. The most common treatments consist of a partial oxidation introducing chemical groups oxidized by modifying the structure of graphitic surface. The presence of chemical groups such as $C=O$, $HC=O$, $C-OH$, designed to increase the reactivity of the surface, an increase in the number and intensity of chemical bonds and physical interactions with the matrix; the resulting increase in surface tension also facilitates the wettability of the fiber by increasing the ease and efficiency of impregnation. In addition, the fibers are clothed with primers (sizing), consisting of solutions/emulsions containing adjuvants of process (lubricants, antistatic, etc.). The primary function of the primers is to protect the fibers during manufacturing operations, spinning, weaving, etc.

The carbon fibers and graphite are thermally and electrically conductive. The electrical conductivity is significantly dependent on the degree of crystallinity achieved in the production

phase. Despite the high conductivity of the fibers, the matrix is a polymer insulator, therefore, the overall composite is partially conductive; also the conductivity characteristics, such as mechanical ones, suffer from the fiber orientation.

The fatigue strength of the fibers is practically equal to the static strength: fiber breakage occurs when the ultimate load is achieved, regardless of the history of solicitation. This property implies that the composite material will have excellent fatigue strength.

2.1.1 – Orthotropic materials

A material is said anisotropic when its characteristics vary with the direction in question. If the material admits three mutually orthogonal planes of symmetry, these are called orthotropic planes. To better understand the difference between an anisotropic material and one orthotropic material is useful to observe that the application of a tensile load to an element of prismatic shape, in an anisotropic material, this load produces deformations and along all sides of the element. This occurs regardless of the particular direction of load application. If the anisotropic material is orthotropic, then there exist three mutually orthogonal directions, such that the application of a tensile stress in these directions produces, as for an isotropic material, a constant deformation without distortion in the plane from these identified. These 3 dimensions are called principal directions of the material.

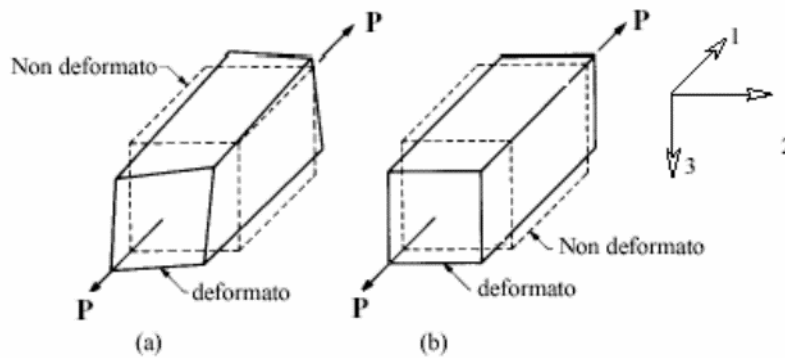


Figure 6 - Typical deformation of an anisotropic material (a) and orthotropic material (b) under stress applied at one principal direction

2.1.2 – Hooke's Law

As is known from the theory of elasticity, the state of tension present in a generic material in the neighborhood of one point is uniquely described by 9 stress components $\sigma_{ij}(i, j = 1, 2, 3)$. The same applies to the state of deformation, described by the nine components $\epsilon_{kl}(k, l = 1, 2, 3)$. consequently, if we assume that the material presents a linear elastic behavior, the relationship between stress and strain (generalized Hooke's law) is written as:

$$\sigma_{ij} = E_{ijkl}\epsilon_{kl} \quad (1)$$

In the case of a fully anisotropic material, therefore, the relationship between stress and strain, involves $9 \times 9 = 81$ elastic constants, $E_{ijkl}(i, j, k, l = 1, 2, 3)$. In fact, since the tensors σ_{ij} and ϵ_{kl} are symmetrical, thus, only 6 components are independent, the independent elastic constants that describe the behavior of an anisotropic material are $6 \times 6 = 36$. Neglecting the variables with a thermodynamic nature also allow to further reduce these constants to a total of 21.

If the material is anisotropic, in particular, orthotropic, it admits three planes of symmetry mutually orthogonal, then it is easy to show that the relevant constitutive laws involving only 9 independent elastic constants. Indicating with 1,2,3 the three main axes of the material, since, as said before, the application of a tension state σ_{ii} ($i = 1, 2, 3$) does not produce distortions ϵ_{li} ($i \neq j$).

If the material is orthotropic, with symmetry planes mutually orthogonal, the relations between stress and strain, written in the system of reference defined by the principal directions are:

$$\begin{Bmatrix} \epsilon_{11} \\ \epsilon_{22} \\ \epsilon_{33} \\ \gamma_{12} \\ \gamma_{23} \\ \gamma_{13} \end{Bmatrix} = \begin{bmatrix} \frac{1}{E_1} & -\frac{\nu_{21}}{E_2} & -\frac{\nu_{31}}{E_3} & 0 & 0 & 0 \\ -\frac{\nu_{12}}{E_1} & \frac{1}{E_2} & -\frac{\nu_{32}}{E_3} & 0 & 0 & 0 \\ \frac{\nu_{13}}{E_1} & -\frac{\nu_{23}}{E_2} & \frac{1}{E_3} & 0 & 0 & 0 \\ 0 & 0 & 0 & G_{12} & \frac{1}{G_{23}} & 0 \\ 0 & 0 & 0 & 0 & G_{23} & \frac{1}{G_{13}} \\ 0 & 0 & 0 & 0 & 0 & G_{13} \end{bmatrix} \begin{Bmatrix} \sigma_{11} \\ \sigma_{22} \\ \sigma_{33} \\ \tau_{12} \\ \tau_{23} \\ \tau_{13} \end{Bmatrix} \quad (2)$$

Assuming, a plain stress state ($\sigma_{33} = \tau_{13} = \tau_{23} = 0$), the relationship can be simplified as:

$$\begin{Bmatrix} \epsilon_1 \\ \epsilon_2 \\ \gamma_{12} \end{Bmatrix} = \begin{bmatrix} \frac{1}{E_1} & -\frac{\nu_{21}}{E_2} & 0 \\ -\frac{\nu_{12}}{E_1} & \frac{1}{E_2} & 0 \\ 0 & 0 & \frac{1}{G_{12}} \end{bmatrix} \begin{Bmatrix} \sigma_1 \\ \sigma_2 \\ \tau_{12} \end{Bmatrix} \quad (3)$$

The equation (3) defines the relationship between strain and stresses for an orthotropic layer, defined by only 4 elastic constraints linearly independent.

2.1.3 – Classical laminate theory

The use of a single layer with unidirectional reinforcement is not to be adequate for most engineering applications, due to the low elastic characteristics of the lamina in a direction perpendicular to the fiber reinforcement. This drawback is overcome by resorting to the composite laminates consisting of n-layers with unidirectional reinforcement oriented so as to meet the various needs of the project such as, in particular, strength and stiffness.

For the proper design of a composite laminate is necessary to know the relationships between, a given type of layer and stacking sequence, between the mechanical properties of the layer and those of the laminate obtained. Under some simplifying assumptions, such relationships are identified by the so-called “classical laminate theory”.

A laminate is composed of an ordered stacking of plies such as to form a composite thin plate. The elastic characteristics and mechanical properties of the laminate depend on the number of sheets, the elastic characteristics and mechanical properties of the individual lamina, and the orientation of the intrinsic axes of each lamina (1-2) with respect to the axes of the laminate (xy).

The simplifying assumptions used are:

- The plies are perfectly matched to each other
- The state of deformation is planar
- In bending, the sections rotate remaining straight and orthogonal to the plane of symmetry (Kirchhoff hypothesis)
- the deformation ϵ_z is negligible small compared to the other deformation ϵ_x and ϵ_y
- the thickness of the laminate is small relative to the other dimensions

To derive the constitutive equation of the laminate, displacement method is used. Denoting by u_0 , v_0 and w_0 components along x, y and z displacement measured with respect a point on the mid-plane of the laminate, then have that the displacement u along x suffered by the generic point of the segment distance z from the middle plane is given by:

$$u_z = u_0 - \alpha z \quad (4)$$

Being α , the rotation of the element being considered. Taking into account the assumptions taken before, such rotation is linked to the displacement about z using the following relationship:

$$\alpha(z) = \frac{\partial w}{\partial x} = \frac{\partial w_0}{\partial x} \quad (5)$$

From (4) and (5) we obtain

$$\mathbf{u}(z) = \mathbf{u}_0 - z \frac{\partial w_0}{\partial x} \quad (1)$$

On a similar way, for the component on y direction:

$$\mathbf{v}(z) = \mathbf{v}_0 - z \frac{\partial w_0}{\partial y} \quad (2)$$

The strain relationships on the xy plane are obtained from the following expressions:

$$\left\{ \begin{array}{l} \epsilon_x = \frac{\partial u}{\partial x} = \frac{\partial u_0}{\partial x} - z \frac{\partial^2 w}{\partial x^2} = \epsilon_x^0 + z k_x \\ \epsilon_y = \frac{\partial v}{\partial y} = \frac{\partial v_0}{\partial y} - z \frac{\partial^2 w}{\partial y^2} = \epsilon_y^0 + z k_y \\ \gamma_{xy} = \frac{\partial u}{\partial y} + \frac{\partial v}{\partial x} = \frac{\partial u_0}{\partial y} + \frac{\partial v_0}{\partial x} - 2z \frac{\partial^2 w}{\partial x \partial y} = \gamma_{xy}^0 + z k_{xy} \end{array} \right. \quad (3)$$

From the equation (8) we can observe how the strains vary linearly inside the laminate thickness z , and the strain is linked to the stiffness matrix of the material. From the Hooke's Law (1), we can now derive the stress-strain relationship for the ply- k of the laminate:

$$\begin{Bmatrix} \sigma_x \\ \sigma_y \\ \tau_{xy} \end{Bmatrix} = [\tilde{E}]_k \begin{Bmatrix} \varepsilon_x \\ \varepsilon_y \\ \gamma_{xy} \end{Bmatrix} = [\tilde{E}]_k \begin{Bmatrix} \varepsilon_x^0 \\ \varepsilon_y^0 \\ \gamma_{xy}^0 \end{Bmatrix} + z[\tilde{E}]_k \begin{Bmatrix} k_x \\ k_y \\ k_{xy} \end{Bmatrix} \quad (4)$$

As we can observe from the last relationship. The stress varies non-linearly inside the laminate, the matrix $[\tilde{E}]_k$ varies from ply to ply, and it's dependent of the mechanical characteristics of ply in question and its relative orientation. Therefore, the stress are linear inside a single ply but are discontinuous from one ply to the other.

Once the stress-strain relationship of each ply is defined, we can now find the relationship between the loads applied to the laminate, the axial and shear stresses, the flexural moment, the torsional moment by unit's length and the displacements of the mean plane.

Considering a laminate made of n -ply's, with a total thickness of h . See figure 7.

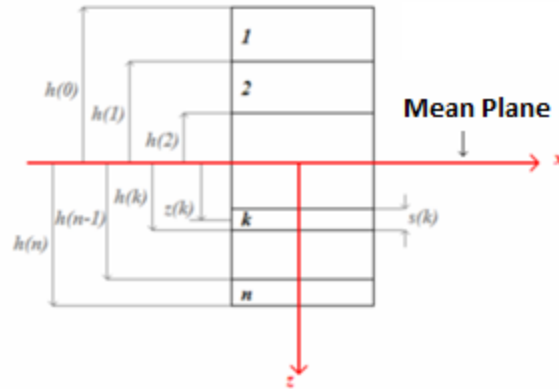


Figure 7- n -ply's laminate and its mean plane location

The axial stresses and the shear stress per unit length on the system of reference defined on the laminate are given by:

$$\begin{aligned} N_x &= \int_{-h/2}^{h/2} \sigma_x dz \\ N_y &= \int_{-h/2}^{h/2} \sigma_y dz \\ T_{xy} &= \int_{-h/2}^{h/2} \tau_{xy} dz \end{aligned}$$

Axial and shear stresses on the xy plane of the laminate (5)

And the flexural and torsional moments are given by:

$$\begin{aligned}
M_x &= \int_{-h/2}^{h/2} \sigma_x z dz \\
M_y &= \int_{-h/2}^{h/2} \sigma_y z dz \\
M_{xy} &= \int_{-h/2}^{h/2} \tau_{xy} z dz
\end{aligned}$$

Flexural and Torsional moments present on the laminate (6)

From the equations (10), (11) and (9) we obtain the loads in function the deformation of the mean plane of the laminate:

$$\begin{aligned}
\begin{Bmatrix} N_x \\ N_y \\ T_{xy} \end{Bmatrix} &= \int_{-h/2}^{h/2} \begin{Bmatrix} \sigma_x \\ \sigma_y \\ \tau_{xy} \end{Bmatrix} dz = \sum_{k=1}^n \int_{-\frac{h}{2}}^{\frac{h}{2}} \begin{Bmatrix} \sigma_x \\ \sigma_y \\ \tau_{xy} \end{Bmatrix} dz = \\
&= \sum_{k=1}^n \int_{-h/2}^{h/2} \left([\tilde{E}]_k \begin{Bmatrix} \varepsilon_x^0 \\ \varepsilon_y^0 \\ \gamma_{xy}^0 \end{Bmatrix} + z [\tilde{E}]_k \begin{Bmatrix} k_x \\ k_y \\ k_{xy} \end{Bmatrix} \right) dz = \\
&= \left(\sum_{k=1}^n [\tilde{E}]_k \int_{-\frac{h}{2}}^{\frac{h}{2}} dz \right) \begin{Bmatrix} \varepsilon_x^0 \\ \varepsilon_y^0 \\ \gamma_{xy}^0 \end{Bmatrix} + \left(\sum_{k=1}^n [\tilde{E}]_k \int_{-\frac{h}{2}}^{\frac{h}{2}} z dz \right) \begin{Bmatrix} k_x \\ k_y \\ k_{xy} \end{Bmatrix} = \\
&= \left(\sum_{k=1}^n [\tilde{E}]_k (h_k - h_{k-1}) \right) \begin{Bmatrix} \varepsilon_x^0 \\ \varepsilon_y^0 \\ \gamma_{xy}^0 \end{Bmatrix} + \left(\sum_{k=1}^n [\tilde{E}]_k \left(\frac{h_k^2 - h_{k-1}^2}{2} \right) \right) \begin{Bmatrix} k_x \\ k_y \\ k_{xy} \end{Bmatrix}
\end{aligned}$$

Stating that:

$$\begin{aligned}
[A] &= \sum_{k=1}^n [\tilde{E}]_k (h_k - h_{k-1}) \\
[B] &= \sum_{k=1}^n [\tilde{E}]_k \left(\frac{h_k^2 - h_{k-1}^2}{2} \right)
\end{aligned}$$

We obtain

$$\begin{Bmatrix} N_x \\ N_y \\ T_{xy} \end{Bmatrix} = [A] \begin{Bmatrix} \varepsilon_x^0 \\ \varepsilon_y^0 \\ \gamma_{xy}^0 \end{Bmatrix} + [B] \begin{Bmatrix} k_x \\ k_y \\ k_{xy} \end{Bmatrix}$$

For the flexural and torsional moments we obtain the following expressions:

$$\begin{aligned}
\begin{Bmatrix} M_x \\ M_y \\ M_{xy} \end{Bmatrix} &= \int_{-h/2}^{h/2} \begin{Bmatrix} \sigma_x \\ \sigma_y \\ \tau_{xy} \end{Bmatrix} z dz = \sum_{k=1}^n \int_{-\frac{h}{2}}^{\frac{h}{2}} \begin{Bmatrix} \sigma_x \\ \sigma_y \\ \tau_{xy} \end{Bmatrix} z dz = \\
&= \sum_{k=1}^n \int_{-h/2}^{h/2} \left(z [\tilde{E}]_k \begin{Bmatrix} \varepsilon_x^0 \\ \varepsilon_y^0 \\ \gamma_{xy}^0 \end{Bmatrix} + z^2 [\tilde{E}]_k \begin{Bmatrix} k_x \\ k_y \\ k_{xy} \end{Bmatrix} \right) dz = \\
&= \left(\sum_{k=1}^n [\tilde{E}]_k \int_{-\frac{h}{2}}^{\frac{h}{2}} z dz \right) \begin{Bmatrix} \varepsilon_x^0 \\ \varepsilon_y^0 \\ \gamma_{xy}^0 \end{Bmatrix} + \left(\sum_{k=1}^n [\tilde{E}]_k \int_{-\frac{h}{2}}^{\frac{h}{2}} z^2 dz \right) \begin{Bmatrix} k_x \\ k_y \\ k_{xy} \end{Bmatrix} = \\
&= \left(\sum_{k=1}^n [\tilde{E}]_k \left(\frac{h_k^2 - h_{k-1}^2}{2} \right) \right) \begin{Bmatrix} \varepsilon_x^0 \\ \varepsilon_y^0 \\ \gamma_{xy}^0 \end{Bmatrix} + \left(\sum_{k=1}^n [\tilde{E}]_k \left(\frac{h_k^3 - h_{k-1}^3}{3} \right) \right) \begin{Bmatrix} k_x \\ k_y \\ k_{xy} \end{Bmatrix}
\end{aligned}$$

Where we can define

$$[D] = \sum_{k=1}^n [\tilde{E}]_k \left(\frac{h_k^3 - h_{k-1}^3}{3} \right)$$

We obtain

$$\begin{Bmatrix} M_x \\ M_y \\ M_{xy} \end{Bmatrix} = [B] \begin{Bmatrix} \varepsilon_x^0 \\ \varepsilon_y^0 \\ \gamma_{xy}^0 \end{Bmatrix} + [D] \begin{Bmatrix} k_x \\ k_y \\ k_{xy} \end{Bmatrix}$$

Joining all the equations defined before, we obtain a single expression that represents the relationship between forces, strains and stiffness.

$$\begin{Bmatrix} \{N\} \\ \{M\} \end{Bmatrix} = \begin{bmatrix} [A] & [B] \\ [B] & [D] \end{bmatrix} \begin{Bmatrix} \{\varepsilon^0\} \\ \{k\} \end{Bmatrix}$$

The matrix [A] is commonly referred as the extensional matrix, the matrix [B] is the coupling matrix and the matrix [D] is the flexural stiffness matrix.

The equation stated before shows how in a laminate an axial or shear load in general induce planar deformation and a variation of the curvature in flexion or torsion of the mean plane. On the other hand, the equation also shows how a flexural or torsional moment induces not only changes in curvature but also generates deformations on the plane of the laminate. This effects are consequences of the stacking sequence of each ply inside the laminate and their mechanical characteristic's and are not related to their anisotropy.

The coupling effects between axial and flexural stresses are generally undesired, this coupling is cancelled when the laminate is created in order to have a null [B] matrix. This condition is achieved

For a particular type of laminate called “symmetrical laminate”, on which each ply of the laminate above the mean plane has a symmetrical ply under the mean plane. The resultant [D] matrix of a laminate with the symmetrical stacking condition of the ply’s is null.

On the literature is common to denote a symmetrical laminate using the letter S (Symmetrical) outside the parenthesis that defines the laminate. i.e. a laminate $[0_2/\pm 45]_s$ refers to a symmetrical laminate made of 6 plies, 2 oriented at 0 degrees and one oriented at ± 45 degrees with respect the laminate reference axis and another 3 plies stacked symmetrically at the other side of the mean plane.

There are other typologies of symmetrical laminates such as cross-ply or angle-ply. In the cross-ply laminate all the plies are oriented 0/90 degrees. Being a symmetrical laminate the [B] matrix is null and the components A_{16}, A_{26}, D_{16} and D_{26} are also null. (see figure 8).

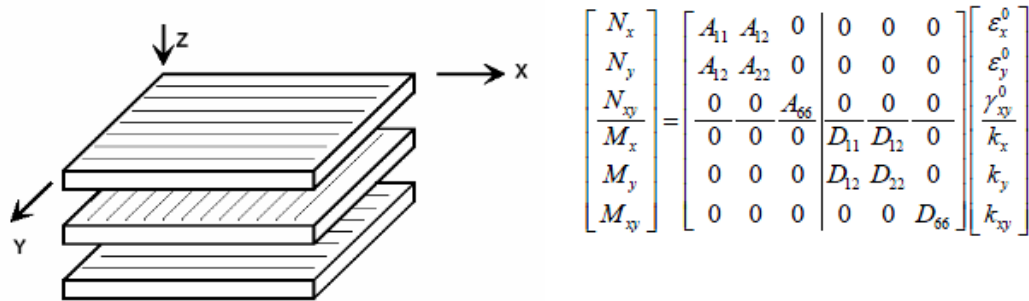


Figure 8 - Cross-ply symmetrical laminate

On the other hand, the angle-ply symmetrical laminate has only plies oriented at ± 45 degrees. (see figure 9).

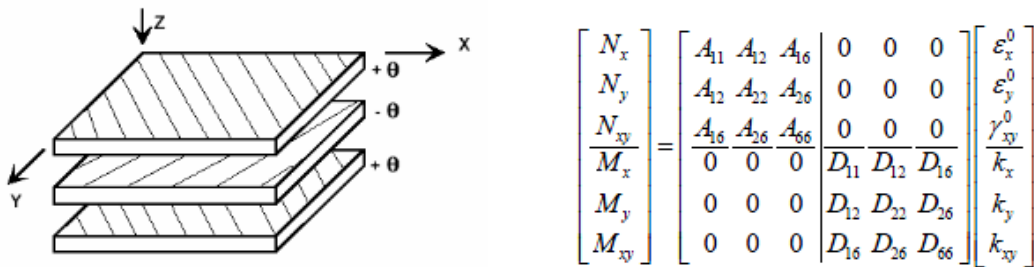


Figure 9 - Angle-Ply symmetrical laminate

2.2 – Sandwich structures [4]

The sandwich structures are made by joining 2 thin layers named “skins” made of a strong and stiff material to a core material or filler material (see figure 10). The external skins support almost all the loads applied on the plane of the sandwich structure. When to the laminate out of plane

loads or flexural moments are applied, the thin skins separated by the core support the loads or moments.

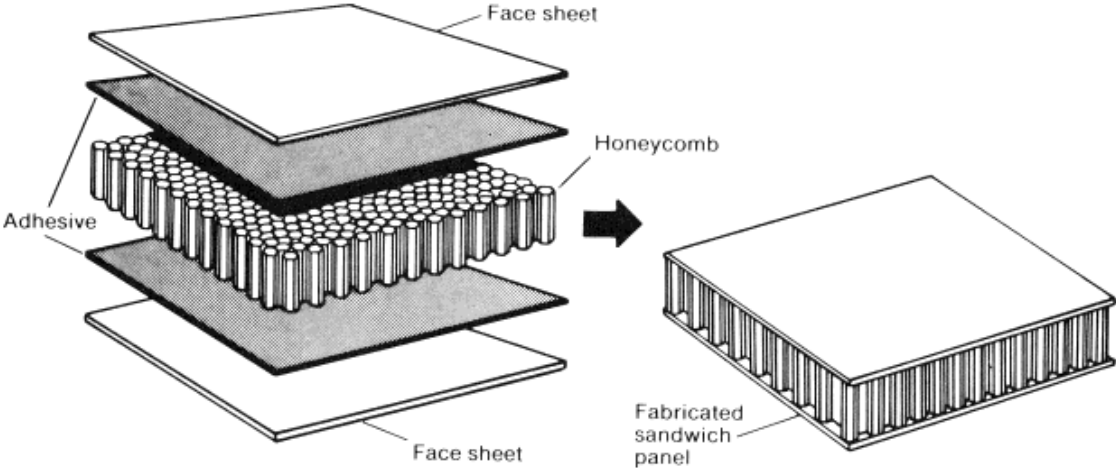


Figure 10- Composite sandwich

Chapter 3 – Monocoque Specifications

3.1 - Problem statement

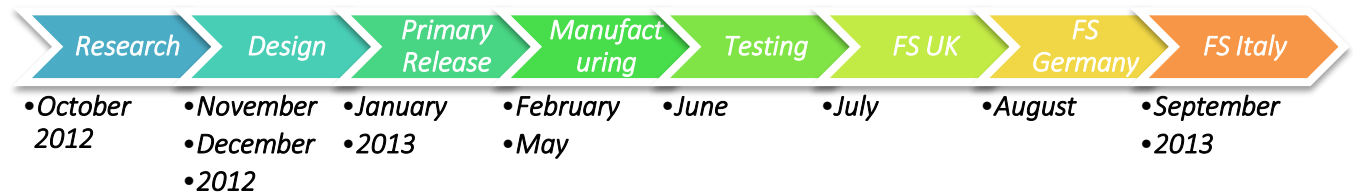
In order to develop the composite monocoque chassis the different goals and performance specifications should be defined. Ideally the chassis would exhibit the following characteristics:

1. Guarantee the driver's safety in case of an accident
2. Sufficiently stiff
3. Lightweight
4. Allows easy access to internally mounted components
5. Easy to manufacture
6. Inexpensive

Characteristics such as Cost, Stiffness and weight are in direct competition with each other. Therefore, setting the targets and overall weight of the different characteristics will give the design constraints that should be followed.

3.2 - Project schedule

The Formula SAE 2013 States that each team should design and manufacture a race car in one year, therefore we planned the activities using the following timeline:



3.3 - Requirements discussion

There are many requirements that the chassis must be able to meet in order to be deemed suitable for a race car, by studying the previous chassis of the team a starting point for the design objectives can be set. But first, we will do a discussion of how the different performance characteristics are correlated to each other.

Safety

The monocoque will be designed compliant with the Formula SAE 2013 Rules, that as stated on chapter one, imposes a set of rules to guarantee the driver's, judges, team members and spectators are safe during the competition's events.

Accessibility and ergonomics

All the components of the car should be integrated somehow to the vehicle, one of the main functions of the chassis is to allow the fitting of all these components and support all the loads that might arise in dynamic or static conditions. As stated by the rules, a 95th percentile male manikin and a 5th percentile female manikin should be able to fit and drive the race car, therefore packaging and ergonomic studies should be performed to guarantee both, comfort and safety.

Weight and Stiffness

The weight is one of the most important requirement of a race car, generally the lightest the faster the car will be. On the other hand, the stiffness of the chassis itself should be high enough to avoid excessive deformations that will affect the suspension kinematics, thus, handling and stability will be compromised. Also, a stiff chassis would allow a very responsive race car to suspension variations, for example, is very common to encounter a race car that no matter what damping and suspension stiffness variations are made the change in performance it's hard to notice due to the fact that the chassis and/or suspension components are not stiff enough to allow all the components to work properly. As a rule of thumb, the chassis torsional stiffness should be at least 10 times that those of the suspension. Therefore, a higher stiffness is desired but it comes at a cost, supposing a baseline chassis, if the highest performing materials are used, and the chassis geometry cannot be changed, to increase its stiffness more material should be added implying an increase of weight.

Cost

As said before, the weight and stiffness of the chassis are proportional to each other. Cost on the other hand, it's mostly related to the cost of the materials used, tooling, transportation, etc. Using the highest performing materials will probably increase the overall cost of the monocoque with respect the use of common materials. The manufacturing solution of this type of component will represent about 70% of the total cost, therefore a compromise should be found in order to found the optimal solution.

Particularly for the 2013 season, the team Squadracorse Polito found the support of a Turin based company called "ERRE TI compositi", that supported the team and covered the manufacturing cost of the monocoque in exchange of know-how and visibility. Thus, the cost was partially limited by ERRE TI but a maximum budget was never established.

Manufacturability

The monocoque should be manufactured on a finite time set by the requirements of the project, the team should every year produce and manufacture a new race car in order to enter that year's competitions. On that period of time, the team should design, manufacture and test the race car before the competition. The most successful Formula SAE/Student teams finish the design and manufacturing of the vehicle 3 months before the competition in order to be able to test and improve the race car and drivers during that time. The design of a new prototype usually takes about 3 months, and the competitions are taken into place during a range of 3-4 months. That

leaves 2-3 months for the production and assembly of all the components for the project to be feasible.

3.4 – Benchmarking

To design a new chassis several tools can be used to define its performance characteristics, the use of benchmarking is one of the most well developed processes on the automotive industry to compare technical products. In order to define a baseline requirements for the monocoque of the SCR we determined the characteristics of the SC12e chassis (2012 race car).

3.4.1 - Technical specifications of the Steel frame of the SC12e race car (2012)

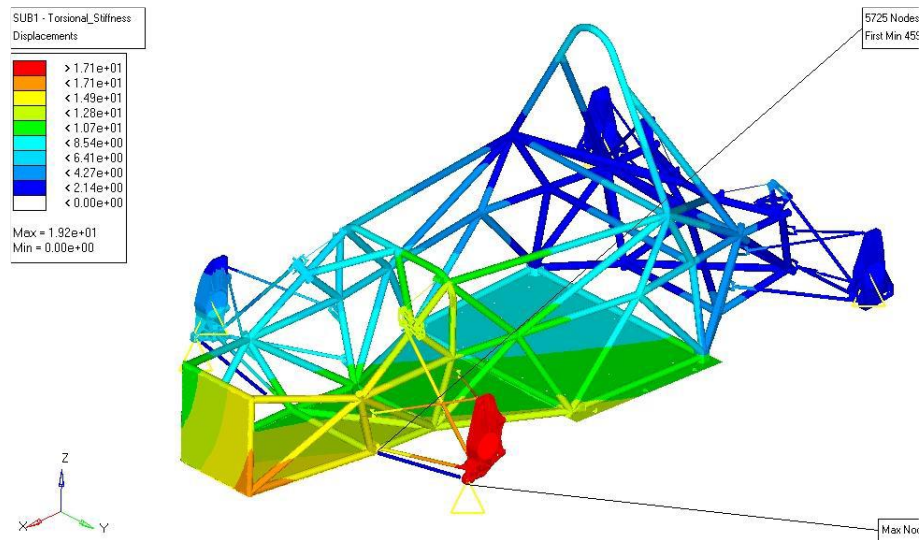


Figure 11 - SC12e Frame Displacements under torsion

| | |
|------------------------------------------|---------|
| Mass [kg] | 44.51 |
| Force [N] | 1000 |
| Displacement [mm] | 19.20 |
| Arm [mm] | 1179 |
| Torsional Stiffness [N*m/rad] | 72404 |
| Stiffness to Weight Ratio [N*m/(rad*kg)] | 1509 |
| Manufacturing time | 1 month |

Table 2 - SC12e Chassis Specs

3.5 - SCR Monocoque specific objectives

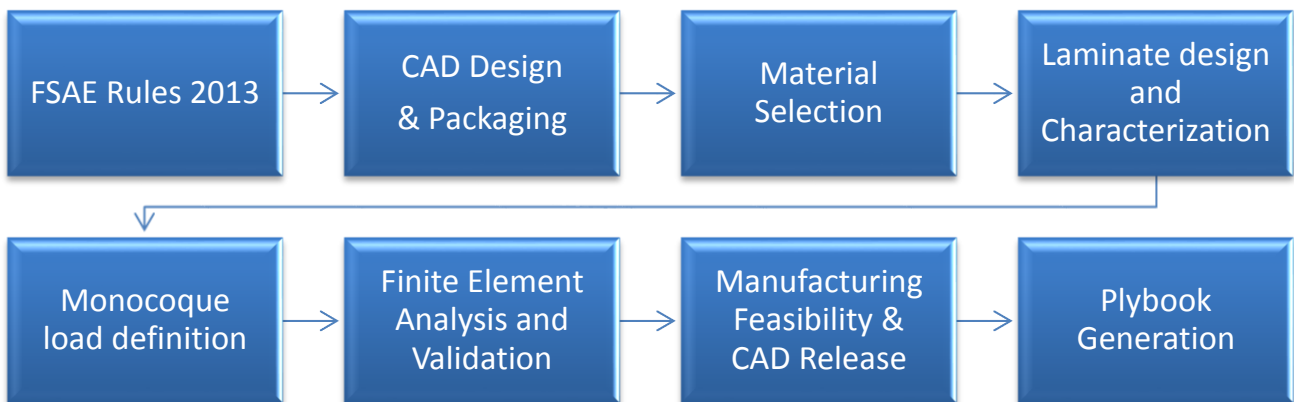
- Compliant with the Formula SAE 2013 Rules
- Torsional stiffness higher or equal than 72404 [N*m/rad]
- Suspension angles variation < 0.1 deg under loads
- Weight less than < 25kg
- Manufacturing time < 1 month

Chapter 4 - Monocoque Design

4.1 - Design Process

There are many compromises in the overall design of a successful race car. It is practically impossible to design something so complicated in a continuous (sequential) way.

The approach followed for the design of the SCR monocoque chassis starts with an overall concept, proceeds to preliminary design, then it is continuously updated through several stages of reviews and refinements and finally is detailed until the required level is reached.



Our starting point is the knowledge of the rules. The successful designer arrives at a realistic interpretation of the various constraints as they are applied in practice. In order to be successful in a competition it is necessary to work in the absolute limits of the constraints.

After that, the first most important specifications are considered: the basic parameter of the vehicle dynamic behavior (decided after several vehicle dynamics simulations confronted with the track tests) such as the tracks and the wheelbase are established (other responses of this specific part as the mass distribution, a target mass, and hypothetic height of the center of gravity have been considered, for the global arrangement and layout of the vehicle itself). The suspension geometry, the pedals encumbrances, the engine and rear box encumbrance with its attachments points were hypothesized.

This make possible to deliver the driving position in order to achieve the best compromise between comfort, visibility and center of gravity height.

4.2 - Vehicle Package

The design and its implementation has the objective to be simple and cpu build. While the use of exotic technologies is common on the motorsport industry, we decided that was far better to be reliable with proven technologies.

The monocoque was designed to fit every component of the racing car, provide a correct driver position and posture satisfying the rules of the competition.

The following images show the final design with every component installed.

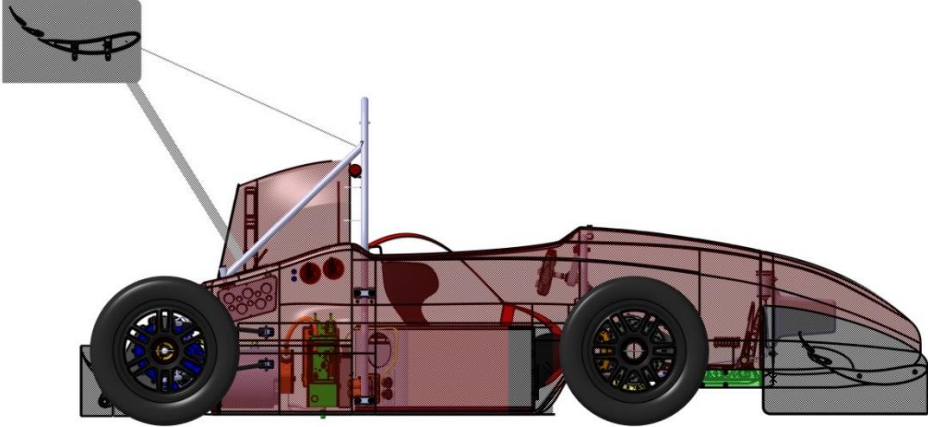


Figure 12 - SCR side view

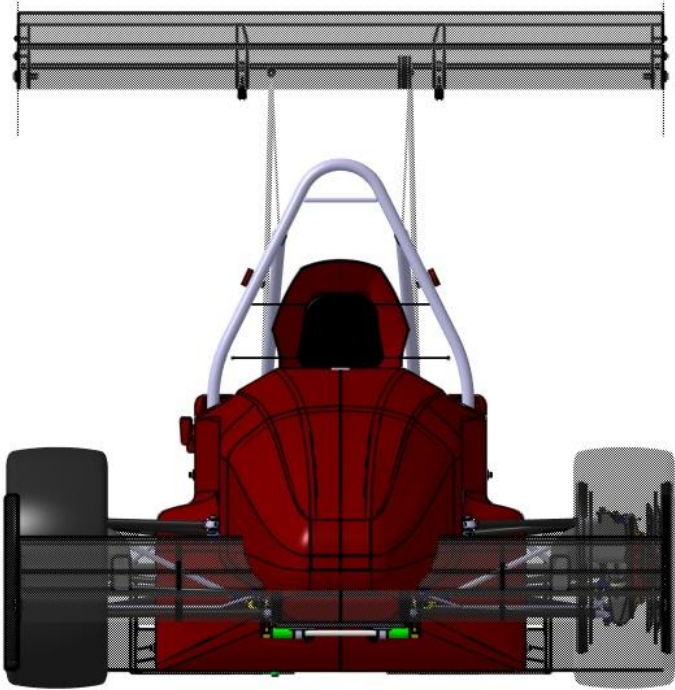


Figure 13- SCR Front view

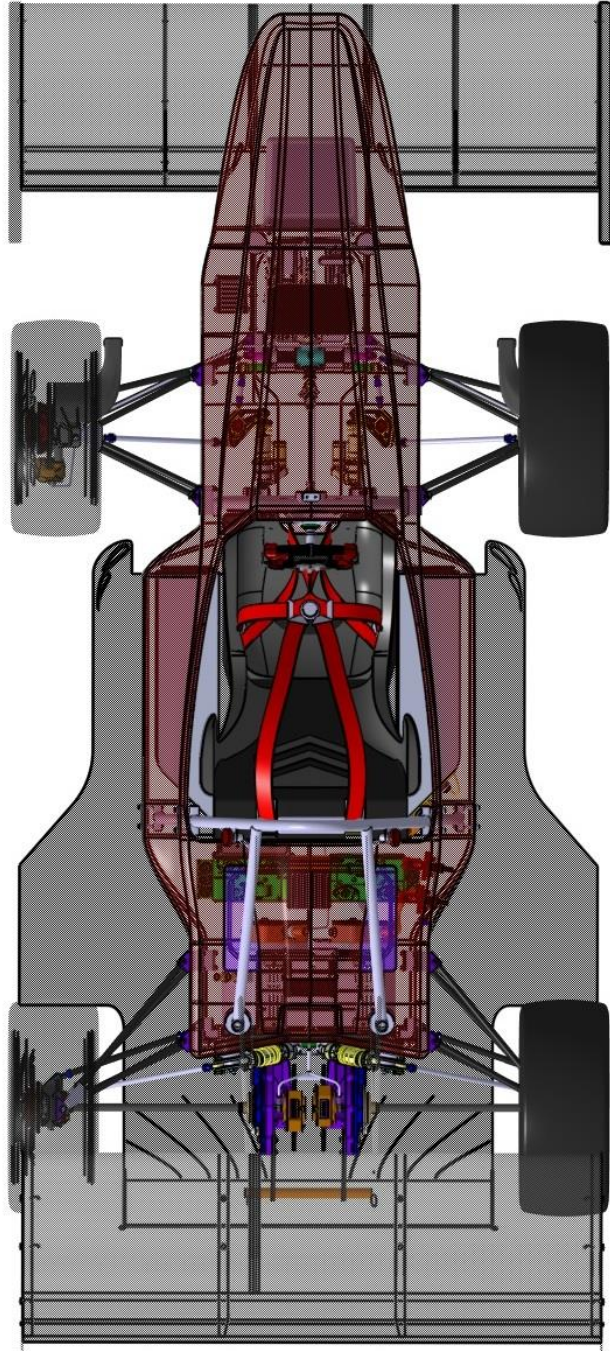


Figure 14- SCR Top view

| Angle | SCX | SCXX | SC12e | SCR |
|------------------|-----|------|-------|-----|
| α | 81 | 85 | 85 | 85 |
| β | 129 | 109 | 120 | 120 |
| γ | 106 | 92 | 100 | 100 |
| δ | 41 | 35 | 38 | 38 |
| τ | 116 | 101 | 105 | 105 |
| Head inclination | 0 | 9 | 0 | 0 |

Table 3 - Comparison between the angles adopted for several SC race cars

These values are referred to a 50 percentile male, which is representative of the size of our drivers.

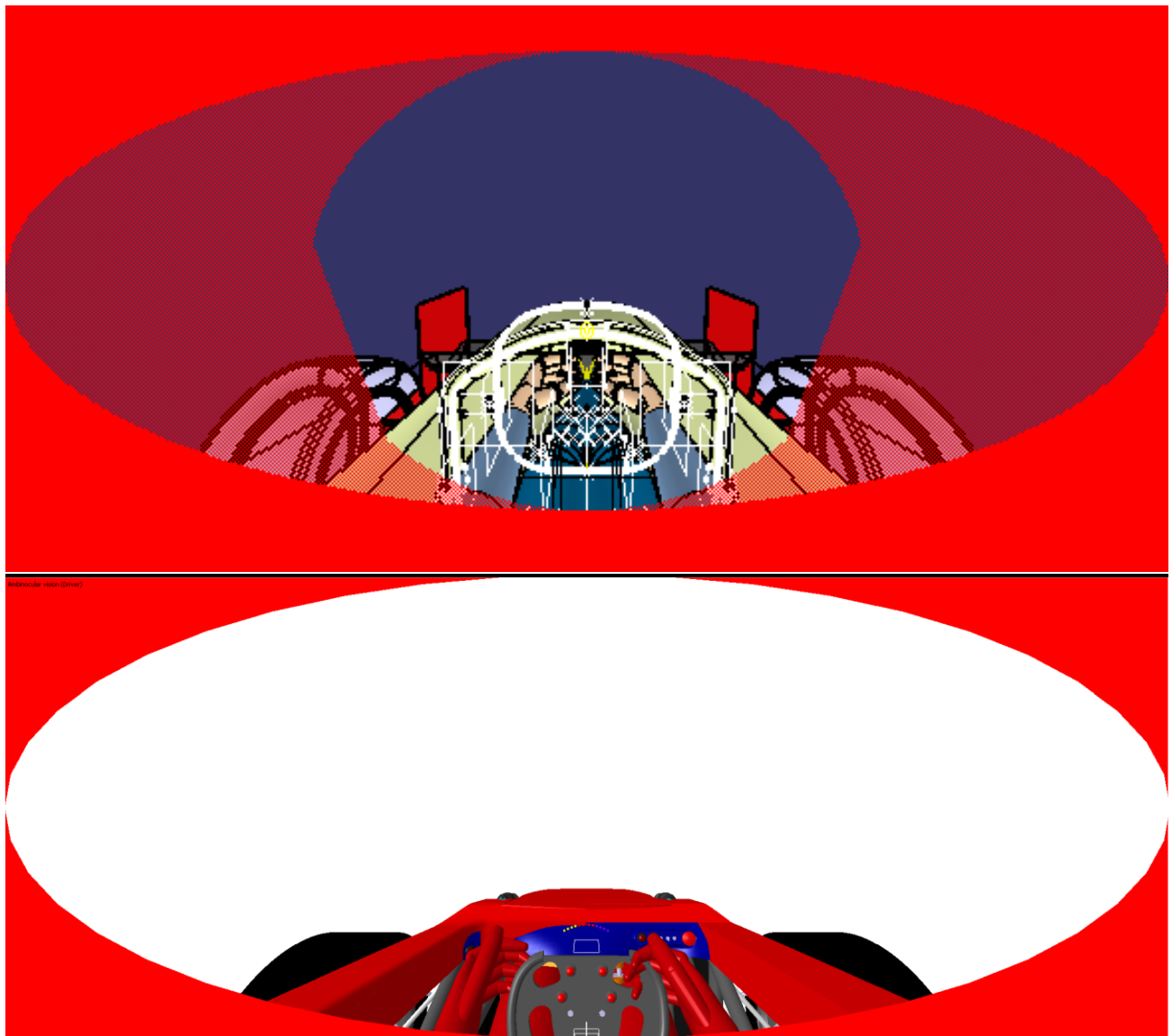


Figure 16 - Viewpoint comparison (up) SCR driving position, (bottom) SCXX driving position

Also the visibility was studied to verify that no component gets in the way of the driver's view and allows him to have a clear view of the track. The SCXX (2011 season) is used as reference which according to the drivers had a nice viewing position. As it can be seen, the fact that the monocoque forms an integral structure the dimensions could be reduced and therefore an increased field of view was obtained

4.4 - Final monocoque CAD Model

After several iterations, the final CAD model was finished, taking into account packaging, ergonomics, accessibility, manufacturability, and its compliance with the articles described at the Formula SAE Rules 2013.

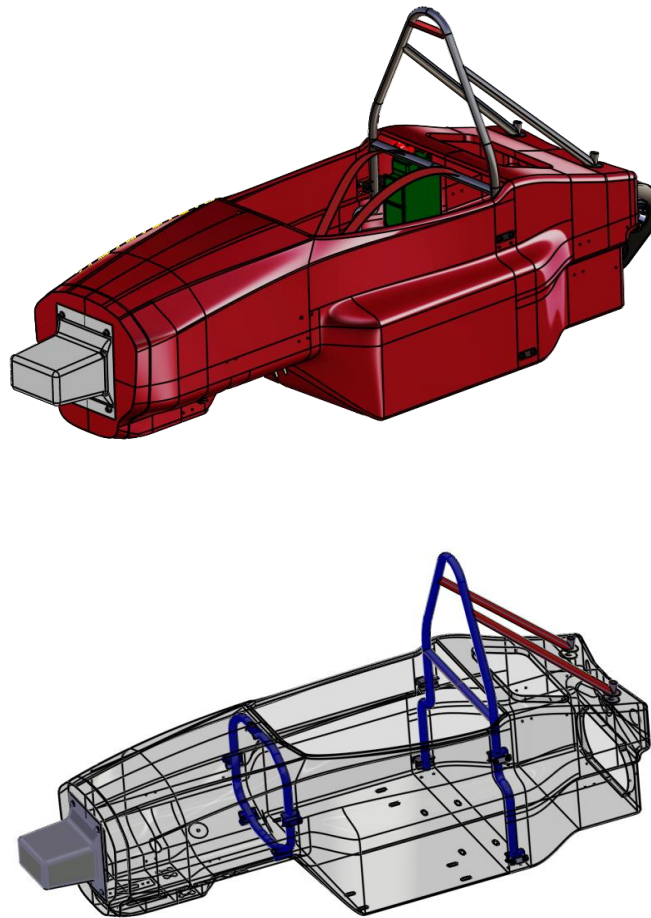


Figure 17 - (Top) Isometric view of the monocoque with its internal components, (Bottom) Transparency view of the monocoque, the steel front and main anti roll bars are present

4.5 – Vehicle Loads

Initially, as most of the components of a vehicle, the monocoque must be validated by a virtual simulations of real case loading. When the main components locations have been defined and the suspension links are frozen, we proceeded to determine the loads that should stress the monocoque in real life scenarios.

Dynamic loads

The external loads that they are applied during the life of the chassis can be divided in the different categories:

1. High longitudinal deceleration
2. High lateral acceleration
3. Combined case

Each case represents the following events: the initial start of the vehicle when the throttle is pressed from a rest position of the car where is a high friction coefficient between wheels and the ground; the second, takes into consideration a pure braking event that occurs in usually on a corner entry, especially after a long straight; and finally, we took into consideration a rapid corner with high load transfer.

It is common practice to consider these loads as static loads, to simplify the simulation, assuming a suspension locked.

On the other hand, another instantaneous load that we could consider in the analysis of the monocoque is the force generated on a frontal crash or lateral crash scenario; but as it will be shown on the following chapters, the monocoque will be able to resist these loads due to the structural constraints defined by the rules.

Fatigue loads will not be considered, due to the fact that a formula student prototype only races about 100km therefore is assumed that there will not be enough cycles to overcome the fatigue limit.

In order to determine the maximum accelerations to which the vehicle will be subjected the workgroup of vehicle dynamics from the team, used VI-GRADE, a multi body dynamics solution package to simulate the track and the different events of the 2012 competition.

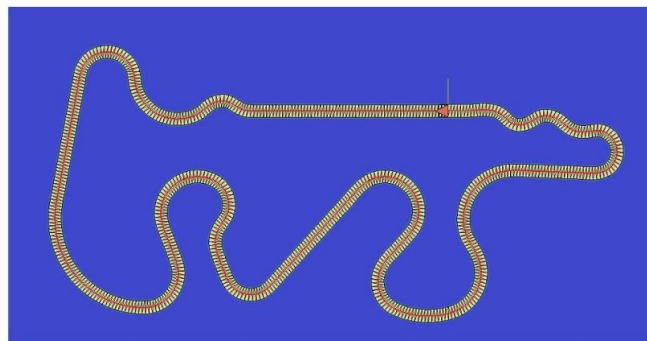


Figure 18 - Gyor Track vi-grade model

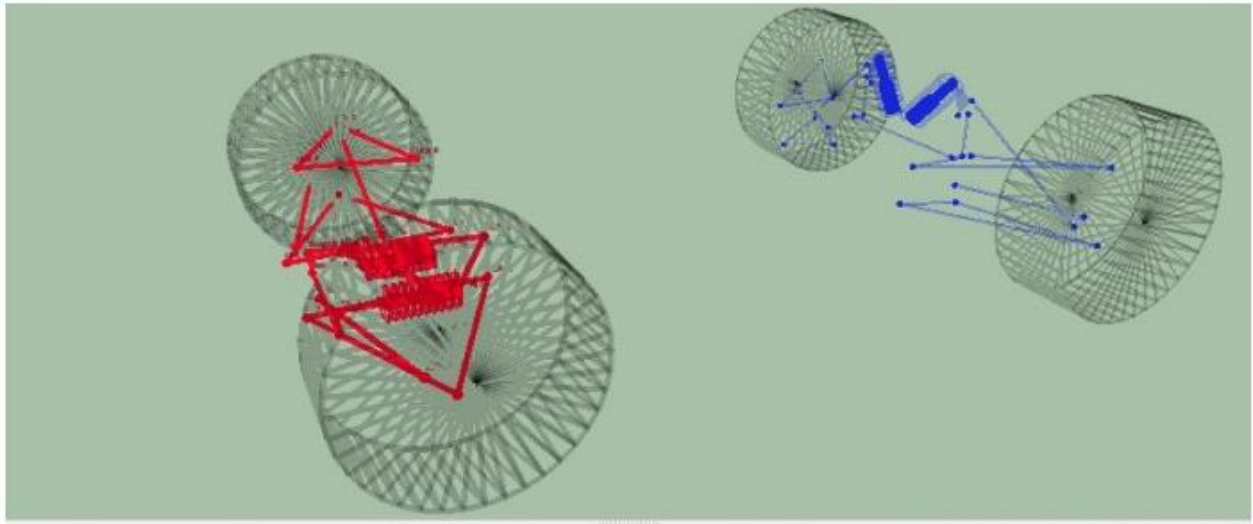


Figure 19 - Front suspension geometry (RED), Rear suspension geometry (Blue)

After several iterations searching for an optimal suspension design, the vehicle dynamic team achieved a desired configuration and provided the loads on each suspension point of the monocoque from the results of a multibody simulation.

Front Suspension Loads

From the Simulation using VI-grade the following forces on the Front suspension joints were obtained.

- a) The maximum lateral force on the tire is 3500N.
- b) The maximum longitudinal force is -3000N.
- c) The maximum combined force is lateral force of 2400N with a longitudinal force of -2000N.

Loadcase A, maximum lateral force applied on the front suspension tire contact patch with the ground

Table 4 - Forces on each front suspension joint at maximum lateral load

| | Fx | Fy | Fz | Fm |
|-------------------------|--------|---------|--------|--------|
| Lower control arm front | -29.4 | -3306 | -23.3 | 3309 |
| Lower control arm rear | -28.8 | -3249.2 | -23.3 | 3256 |
| Upper control arm front | -134.7 | -1467.5 | -37 | 1474 |
| Upper control arm rear | 145.1 | -1638.7 | -37 | 1648 |
| Tierod to rack | 139.2 | -552.8 | 35.3 | 571.3 |
| Tierod to upright | -139 | 553 | -33.9 | 571.3 |
| Rocker to pullrod | -17.6 | -596 | 324.4 | 678.8 |
| Rocker to body | -531.5 | 622 | -314.5 | 877.9 |
| Upright to LCA | -48 | 6560 | 53.6 | 6560.1 |

| | | | | |
|----------------|------|--------|------|--------|
| UCA to upright | 72.3 | 2511.8 | 43.7 | 2514.2 |
|----------------|------|--------|------|--------|

Loadcase B, maximum longitudinal force applied on the front suspension tire contact patch with the ground

Table 5- Forces on each front suspension joint at maximum longitudinal force

| | Fx | Fy | Fz | Fm |
|-------------------------|---------|---------|---------|--------|
| Lower control arm front | -169 | -2738.4 | 1146.1 | 2973.4 |
| Lower control arm rear | -96.1 | 1799.6 | -1181.6 | 2155 |
| Upper control arm front | -1.25 | -8.4 | 9 | 12.3 |
| Upper control arm rear | -2.2 | -45.8 | 9 | 46.7 |
| Tierod to rack | -271.5 | 1041.5 | -37.2 | 1077 |
| Tierod to upright | 271.5 | -1041.5 | 38.5 | 1077 |
| Rocker to pullrod | 7.6 | -501 | 265.1 | 567.2 |
| Rocker to body | -489.7 | 498.2 | -364.3 | 746.9 |
| Upright to LCA | -5048 | -576.5 | -169.9 | 5083.7 |
| UCA to upright | -2319.6 | 437.4 | 355.6 | 2387.1 |

Loadcase C, maximum combined force applied on the front suspension tire contact patch with the ground

Table 6 - Forces on each front suspension joint at maximum combined force

| | Fx | Fy | Fz | Fm |
|-------------------------|---------|---------|---------|--------|
| Lower control arm front | -143.4 | 5356.8 | -1680.8 | 5616.2 |
| Lower control arm rear | 40.5 | -1565.8 | -1679.4 | 2296.5 |
| Upper control arm front | -173.4 | -2801.3 | 773.3 | 2911.3 |
| Upper control arm rear | -2.2 | 259.4 | -789.5 | 830 |
| Tierod to rack | -185 | 718.6 | -27.4 | 742.5 |
| Tierod to upright | 185 | -718.6 | 28.7 | 742.6 |
| Rocker to pullrod | 8.6 | -445 | 235.1 | 503.4 |
| Rocker to body | -472.6 | 424.4 | -239.1 | 678.7 |
| Upright to LCA | -3361.8 | 3791 | -2.7 | 5066.9 |
| UCA to upright | -1562.3 | 2096.9 | 175.2 | 2620.7 |

Rear Suspension Loads

As it was made for the front suspension, from the VI-grade Simulation of the SCR performance the forces on the rear suspension joints were calculated.

- The maximum lateral force on the tire is -3000N.
- The maximum longitudinal force is -2500N.
- The maximum combined force is lateral force of 2000N with longitudinal force of -500N.

Loadcase A, maximum longitudinal force applied on the front suspension tire contact patch with the ground

Table 7- Forces on each rear suspension joint at maximum longitudinal force

| | Fx | Fy | Fz | Fm |
|-------------------------|--------|---------|--------|--------|
| Lower control arm front | -0.4 | -140.7 | -1.3 | 140.7 |
| Lower control arm rear | 63.9 | -5042 | -0.3 | 5042 |
| Upper control arm front | -19.9 | 143.4 | -33 | 148.4 |
| Upper control arm rear | -144.5 | 2427.9 | 23.2 | 2432.4 |
| Tierod to rack | 13.7 | -134.2 | 19.8 | 136.3 |
| Tierod to upright | -13.7 | 134.2 | -18.4 | 136.1 |
| Rocker to pullrod | -48.4 | 254.4 | 212.7 | 335.1 |
| Rocker to body | -369.1 | -255 | -211.4 | 496 |
| Upright to LCA | -13.6 | -5182.7 | -68.9 | 5183.2 |
| UCA to upright | 7.7 | -2316.9 | 343.7 | 2342.3 |

Loadcase B, maximum lateral force applied on the front suspension tire contact patch with the ground

Table 8 - Forces on each rear suspension joint at maximum lateral force

| | Fx | Fy | Fz | Fm |
|-------------------------|---------|---------|---------|--------|
| Lower control arm front | -47.4 | 5315.9 | -2274.6 | 5782.3 |
| Lower control arm rear | 45 | -5377 | -2269.9 | 5836.7 |
| Upper control arm front | -272.6 | -2056.4 | 940.8 | 2277.8 |
| Upper control arm rear | -108.8 | 2330 | -977.3 | 2529.1 |
| Tierod to rack | -6 | 54.4 | -6.4 | 55.1 |
| Tierod to upright | 6 | -54.4 | 7.8 | 55.3 |
| Rocker to pullrod | -49.9 | 272.8 | -227 | 359.3 |
| Rocker to body | -398.5 | -273 | -211.4 | 533.8 |
| Upright to LCA | -4461.5 | -61.1 | 857.5 | 4543.7 |
| UCA to upright | -1967.5 | -0.8 | 68 | 1968.7 |

Loadcase C, maximum combined force applied on the front suspension tire contact patch with the ground

Table 9 - Forces on each rear suspension joint at maximum combined forces

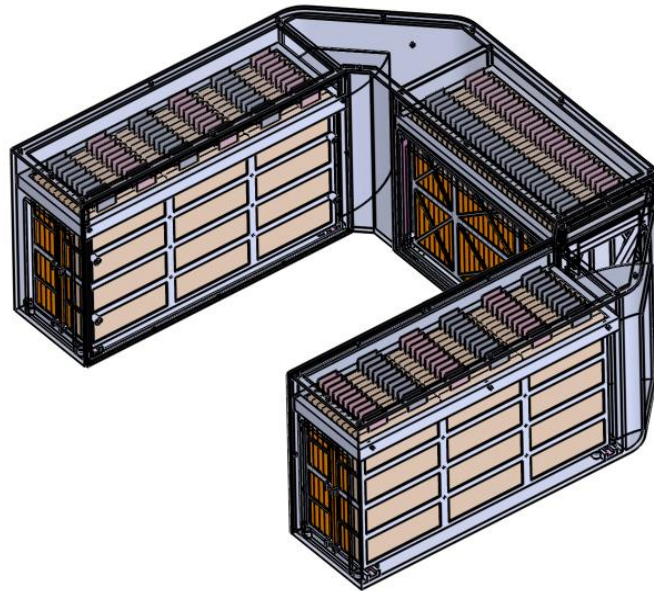
| | Fx | Fy | Fz | Fm |
|-------------------------|--------|--------|--------|--------|
| Lower control arm front | -18.9 | 1191.4 | -457.7 | 1276.5 |
| Lower control arm rear | -34.9 | 2340.3 | -457.7 | 2384.9 |
| Upper control arm front | -111.5 | -365.7 | 161.6 | 415.1 |
| Upper control arm rear | 260.3 | -833.4 | -162.1 | 888 |
| Tierod to rack | 1.9 | -18.3 | 3.4 | 18.7 |
| Tierod to upright | -1.9 | -18.3 | -2 | 18.5 |

| | | | | |
|-------------------|--------|--------|--------|---------|
| Rocker to pullrod | -62.3 | 314.7 | 266.1 | 416.8 |
| Rocker to body | -457.6 | -314.7 | -264.8 | 615.3 |
| Upright to LCA | -888.6 | 3531.8 | 219.6 | 3648.5 |
| UCA to upright | -385.4 | 1513.7 | -100 | 11565.2 |

As it will be seen on the following chapters, the loads presented on the previous tables will be used for the calculation of the suspension attachments inserts of the monocoque, for the overall structure analysis only the tire forces will be applied on finite element model with its suspension components modeled in place to avoid imputing a huge amount of force vectors that will make the job hard to check and debug.

Battery Pack Loads

The battery accumulator attachments on the vehicle must withstand a 20g longitudinal and deceleration, and a 10g deceleration on every other direction to comply with the EV3.4.2 rule.



The Battery accumulator of the SCR consists of 3 internal modules of 33 batteries connected together forming a unique container. Every module has been designed in order to comply with the FSAE Rules 2013.

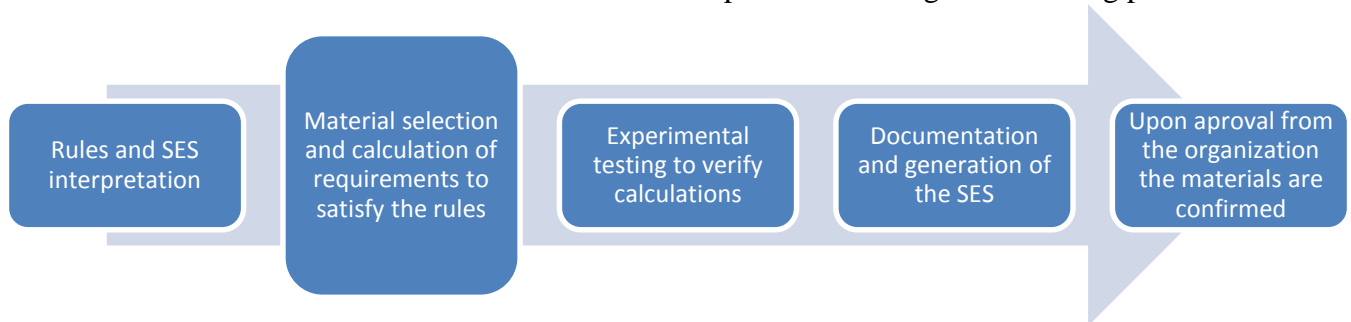
Every internal module has an approximated weight of 24kg, with a total weight of about 72.57kg. Assuming that the Accumulator it's a rigid structure, the forces applied to the monocoque trough the attached points are:

| | |
|-----------------------|-----------|
| Accumulator Mass (kg) | 72,57 |
| Horizontal Force (N) | 14238,234 |
| Vertical Force (N) | 7119,117 |

Table 10 - Forces derivated by the inertia of the battery pack.

4.6 - Process followed to define the monocoque materials and safety zones

Once the main loads due dynamic events applied to the monocoque where defined we can proceed to the evaluation of the materials that will be used to its production using the following process.



4.7 – Material Selection

The formula SAE Rules are designed for a classic chassis made entirely of steel tubes, therefore any deviation from these materials a proven Safety equivalence Spreadsheet that demonstrates the equivalence by calculations which data it's derived from tested materials. This implies that even if another technology can be implemented extra effort should be made to proof that the design of the chassis will have the minimum structural requirements stated by the rules.

As stated on the objectives for the monocoque design, a higher stiffness to weight ratio than the steel chassis should be achieved, therefore the research team of squadracorse politico started screening with several manufacturers datasheet to select the best performing materials and then depending on cost and availability the selection would be made.

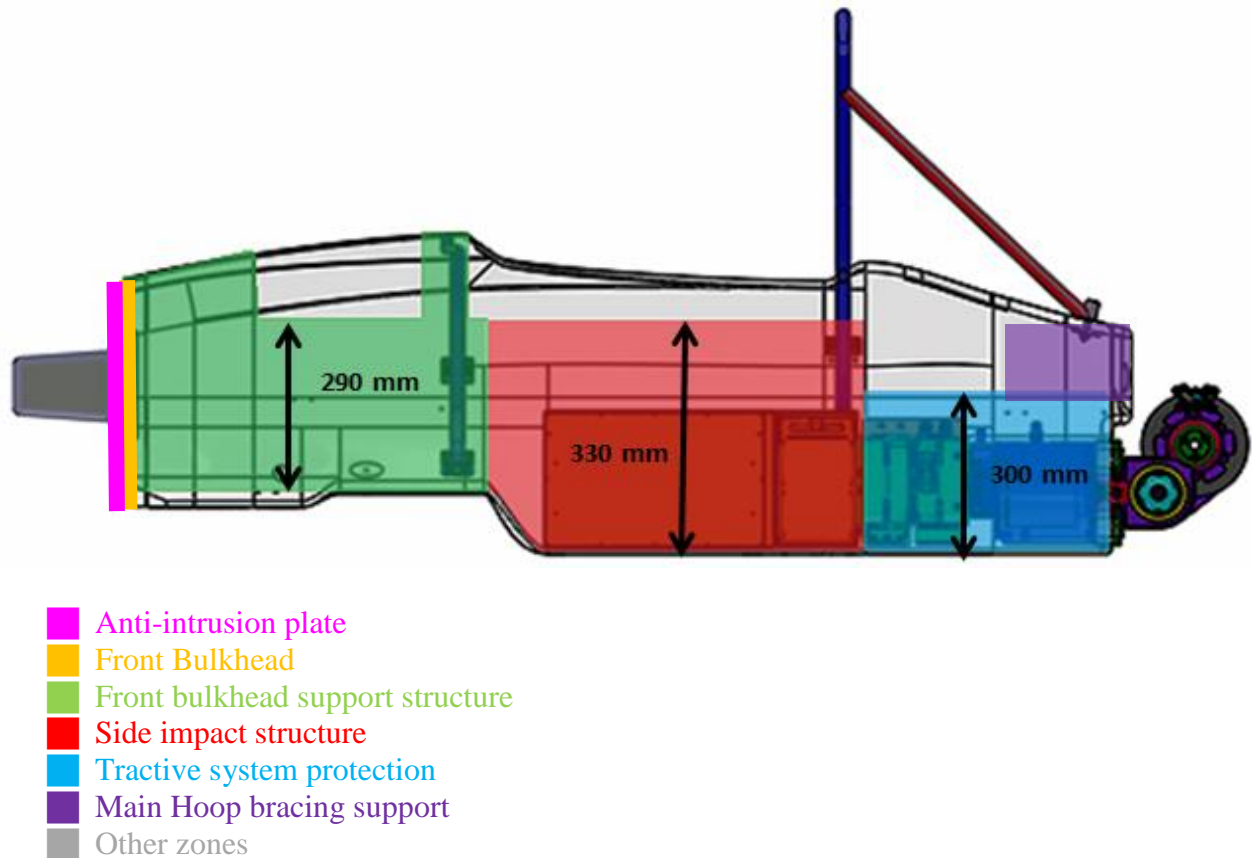
The safety equivalence that we stated before is basically an equivalence calculation between the bending properties of a tubular steel structure and a composite panel of our design. Therefore the “Bending characteristics” are critical to be able to have a structure that is safe, on the other hand, if we imagine the monocoque made of several composite panels the bending characteristics of these panels will affect the overall stiffness and the final weight.

From the theory, assuming that we have a tube made of a laminate using a twill pre-preg carbon fiber ply, the best torsional stiffness and torsional strength that can be achieved is when the fibers are oriented to [45/-45] degrees from the tube axis. But on the other hand, the bending stiffness and strength this will be at its minimum. Therefore, if our objective is to maximize torsional stiffness and have a minimum bending strength and stiffness a combination of both angle configurations should give the optimal layup.

4.8 - Safety zones defined by the rules

The Formula SAE Rules link the design of several areas of the monocoque to the safety equivalence spreadsheet and therefore to the results of the experimental testing, the other zones are not relevant for the safety and therefore are left for the designer to design and optimize. The

following figure show what are the relevant zones stated by the rules that are critical for the safety of the driver.



Summary of the chassis baseline requirements defined by the Formula SAE 2013 Rules

The following table summarizes the mechanical characteristics of the monocoque that should be achieved to comply with the regulations.

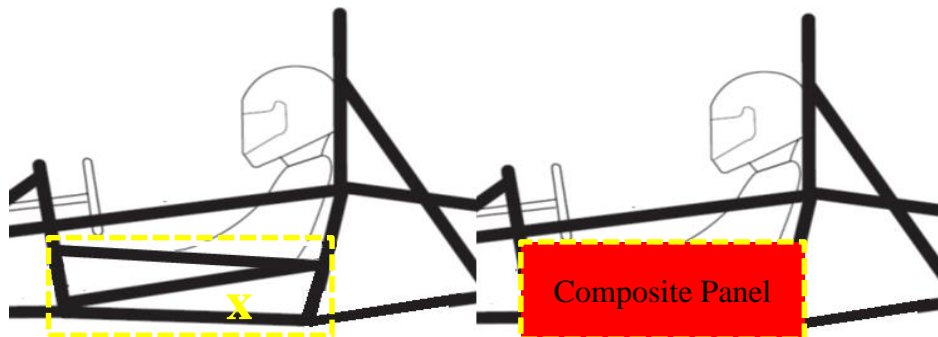
| | Front bulkhead | Front Bulkhead support | Side impact structure | Accumulator protection | Main Hoop bracing Support |
|----------------------------|----------------|------------------------|-----------------------|------------------------|---------------------------|
| Material Property | Baseline | Baseline | Baseline | Baseline | Baseline |
| Material type | Steel | Steel | Steel | Steel | Steel |
| Tubing Type | Round | Round | Round | Round | Round |
| Material name /grade | Steel | Steel | Steel | Steel | Steel |
| Youngs Modulus, E | 2,00E+11 | 2,00E+11 | 2,00E+11 | 2,00E+11 | 2,00E+11 |
| Yield strength, Pa | 3,05E+08 | 3,05E+08 | 3,05E+08 | 3,05E+08 | 3,05E+08 |
| UTS, Pa | 3,65E+08 | 3,65E+08 | 3,65E+08 | 3,65E+08 | 3,65E+08 |
| Yield strength, welded, Pa | 1,80E+08 | 1,80E+08 | 1,80E+08 | 1,80E+08 | 1,80E+08 |

| | | | | | |
|------------------------------------------------------|----------|----------|----------|----------|----------|
| UTS welded, Pa | 3,00E+08 | 3,00E+08 | 3,00E+08 | 3,00E+08 | 3,00E+08 |
| Geometrical Properties | | | | | |
| Number of tubes | 2,00E+00 | 3,00E+00 | 3,00E+00 | 3,00E+00 | 2,00E+00 |
| Tube OD, mm | 2,54E+01 | 2,54E+01 | 2,54E+01 | 2,54E+01 | 2,50E+01 |
| Wall, mm | 1,60E+00 | 1,25E+00 | 1,60E+00 | 1,60E+00 | 1,50E+00 |
| Panel height,mm | 6,90E+01 | 2,90E+02 | 3,30E+02 | 3,30E+02 | 3,30E+02 |
| I, m^4 | 8,51E-09 | 6,93E-09 | 8,51E-09 | 8,51E-09 | 7,68E-09 |
| Mechanical Properties | | | | | |
| EI | 3,40E+03 | 4,16E+03 | 5,11E+03 | 5,11E+03 | 3,07E+03 |
| Area, mm^2 | 2,39E+02 | 2,85E+02 | 3,59E+02 | 3,59E+02 | 2,21E+02 |
| Yield tensile strength, N | 7,30E+04 | 8,68E+04 | 1,09E+05 | 1,09E+05 | 6,76E+04 |
| UTS, N | 8,73E+04 | 1,04E+05 | 1,31E+05 | 1,31E+05 | 8,08E+04 |
| Yield tensile strength, N as welded | 4,31E+04 | 5,12E+04 | 6,46E+04 | 6,46E+04 | 3,99E+04 |
| UTS, N as welded | 7,18E+04 | 8,54E+04 | 1,08E+05 | 1,08E+05 | 6,64E+04 |
| Max load at mid span to give UTS for 1m long tube, N | 1,96E+03 | 2,39E+03 | 2,93E+03 | 2,93E+03 | 1,79E+03 |
| Max deflection at baseline load for 1m long tube, m | 1,20E-02 | 1,20E-02 | 1,20E-02 | 1,20E-02 | 1,22E-02 |
| Energy absorbed up to UTS, J | 1,17E+01 | 1,43E+01 | 1,76E+01 | 1,76E+01 | 1,09E+01 |

Table 11 - Summary of the chassis baseline requirements defined by the Formula SAE 2013 Rules

4.9 - Composite Sandwich Equivalence

Each safety zone of the monocoque should be equivalent to their steel tubular structure as stated on the rules. The following calculations should be made and presented to the Judges. The following figure illustrates the tubes that protect the driver in case of a side impact, consisting of 3 tubes that go from the front roll hoop to the main roll hoop. At the right side, an “equivalent” composite flat panel substitutes the 3 tubes defined by the rules and its equivalency should be proven by calculations using experimental data of the materials that will be used to build it.



Z *Figure 20 - (left) tubes of the Side impact zone of a baseline chassis, (right) equivalent composite panel*

In order to prove the equivalence the following mechanical properties of the structure should be provided and it should be higher or equal than the properties of the baseline structure.

Mechanical Properties that should be derived from experimental testing for a Composite sandwich panel by means of a 3-Point bending test and a Perimeter Shear test.



Figure 21 - (left) 3 Point Bending Test, (Right) Perimeter Shear Test

| 3-Point bending | Perimeter shear test |
|-----------------------------------------------------------------------------|-----------------------------------------|
| Gradient of the force vs displacement the Linear elastic region (stiffness) | Maximum shearing force at panel failure |
| Maximum force at panel failure | Shear Stress of the skins |
| Skin Modulus of Elasticity [Ex] | |
| Skin Yield Strength [Sy] | |
| Skin Ultimate Tensile Strength [UTS _{skin}] | |

Figure 22- Mechanical properties of a composite sandwich panel that should be derived from experimental testing

Using the derived data, for each safety zone the following properties should be calculated to determine its equivalence. Assuming that we test a panel that has, length “l”, Height “h”, width “w”, Total thickness “tt”, Skin thickness “ts” and “core thickness “c”.

| Property |
|---------------------------------------------------|
| I, Second Moment of Area |
| Buckling Modulus |
| Yield tensile Force |
| UTS, Ultimate Tensile Force |
| Max load at mid span to give UTS for 1m long tube |
| Max deflection at baseline load for 1m long tube |
| Energy absorbed up to UTS |

Table 23 - Calculations that should be done to proof the equivalence

Selection of the skins of the composite sandwich

As said on the introduction chapters, the team found a sponsor for the manufacturing of the composite monocoque. The company “ERRE Ti” provided a list of materials available from his suppliers in order to select the best materials that can be obtained in a reasonable time.

Once the list was obtained, the main properties liked to stiffness, strength and weight were organized and normalized to a fiber content of 45% (and a Resin content of 55%). The ratios between the Elastic Moduli and strength with respect the weight of a ply with 1m² of area were calculated and normalized to compare and determine the materials that will give the highest performance.

The score is calculated as:

$$Score = \frac{\frac{0.5(E_x + E_y)}{Weight} + \frac{G_{xy}}{Weight} + \frac{0.5(\sigma_x + \sigma_y)}{Weight}}{MaxScore}$$

| |
|---------------------------------|
| Normalized to Vf% fiber content |
| 45% |

| Cabon fiber reinforced epoxy matrix ply | E _x [Gpa] | E _y [Gpa] | G _{xy} [Gpa] | sig _{xt} [Mpa] | sig _{yt} [Mpa] | Rho [kg/m ³] | t [m] | Weight 1m ² [kg] | E/W | G/W | sig/W | Score |
|---------------------------------------------------|----------------------|----------------------|-----------------------|-------------------------|-------------------------|--------------------------|-------|-----------------------------|-------|------|--------|-------|
| HexPly M18/1 Woven G939 | 53,3 | 53,3 | 4,6 | 655,1 | 655,1 | 1472,0 | 0,2 | 0,3 | 164,6 | 14,3 | 2022,9 | 0,99 |
| Hexply 49 200T2x2 CHS-3k | 49,6 | 49,6 | 4,6 | 702,8 | 702,8 | 1363,6 | 0,2 | 0,3 | 154,0 | 14,1 | 2184,0 | 0,96 |
| HexPly F593 Woven T300 (W3G282) nominal | 49,6 | 49,6 | 4,8 | 585,2 | 585,2 | 1462,9 | 0,2 | 0,3 | 151,5 | 14,8 | 1787,5 | 0,93 |
| HexPly 8552 Woven AS4 (AGP280-5H) nominal | 54,1 | 54,1 | 4,6 | 655,1 | 655,1 | 1523,3 | 0,3 | 0,4 | 123,0 | 10,5 | 1488,0 | 0,73 |
| HexPly M21 Woven AS4C T2 | 51,9 | 51,9 | 4,0 | 714,3 | 714,3 | 1505,0 | 0,3 | 0,4 | 121,0 | 9,3 | 1665,3 | 0,73 |
| HexPly M56 AS4C Woven 2x2T | 56,6 | 56,6 | 3,6 | 708,6 | 708,6 | 1472,0 | 0,3 | 0,5 | 121,6 | 7,8 | 1523,4 | 0,67 |
| HexPly 8552 Woven IM7 (SPG370-8H) nominal | 68,9 | 68,9 | 4,6 | 785,2 | 785,2 | 1511,1 | 0,4 | 0,6 | 119,9 | 8,1 | 1367,4 | 0,65 |
| HexPly 922-1 Woven G926 nominal | 50,6 | 50,6 | 5,0 | 539,3 | 539,3 | 1496,8 | 0,3 | 0,5 | 97,6 | 9,5 | 1040,1 | 0,58 |
| HexPly M26 Woven G1070 | 52,5 | 52,5 | 4,6 | 646,9 | 646,9 | 1497,7 | 0,4 | 0,6 | 91,8 | 8,1 | 1130,7 | 0,55 |
| HexPly F593 Woven T300 (F3T584) nominal | 49,7 | 49,7 | 4,8 | 517,3 | 517,3 | 1462,9 | 0,4 | 0,6 | 79,1 | 7,7 | 824,2 | 0,47 |
| Cycom 977-20 RTM PRIFORM 24K IMS WNCF 550 nominal | 64,5 | 64,5 | 4,5 | 788,3 | 788,3 | 1538,0 | 0,5 | 0,8 | 82,3 | 5,7 | 1006,3 | 0,46 |
| Cycom 5276-1 Woven G30-500PW | 49,6 | 49,6 | 4,2 | 671,5 | 671,5 | 1475,7 | 0,5 | 0,8 | 65,1 | 5,5 | 881,0 | 0,40 |

Table 12 - CFRP ply available at “ERRETI composite” and its performance score

After organizing the materials by its performance score, Erreti compositi contacted its suppliers and the material with the highest score that could be obtained on a 1 month from its order was the

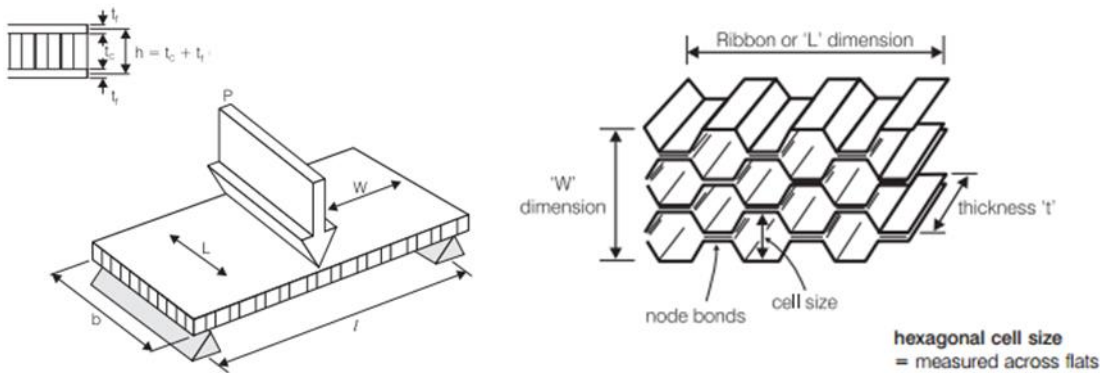
Hexply M49 200T2x2 CHS-3k therefore we selected it as the design material and proceeded with the material characterization required by the rules.

This material is a woven pre-preg with CHS-3K High Strength carbon fibers with the m49 epoxy matrix, is sold at 42% of resin content by weight and manufactured by Hexcel.

Selection of the honeycomb core of the composite sandwich

In order to define the core that will be used to produce the sandwich laminates we did the following considerations: the outer skins of the sandwich will be of CFRP Hexply M49 200T2x2 CHS-3k as it was established before. The dimensioning will be made with the classical beam theory formulae [6] where the stiffness and strength of the panel will be calculated and compared with the requirements reported on table 4.

Considering a panel under a 3-point bending load test simply supported



Panel geometry

| | |
|--------|------|
| b [mm] | 330 |
| l [mm] | 1000 |
| h [mm] | 24.4 |

Skin Data

| Facing skins | Hexply m49 200T2x2 | |
|--------------|--------------------|-----|
| t1 | 1.2 | mm |
| t2 | 1.2 | mm |
| Sig_xt | 700 | Mpa |
| Ex | 49,6 | Gpa |
| v12 | 0,05 | |

The mechanical properties used to define the core where those of the side impact zone, this zone should have the highest strength and stiffness, therefore, it will be used to determine the feasibility of each core.

The most important baseline requirements of the side impact zone are:

| | | |
|-----------------------|------|--------|
| EI | 5110 | Pa*m^4 |
| Max Deflection for 1m | 12 | mm |
| Max load for 1m tube | 2930 | N |
| Energy absorbed | 17,6 | J |

The following core and list data where provided by our supplier to evaluation

| Designation | Cell size | wall thickness [mm] | Density | L direction | | W direction | | Compression | |
|-------------|-----------|---------------------|----------------------|-------------|-----------|-------------|-----------|-------------|----------|
| | | | [kg/m ³] | Sig_L [Mpa] | G_l [Mpa] | Sig_w [Mpa] | G_w [Mpa] | Sig_z [Mpa] | Ez [Mpa] |
| 5052 | 3/16 | 0,01778 | 32 | 0,75845 | 551,6 | 0,4137 | 317,17 | 1,03425 | 234,43 |
| 5052 | 1/8 | 0,01778 | 49,6 | 1,44795 | 310,275 | 0,89635 | 151,69 | 1,86165 | 517,125 |
| 5052 | 3/16 | 0,0254 | 49,6 | 1,44795 | 310,275 | 0,861875 | 151,69 | 1,86165 | 517,125 |
| 5056 | 3/16 | 0,0254 | 49,6 | 1,827175 | 310,275 | 1,03425 | 137,9 | 2,6201 | 668,815 |
| 5052 | 1/4 | 0,0254 | 36,8 | 0,9653 | 220,64 | 0,586075 | 110,32 | 1,206625 | 310,275 |
| 3003 | 1/4 | 0,0508 | 67,2 | 2,102975 | 393,015 | 1,22731 | 193,06 | 3,0338 | 758,45 |
| 3003 | 3/8 | 0,0508 | 43,2 | 1,137675 | 241,325 | 0,75845 | 117,215 | 1,5169 | 399,91 |
| 3003 | 1/4 | 0,0762 | 83,2 | 2,378775 | 434,385 | 1,482425 | 213,745 | 4,20595 | 1020,46 |
| 3003 | 3/8 | 0,0762 | 57,6 | 1,379 | 275,8 | 0,89635 | 137,9 | 2,240875 | 634,34 |
| 3003 | 1/2 | 0,0762 | 38,4 | 0,861875 | 172,375 | 0,48265 | 103,425 | 1,137675 | 275,8 |
| 3003 | 3/4 | 0,0762 | 28,8 | 0,586075 | 110,32 | 0,379225 | 55,16 | 0,75845 | 165,48 |
| 3003 | 2/3 | 0,0762 | 33,6 | 0,655025 | 124,11 | 0,4137 | 68,95 | 0,861875 | 193,06 |

Table 13- Hexcel Aluminum Honeycomb Core available from our supplier

The calculations for each core was performed and the deflection, strength and stiffness where compared with the baseline requirements.

| Designation | Cell size | wall thickness [mm] | Bending Stiffness | Shear Stiffness | Max Force before skin failure | Max force before Core failure | Force considered deflection calculation | Total Deflection | Panel Stiffness | Energy | EI |
|-------------|-----------|---------------------|---------------------|-----------------|-------------------------------|-------------------------------|-----------------------------------------|------------------|-----------------|--------|----------------------|
| | | | [N*m ²] | [N] | [N] | [N] | [N] | [m] | [N/mm] | [J] | [Pa*m ⁴] |
| 5052 | 3/16 | 0,01778 | 5846,9 | 2553852,8 | 24393,6 | 12214,1 | 2930,0 | 0,0 | 273,1 | 31,4 | 5290,7 |
| 5052 | 1/8 | 0,01778 | 5846,9 | 1221407,9 | 24393,6 | 23317,8 | 2930,0 | 0,0 | 265,4 | 32,3 | 5290,7 |
| 5052 | 3/16 | 0,0254 | 5846,9 | 1221407,9 | 24393,6 | 23317,8 | 2930,0 | 0,0 | 265,4 | 32,3 | 5290,7 |
| 5056 | 3/16 | 0,0254 | 5846,9 | 1110370,8 | 24393,6 | 29424,8 | 2930,0 | 0,0 | 264,0 | 32,5 | 5290,7 |
| 5052 | 1/4 | 0,0254 | 5846,9 | 888296,6 | 24393,6 | 15545,2 | 2930,0 | 0,0 | 260,1 | 33,0 | 5290,7 |
| 3003 | 1/4 | 0,0508 | 5846,9 | 1554519,1 | 24393,6 | 33866,3 | 2930,0 | 0,0 | 268,5 | 32,0 | 5290,7 |
| 3003 | 3/8 | 0,0508 | 5846,9 | 943815,2 | 24393,6 | 18321,1 | 2930,0 | 0,0 | 261,2 | 32,9 | 5290,7 |
| 3003 | 1/4 | 0,0762 | 5846,9 | 1721074,7 | 24393,6 | 38307,8 | 2930,0 | 0,0 | 269,7 | 31,8 | 5290,7 |
| 3003 | 3/8 | 0,0762 | 5846,9 | 1110370,8 | 24393,6 | 22207,4 | 2930,0 | 0,0 | 264,0 | 32,5 | 5290,7 |
| 3003 | 1/2 | 0,0762 | 5846,9 | 832778,1 | 24393,6 | 13879,6 | 2930,0 | 0,0 | 258,8 | 33,2 | 5290,7 |
| 3003 | 3/4 | 0,0762 | 5846,9 | 444148,3 | 24393,6 | 9438,2 | 2930,0 | 0,0 | 242,4 | 35,4 | 5290,7 |
| 3003 | 2/3 | 0,0762 | 5846,9 | 555185,4 | 24393,6 | 10548,5 | 2930,0 | 0,0 | 249,2 | 34,5 | 5290,7 |

Compliance with the baseline requirements for each honeycomb core, assuming a core of 22mm due to packaging constraints.

| Designation | Cell size | wall thickness [mm] | Deflection ratio | Max Load ratio | Energy ratio | EI ratio | Min ratio > 1 | Core Weight [kg] |
|-------------|-----------|---------------------|------------------|----------------|--------------|----------|---------------|------------------|
| 5052 | 3/16 | 0,0178 | 1,12 | 4,17 | 1,79 | 1,04 | 1,035 | 0,232 |
| 5052 | 1/8 | 0,0178 | 1,09 | 7,96 | 1,84 | 1,04 | 1,035 | 0,360 |
| 5052 | 3/16 | 0,0254 | 1,09 | 7,96 | 1,84 | 1,04 | 1,035 | 0,360 |
| 5056 | 3/16 | 0,0254 | 1,08 | 8,33 | 1,85 | 1,04 | 1,035 | 0,360 |
| 5052 | 1/4 | 0,0254 | 1,07 | 5,31 | 1,88 | 1,04 | 1,035 | 0,267 |
| 3003 | 1/4 | 0,0508 | 1,10 | 8,33 | 1,82 | 1,04 | 1,035 | 0,488 |
| 3003 | 3/8 | 0,0508 | 1,07 | 6,25 | 1,87 | 1,04 | 1,035 | 0,314 |
| 3003 | 1/4 | 0,0762 | 1,10 | 8,33 | 1,81 | 1,04 | 1,035 | 0,604 |
| 3003 | 3/8 | 0,0762 | 1,08 | 7,58 | 1,85 | 1,04 | 1,035 | 0,418 |
| 3003 | 1/2 | 0,0762 | 1,06 | 4,74 | 1,88 | 1,04 | 1,035 | 0,279 |
| 3003 | 3/4 | 0,0762 | 0,99 | 3,22 | 2,01 | 1,04 | 0,993 | Failed |
| 3003 | 2/3 | 0,0762 | 1,02 | 3,60 | 1,96 | 1,04 | 1,020 | 0,244 |

The previous table reports the calculated value of the designed laminate property with respect the baseline requirements, almost all the core types can be used. Only one core type failed due to insufficient shear stiffness. Therefore, the selection between the feasible core was determined by the one that has the minimum weight. The hexweb 5052 3/16 0.0178 aluminum honeycomb was selected as core material for the monocoque.

4.10 – CFRP skins and Core details

Based on the previous tables, from the materials available from our suppliers the materials selected for the monocoque manufacturing where the following:

- **Hexply M49 200T2x2 CHS-3k**, this material used as skins for the sandwich is a woven pre-preg with CHS-3K High Strength carbon fibers with the m49 epoxy matrix, is sold at 42% of resin content by weight and manufactured by Hexcel. A material considered by Dallara as top quality.
- **The hexweb 5052 3/16 0.0178** aluminum honeycomb was selected as core material for the monocoque, also from Hexcel, features 3/16 in cell sizes, and wall thicknesses of 0.0178 mm, with in order to comply with the calculations should be used with a minimum height of 22mm.
- **Redux 312 Adhesive film**. An epoxy adhesive film was suggested by our supplier, being the most performing available to bond carbon with the honeycomb core.

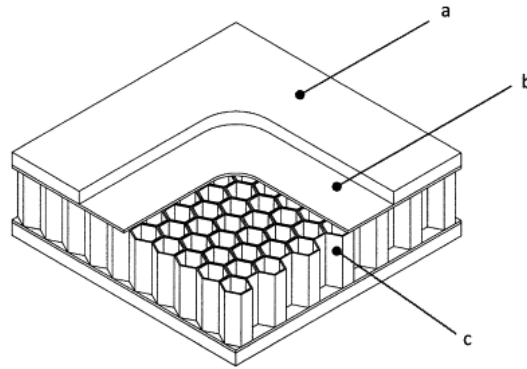


Figure 24 - Skin CFRP plyes (a), Adhesive Layer (b), Aluminium Honeycomb core (c)

After the materials were selected an experimental characterization was performed, here we will present the results of these tests and the different layouts but more detail can be found on the thesis project “Analisi Strutturale di un Telaio in Materiale Sandwich di Una Vettura da Competizione Formula SAE” written by Marco Cairola [7].

3 point bending tests were performed at different layouts to verify the calculations made before

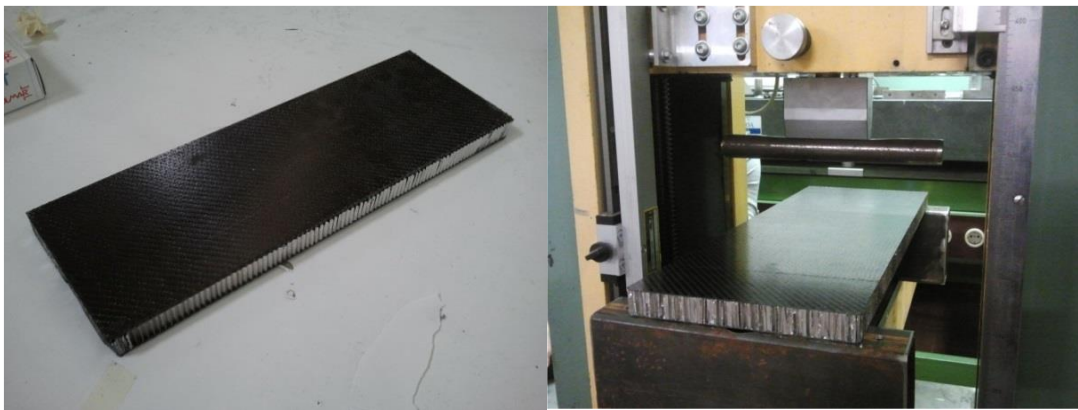
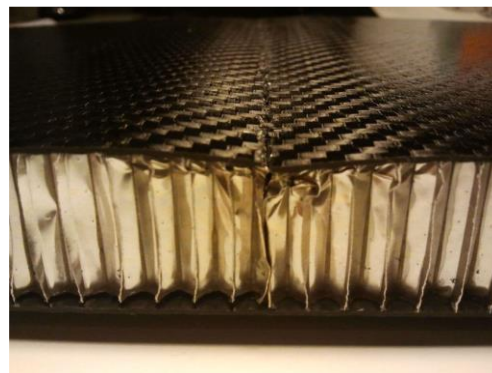
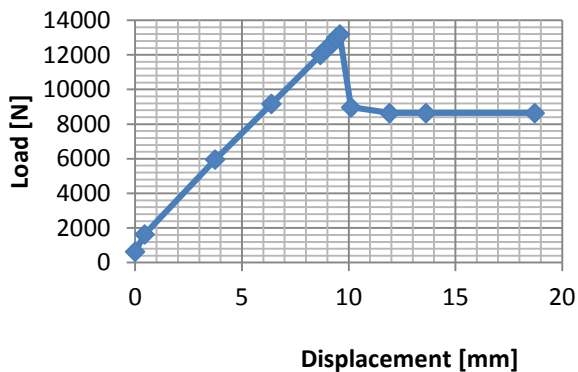


Figure 25 - 3 Point bending test for the Side impact zone laminate

Obtaining the following Force vs displacement curve



By using the beam theory, the inverse process used to define the materials was implemented to derive the Elastic moduli of the skins performing calculations on the elastic region of the graph and the maximum skin stressed where determined by the peak at which the sandwich failure was

achieved. It must be noticed that the sandwich failed by core failure, therefore the actual yielding stress for the plies cannot be correctly defined. But, the formula SAE rules states that its properties should be derived at that load.

| CFRP Skin Properties | Minimum Value | Experimental Value | Expected Value |
|-------------------------------------------------------|---------------|--------------------|----------------|
| Maximum force at panel failure | 7100 N | 13179 N | 12000 N |
| Skin Modulus of Elasticity [Ex] | 32.4 GPa | 67.7 GPa | 63GPa |
| Skin Yield Strength [Sy] | 201 MPa | 296 MPa | 905 MPa |
| Skin Ultimate Tensile Strength [UTS _{skin}] | 201 MPa | 296 MPa | 905 MPa |

On the basis of this test, the following ply-core layout is compliant with the rules therefore it can be used with the side impact structure. As well as, the properties of the skin layers of Hexply M49 200T2x2 CHS-3k were determined and these values will be used for the Finite element method calculations.

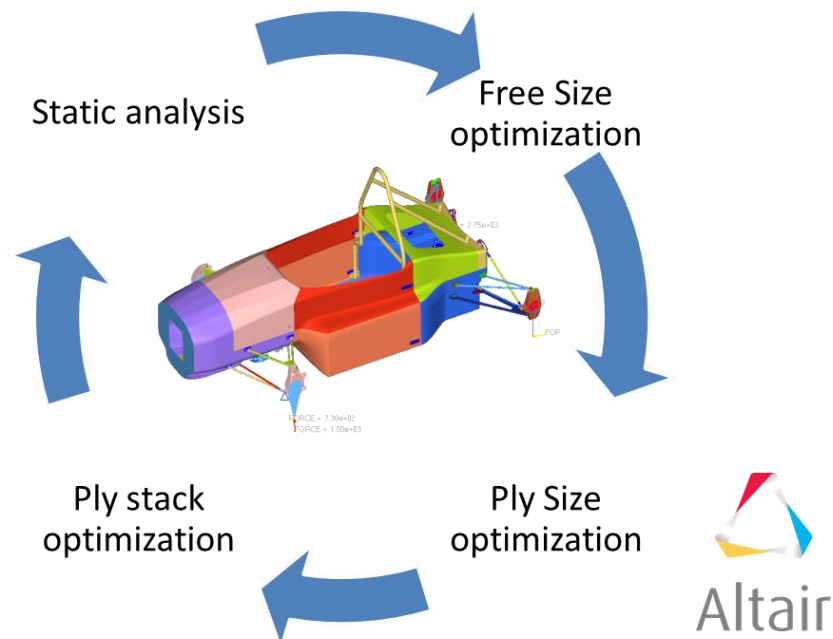
Laminate of the sandwich composite for the Side impact zone

- 4 plies per skin of T200T2 Hexcel M49 42% - t=0,25mm fiber orientation 0/90 deg.
- 5052 Hexcel Aluminum Core t=22mm on W direction

Chapter 5 – Finite Element Analysis

5.1 – FEA process

Before continuing with the definition of the other safety zones, the overall monocoque performance should be determined in order to find an optimum layout for the other zones that provides the required strength and stiffness to support the loads on driving conditions and satisfy the compliance with the rules. In order to do that the following process was implemented using the Altair hyperworks finite element pre-processor Hypermesh to generate the mesh and impose the constraints and the software optistruct as a Finite element solver:



The final Monocoque model includes the model of the front and rear suspensions with the shock absorber modelled as a steel rod to perform the static analysis.

5.2 - FEM model details

- About 60000 Nodes.
- CQUAD4 elements
- CTRIA3 elements < 5%.
- Bolts and shock absorbers modelled as PBEAMS (without pretension).
- Forces applied with RBE3 interpolation elements.
- Rigid connections modelled with RBE2 elements.

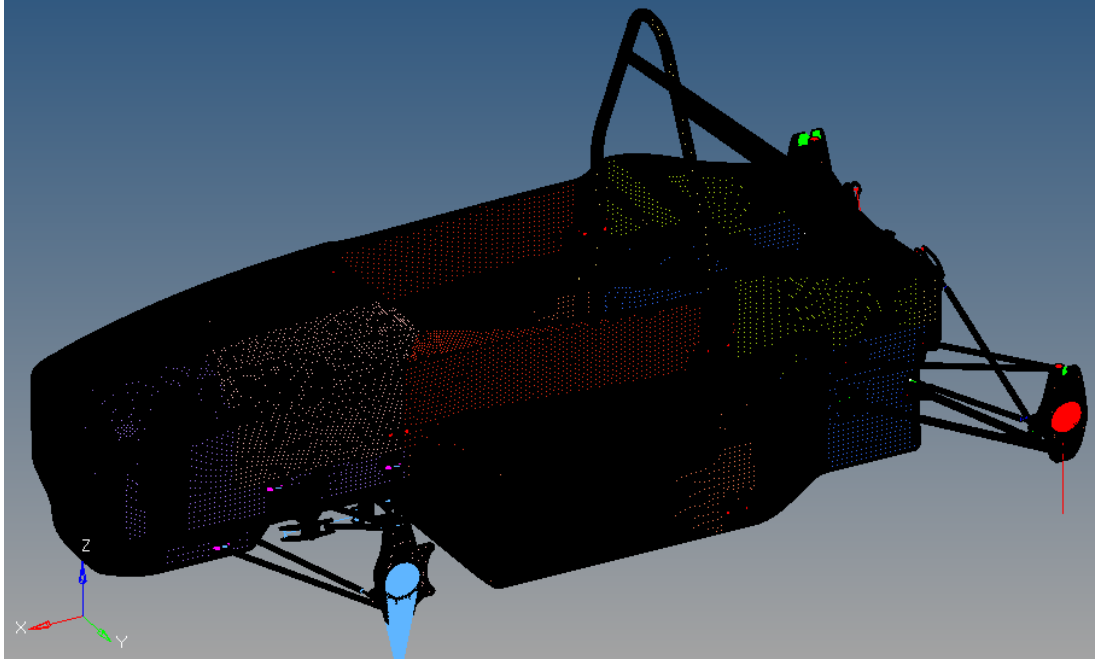
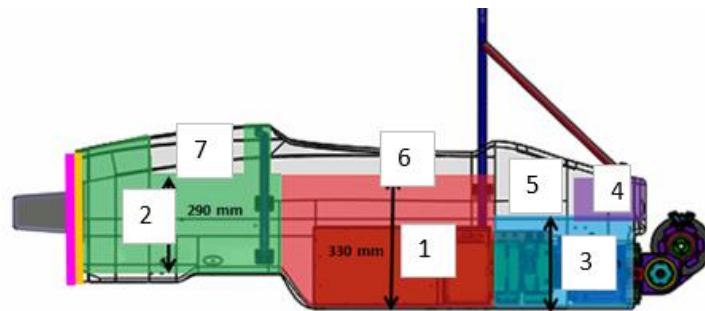


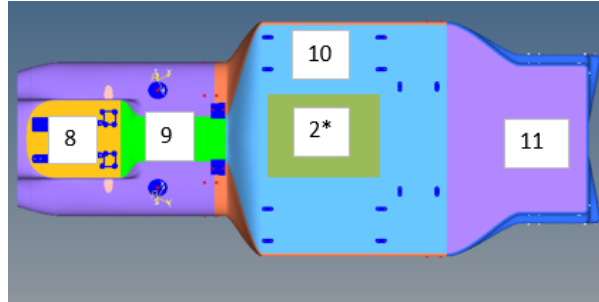
Figure 1 - Monocoque Finite Element Model

After several iterations applying the static loads on dynamic conditions to the monocoque as well as, the measuring the resulting torsional stiffness the design converged. The design angles of the monocoque where chosen to be only of 0deg/45deg with respect the x axis projection to the surface due to the lack of precision that could be achieved by laminating by hand by unexperienced students.

5.3 – Final layup stacking sequence

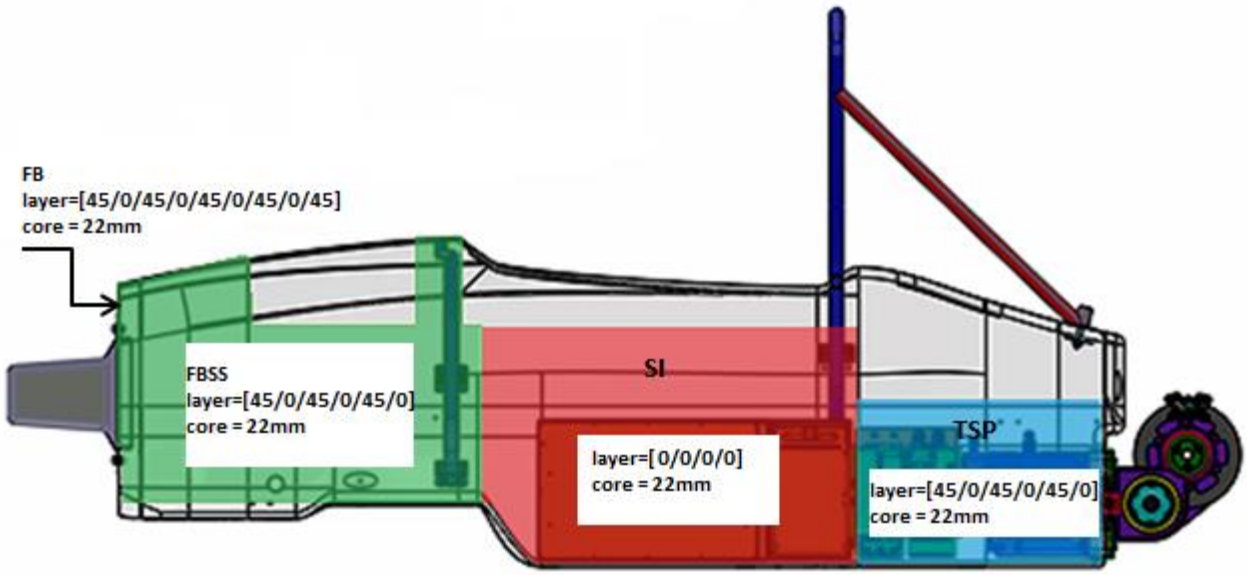
The final stacking of the monocoque resulting from the optimization cycle is the following.





| | Material | Zone 1 - Side impact | Zone 2 - FBS | Zone 3 - TSS | Zone 4 - Rear Structural | Zone 5 Rear Design | Zone 6 SI design | Zone 7 Front Design | Zone 8 - Floor pedal box | Zone 9 Floor FBS | Zone 10 Floor SI | Zone 11 Floor Rear | CFRP Inserts |
|-------------|-----------------|----------------------|-----------------|-----------------|--------------------------|--------------------|------------------|---------------------|--------------------------|------------------|------------------|--------------------|------------------|
| Outer Layer | CFRP M49 T200T2 | Ply 10 - 45 deg | Ply 10 - 45 deg | Ply 10 - 45 deg | Ply 10 - 45 deg | | | | | | | | |
| | CFRP M49 T200T2 | | Ply 9 - 0 deg | Ply 9 - 0 deg | Ply 9 - 0 deg | | | | | | | | |
| | CFRP M49 T200T2 | | Ply 8 - 45deg | Ply 8 - 45deg | Ply 8 - 45deg | | | | | | | | |
| | CFRP M49 T200T2 | Ply 7 - 0deg | | | | | | | | | | | |
| | CFRP M49 T200T2 | Ply 6 - 0deg | | | | | | | | | | | |
| | CFRP M49 T200T2 | Ply 5 - 0deg | Ply 5 - 0deg | Ply 5 - 0deg | Ply 5 - 0deg | | | | | | | | |
| | CFRP M49 T200T2 | | Ply 4 - 45deg | Ply 4 - 45deg | Ply 4 - 45deg | Ply 4 - 45deg | Ply 4 - 45deg | Ply 4 - 45deg | Ply 4 - 45deg | Ply 4 - 45deg | Ply 4 - 45deg | Ply 4 - 45deg | Ply 4 - 45deg |
| | CFRP M49 T200T2 | Ply 3 - 0deg | Ply 3 - 0deg | Ply 3 - 0deg | Ply 3 - 0deg | Ply 3 - 0deg | Ply 3 - 0deg | Ply 3 - 0deg | Ply 3 - 0deg | Ply 3 - 0deg | Ply 3 - 0deg | Ply 3 - 0deg | Ply 3 - 0deg |
| CORE | 5052 Hexcel | Ply 1 - 22mm | Ply 1 - 22mm | Ply 1 - 22mm | Ply 1 - 22mm | Ply 2 - 10mm | Ply 2 - 10mm | Ply 2 - 10mm | Ply 2 - 10mm | Ply 2 - 10mm | Ply 2 - 10mm | Ply 2 - 10mm | Ply 1000 Hextool |
| Inner Layer | Symmetrical | Symmetrical | Symmetrical | Symmetrical | Symmetrical | Symmetrical | Symmetrical | Symmetrical | Symmetrical | Symmetrical | Symmetrical | Symmetrical | Symmetrical |

Table 14 - Stacking sequence and ply number for each zone



5.4 – FEA Static Linear Simulation results

5.4.1 - Torsional Stiffness Results

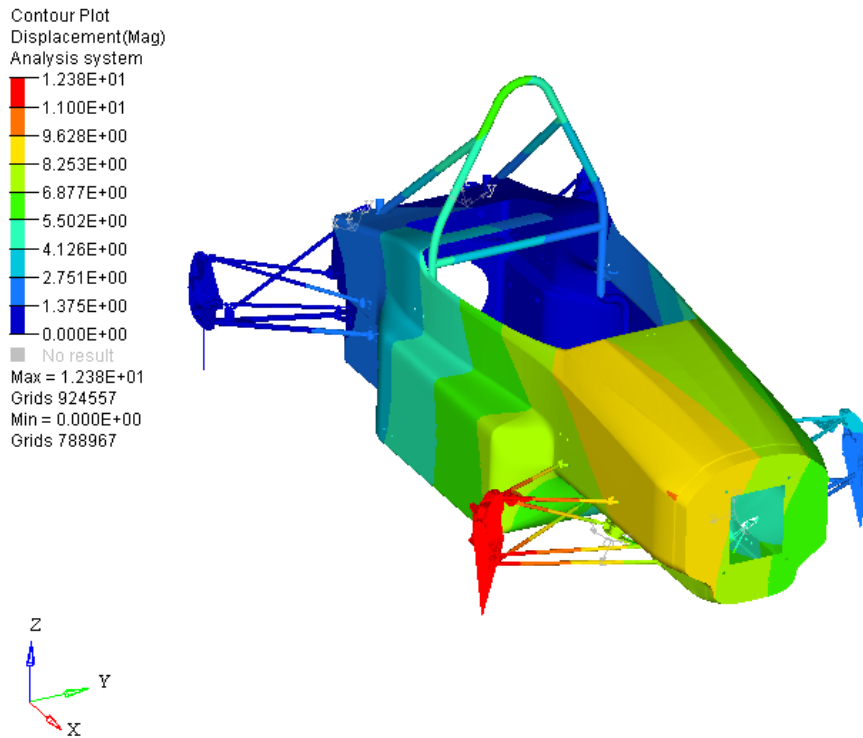


Figure 26 - Optimized Monocoque - Static linear case: torsional stiffness

| | SC12e | SCR FEM Simulation |
|-------------------|------------|--------------------|
| Force [N] | 1000 | 1000 |
| Track [m] | 1,179 | 1,2 |
| displacement [mm] | 19,2 | 12,38 |
| Kt [N*m/rad] | 72404,3683 | 116320,7663 |

Table 15 - FEM Linear Static Torsional Stiffness comparison

For the torsional stiffness, a 40 % increase of the monocoque target stiffness was implemented to take into account for manufacturing defects and to cover the modelling assumptions made on the finite element model.

5.4.2 - Static loadcase results – Braking condition

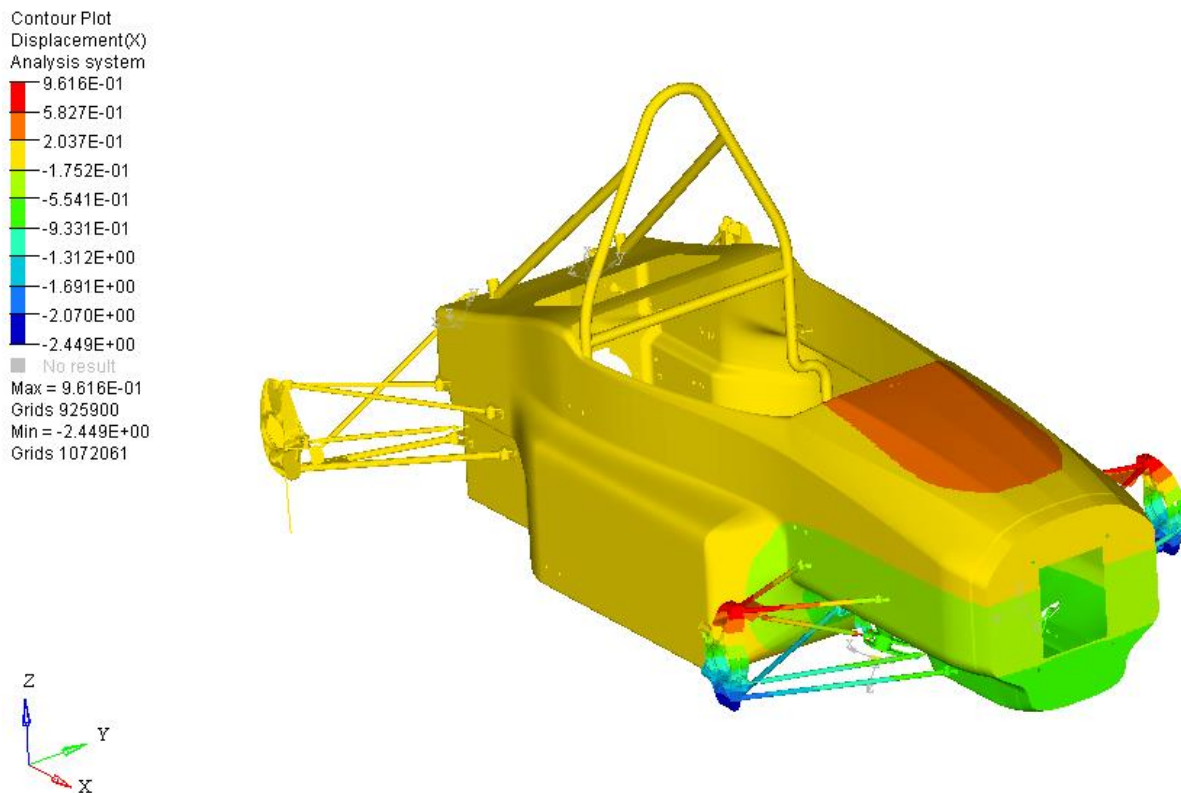


Figure 27- X displacement (Braking Condition)

Contour Plot
 Composite Failure Index(Failure Index)

| |
|-----------|
| 3.083E-01 |
| 2.740E-01 |
| 2.398E-01 |
| 2.055E-01 |
| 1.713E-01 |
| 1.370E-01 |
| 1.028E-01 |
| 6.850E-02 |
| 3.425E-02 |
| 2.003E-19 |
| No result |

Max = 3.083E-01
 2D 521037
 Min = 2.003E-19
 2D 73546

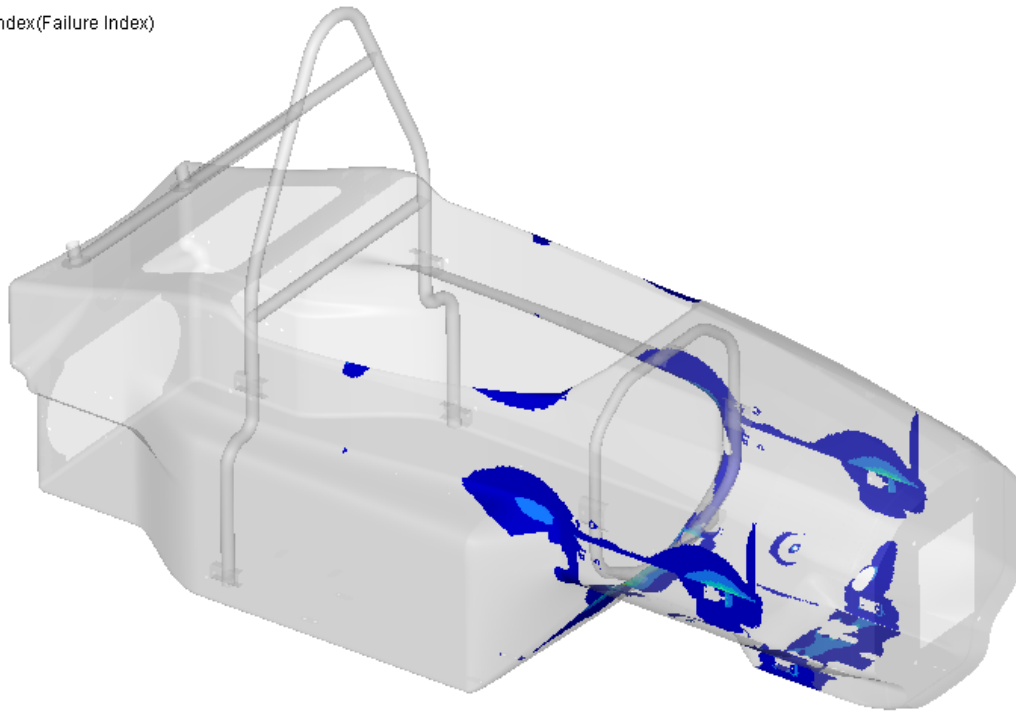


Figure 28- Tsai Wu Failure Coefficient when braking

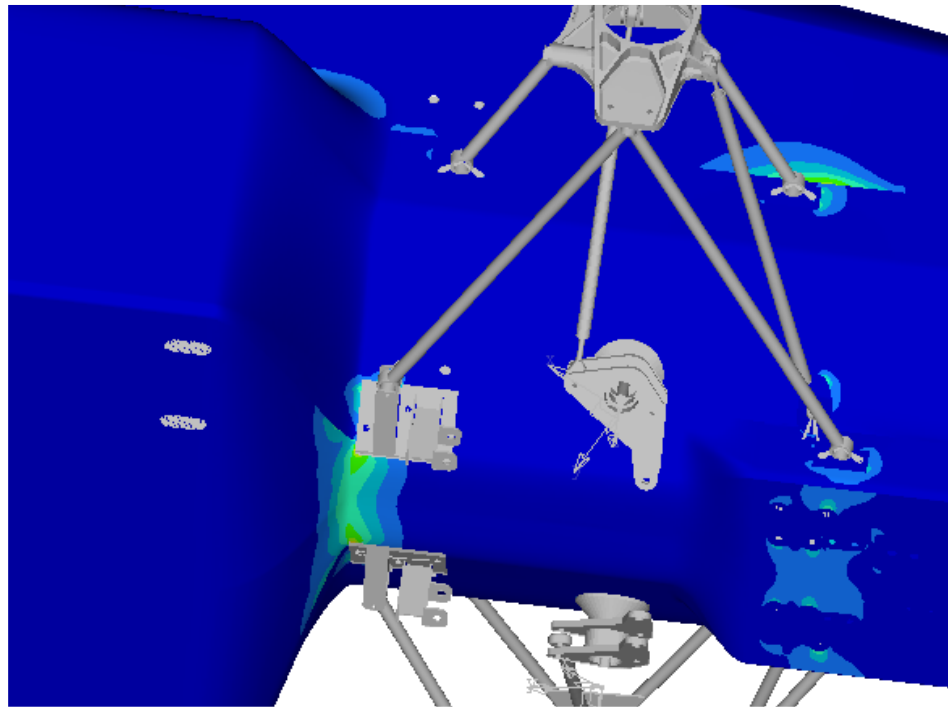


Figure 29- Zoom of the critical zone when braking

5.4.3 - Static loadcase results – Max lateral Acceleration

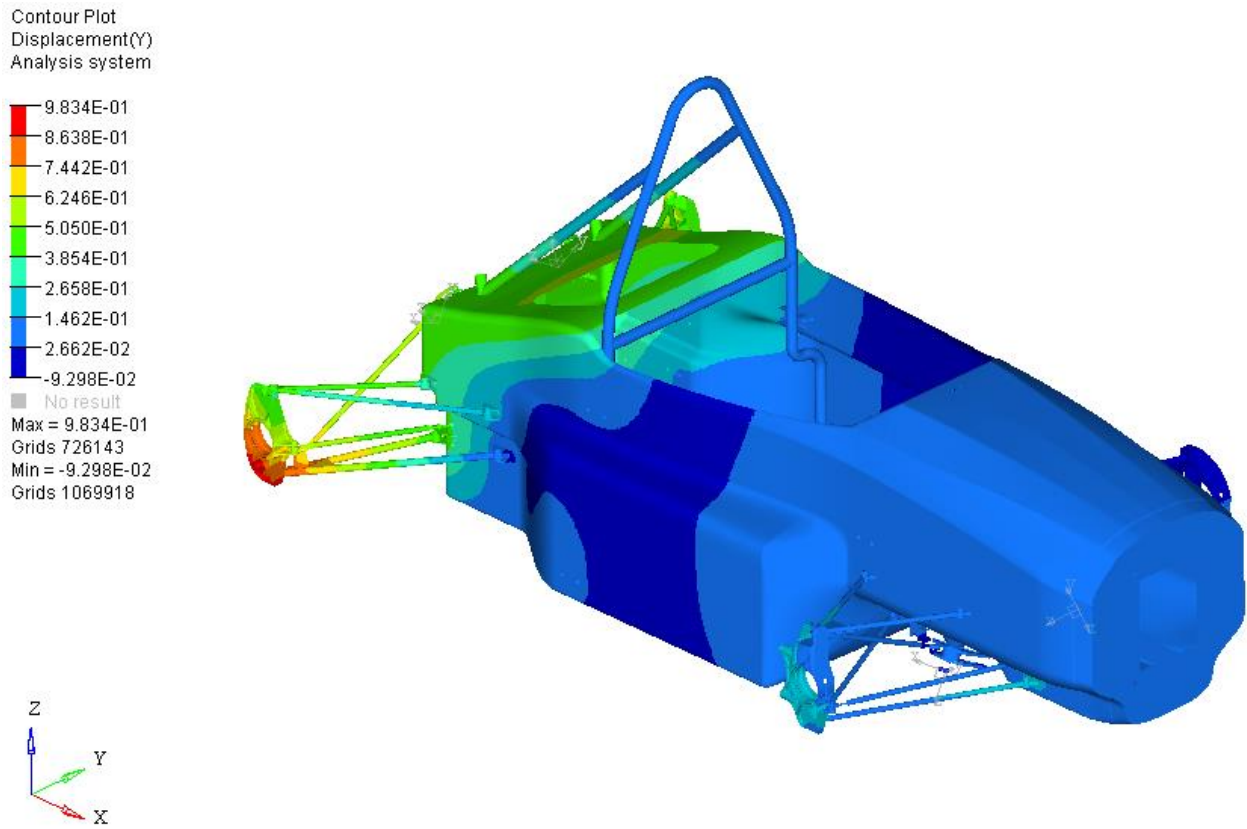


Figure 30 - Y displacement at Maximum lateral Acceleration

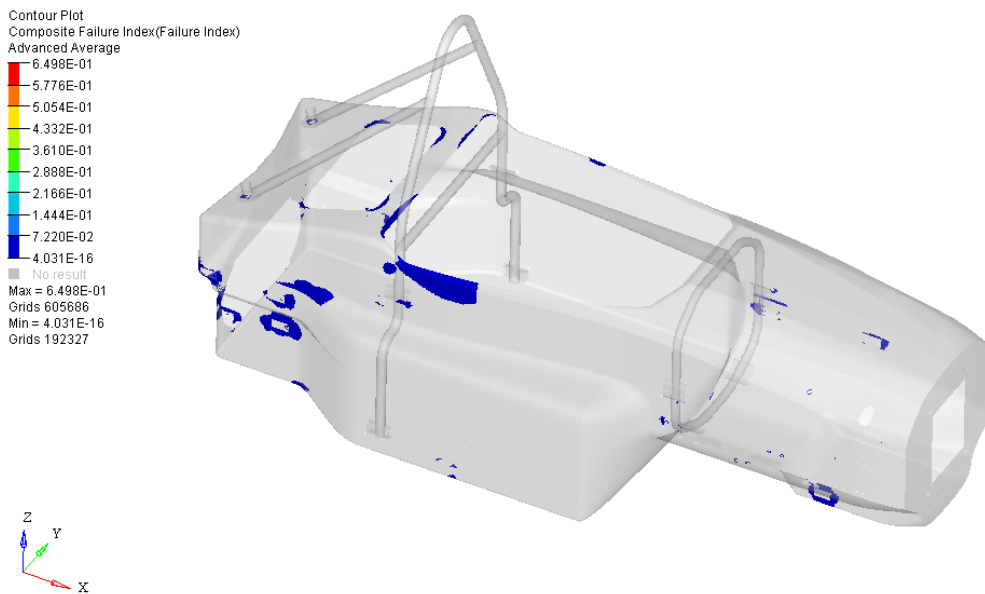


Figure 31- Tsai Wu failure coefficient for the maximum acceleration loadcase

5.4.4 - Static loadcase results – Maximum Combined accelerations

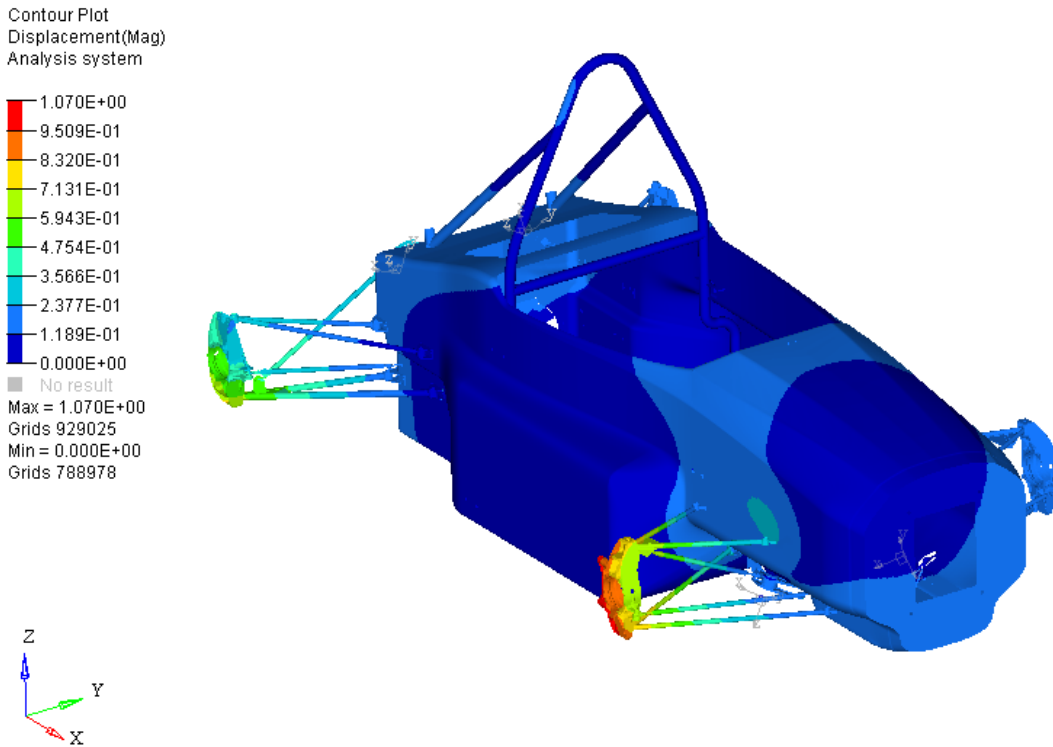


Figure 32 - Displacements - Static loadcase: Maximum combined accelerations

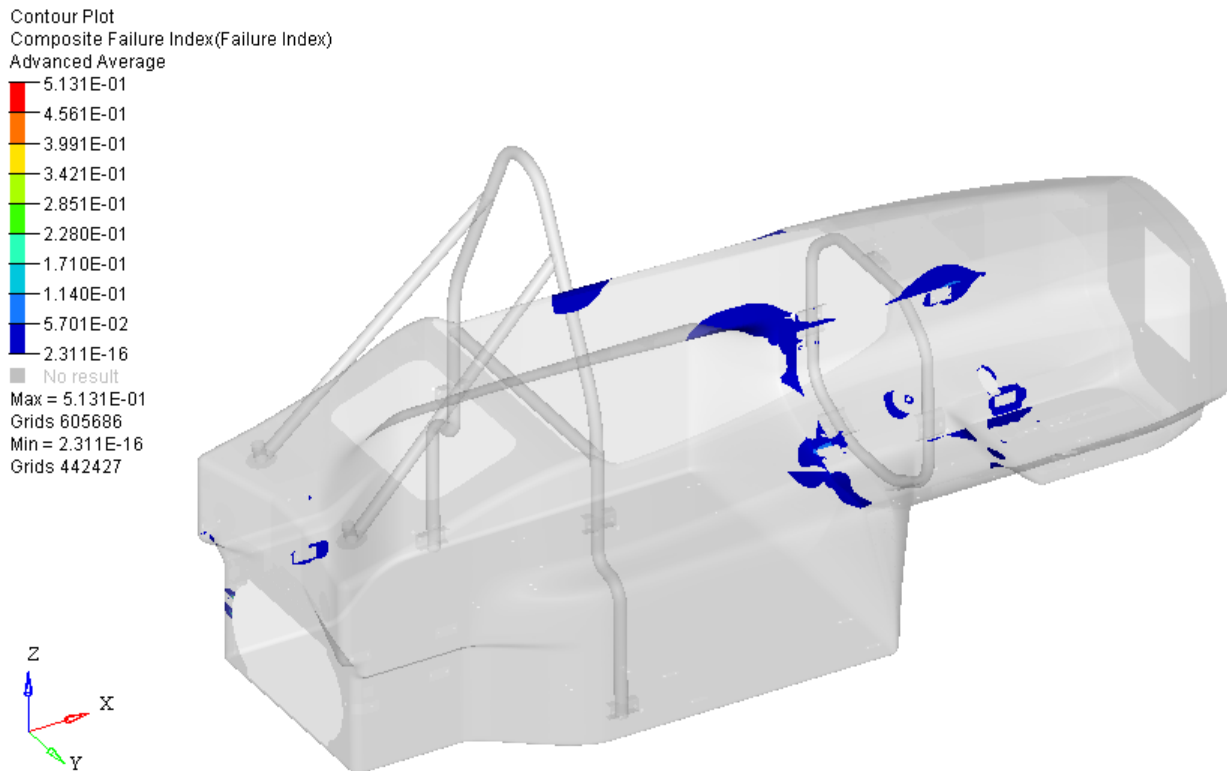


Figure 33- Tsai wu failure coefficient at maximum combined acceleration loadcase

5.5 - Summary of the results of the FEA linear static simulations

Stiffness

One of the objectives that the monocoque with its suspension should guarantee that under loads the kinematics of the suspension does not vary considerably due to deformations to maintain the handling behavior of the race car. The following calculations show the variations of the characteristics angles of the suspension under the considered loadcases determined by FEM.

| | Front Suspension | | | Rear Suspension | | |
|-----------------------|------------------|-------------|----------|-----------------|-------------|----------|
| | Braking | Max Lateral | Combined | Braking | Max Lateral | Combined |
| Δ Caster [deg] | 0,076 | 0,048 | 0,074 | - | 0,052 | 0,073 |
| Δ Camber [deg] | 0,084 | 0,085 | 0,092 | - | 0,064 | 0,080 |
| Δ Toe [deg] | 0,052 | 0,073 | 0,071 | - | 0,071 | 0,058 |

Table 16 - Suspension angle variation under load

These results show that the angle variation of the suspension's angles under load is below 0.2deg. Only for the maximum lateral loadcase the rear suspension exceeds this value for the caster angle but we can consider it acceptable due to the lack of influence at pure lateral acceleration, a stiffening of the structure should have been performed if a big caster variation under braking were presented at the front suspension to avoid losses braking performance.

Failure Index

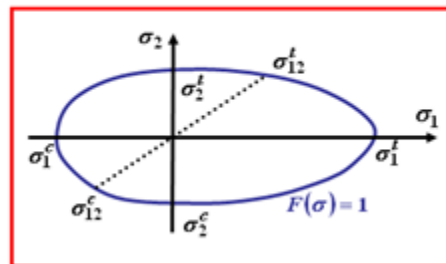
The Tsai–Wu failure criterion is a phenomenological material failure theory which is widely used for anisotropic composite materials which have different strengths in tension and compression.

$$F(\sigma) = F_1\sigma_1 + F_2\sigma_2 + F_{11}\sigma_1^2 + F_{22}\sigma_2^2 + F_{44}\sigma_{12}^2 + 2F_{12}\sigma_1\sigma_2$$

$$F_1 = -\frac{1}{\sigma_{1y}^c} + \frac{1}{\sigma_{1y}^t} \quad ; \quad F_{22} = \frac{1}{\sigma_{2y}^c \sigma_{2y}^t}$$

$$F_2 = -\frac{1}{\sigma_{2y}^c} + \frac{1}{\sigma_{2y}^t} \quad ; \quad F_{44} = \frac{1}{\sigma_{12y}^c \sigma_{12y}^t}$$

$$F_{11} = \frac{1}{\sigma_{1y}^c \sigma_{1y}^t} \quad ; \quad F_{12} = -\frac{\alpha}{2} \sqrt{F_{11} F_{22}}$$



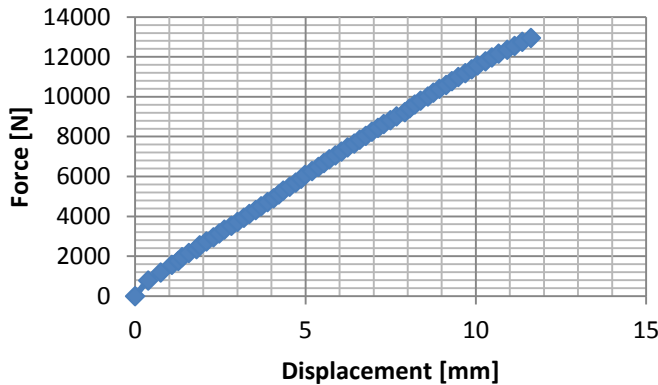
The following table summarizes the safety factors of the monocoque under the static linear loadcases.

| | Braking | Max Lateral | Combined |
|---------------|---------|-------------|----------|
| Failure Index | 0,308 | 0,649 | 0,513 |
| Safety Factor | 3,247 | 1,541 | 1,949 |

The safety factor obtained were all above 1, therefore the monocoque should be able to withstand the loads under driving conditions with a considerable margin for non-expected loading events. Good engineering practices are applied when safety factors above 1.5 are used according to some authors. Therefore these results were considered acceptable.

5.6 – Different Layup experimental validation

After defining the Monocoque material and layups, the rules state that every time a different layup is used on the monocoque safety zones the 3 point bending test should be performed in order to verify its mechanical properties. Therefore we proceeded to test the other layup present at the Front bulkhead support area and the tractive system support area.



| CFRP Skin Properties | Minimum Value | Experimental Value | Expected Value |
|-------------------------------------------------------|---------------|--------------------|----------------|
| Maximum force at panel failure | 6400 N | 12949.2 N | 14363 N |
| Skin Modulus of Elasticity [Ex] | 37 GPa | 43.2 GPa | 45 GPa |
| Skin Yield Strength [Sy] | 124 MPa | 358 MPa | 700 MPa |
| Skin Ultimate Tensile Strength [UTS _{skin}] | 124 MPa | 358 MPa | 700 MPa |

From the results shown above, the laminates for the other safety zones were validated by experimental testing. Thus, the following laminate is compliant with the Formula SAE Rules 2013

- Laminate - 6 plies per skin of T200T2 Hexcel M49 42% - t=0,25mm fiber orientation 45/0/45/0/45/0 deg.
- 5052 Hexcel Aluminum Core t=22mm on W direction

5.7 - Safety Attachments verification according to the FSAE Rules 2013

At this point, all the laminates that define the entire layups used as safety structure were determined and are compliant with the Formula SAE 2013 Rules. We moved on to the attachments of the different safety devices that must be fixed to the monocoque, such as the front hoop, the main roll hoops and the safety harnesses attachments.

A perimeter shear test was performed to determine the ultimate shear stress of the skins of the 2 laminates validated. The rules state that a minimum load strength of the attachments should be guaranteed. For the out of plane loads a pure shear calculation was performed to determine the minimum perimeters of the inserts or backing plate attachments with the data derived from a perimeter shear testing.

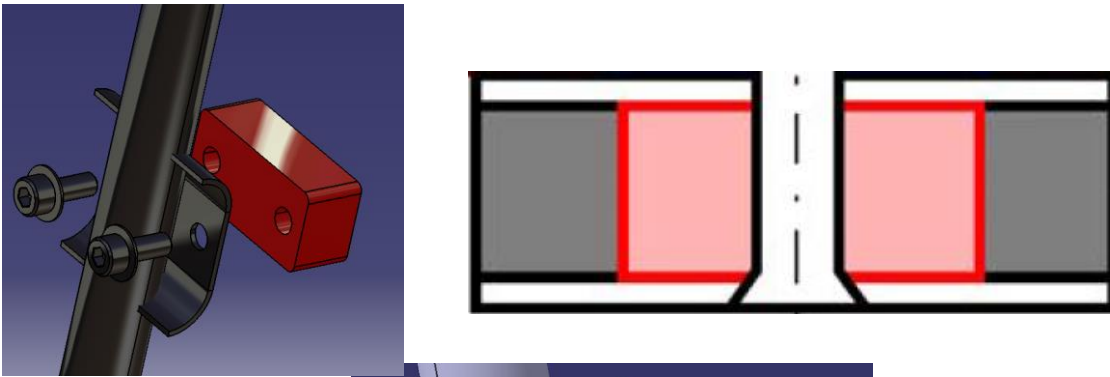


Figure 34 - attachment to insert solution

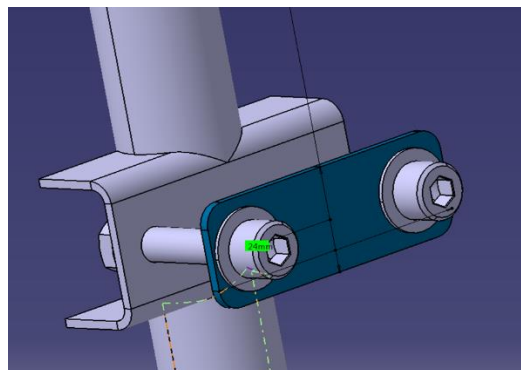


Figure 35 - Backing plate solution

5.8 - Perimeter shear testing

The following shear test experiment was performed to determine the shear strength of the carbon fiber skins. With an indentator of 25mm

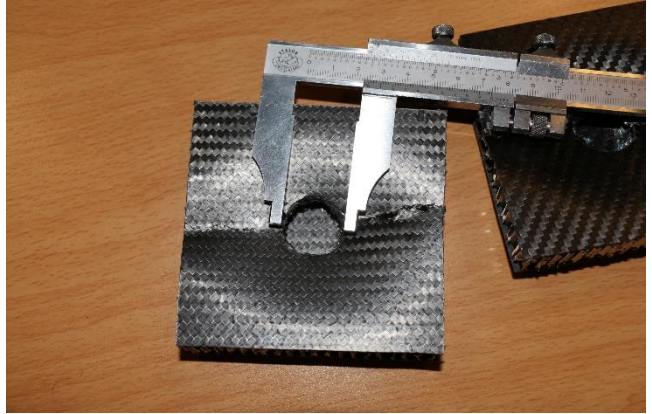
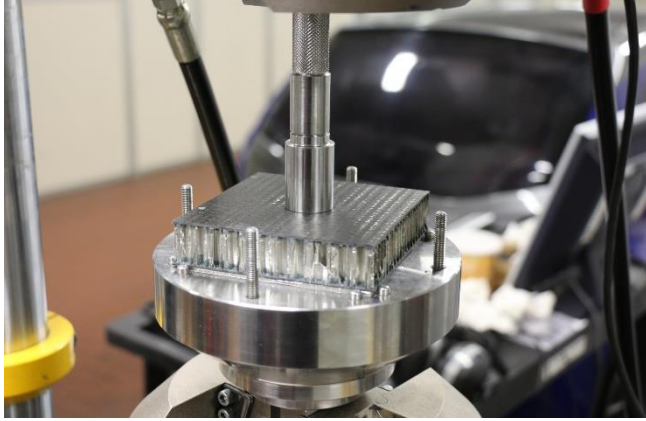
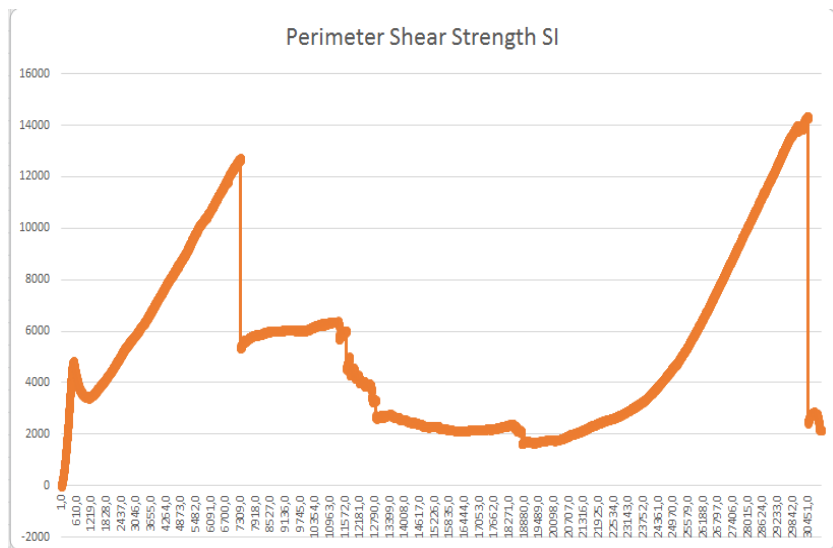


Figure 36- Perimeter shear testing

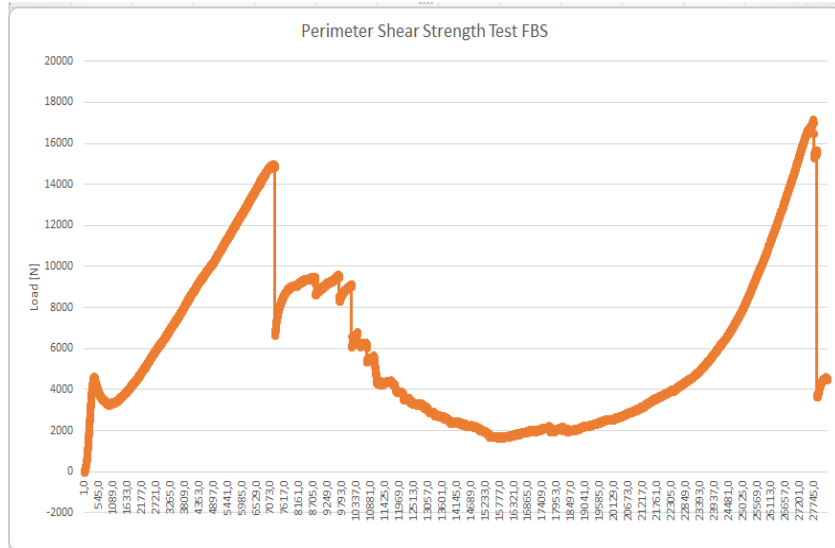


Figure 37 - Tooling details to perform the test. Support (left), Indentator (right)

Perimeter shear test results for the first laminate



Perimeter shear test results of the second laminate



5.9 - Summary of the perimeter shear test results

Laminate 1 (Side impact zone)

- 4 plies per skin of T200T2 Hexcel M49 42% - t=0,25mm fiber orientation 0/90 deg.
- 5052 Hexcel Aluminum Core t=22mm on W direction

| | |
|-------------------------------|-------|
| Peak force 1(N) | 12830 |
| Peak Force 2 (N) | 14250 |
| Skin cured thickness t (mm) | 1 |
| σ_{shear} (Mpa) | 163,4 |

Laminate 2 (Front Bulkhead Zone, TSS)

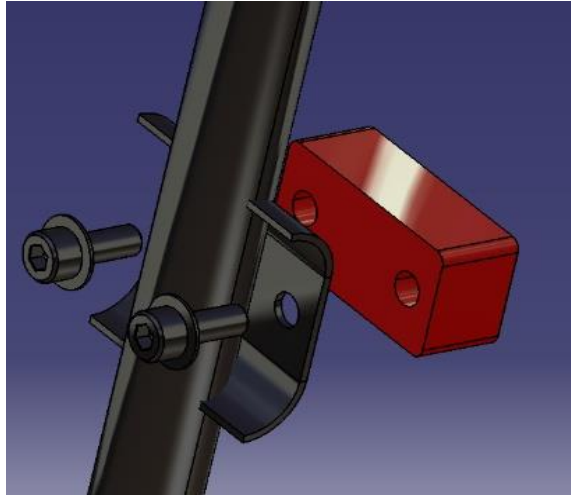
- Laminate - 6 plies per skin of T200T2 Hexcel M49 42% - t=0,25mm fiber orientation 45/0/45/0/45/0 deg.
- 5052 Hexcel Aluminum Core t=22mm on W direction

| | |
|-------------------------------|-------|
| Peak force 1(N) | 14950 |
| Peak Force 2 (N) | 16980 |
| Skin cured thickness t (mm) | 1,40 |
| σ_{shear} (Mpa) | 136,0 |

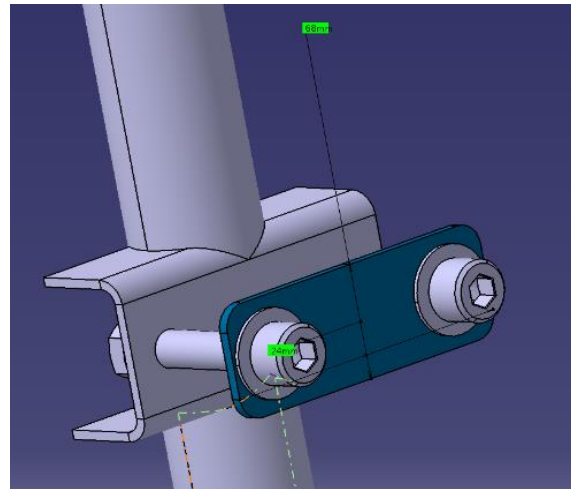
5.10 - Safety attachments and suspension inserts calculation results

The following table shows the attachment location, bolts numbers defined by the rules, and strength calculations to comply with the Formula SAE 2013 rules. For the determination of the insert/backing plate perimeter the minimum shear strength of the 2 tests performed was used.

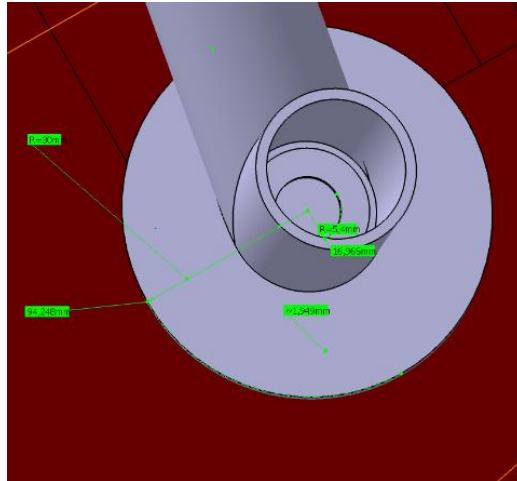
| Front Hoop Attachments | | |
|---------------------------------|-----|------|
| Fastener dia., mm | 8 | PASS |
| No. of fasteners | 2 | PASS |
| Bracket to hoop weld length, mm | 126 | PASS |
| Bracket thickness, mm | 2 | PASS |
| Bracket perimeter, mm | 180 | |
| Skin thickness, mm | 1,4 | |
| Skin shear strength, MPa | 136 | |
| Perimeter shear strength, kN | 34 | PASS |
| Backing plate thickness, mm | 20 | PASS |
| Backing plate perimeter, mm | 180 | |
| Perimeter shear strength, kN | 34 | PASS |



| Main Hoop Attachments | | |
|---------------------------------|-----|------|
| Fastener dia., mm | 8 | PASS |
| No. of fasteners | 2 | PASS |
| Bracket to hoop weld length, mm | 115 | PASS |
| Bracket thickness, mm | 2 | PASS |
| Bracket perimeter, mm | 184 | |
| Skin thickness, mm | 1,4 | |
| Skin shear strength, MPa | 136 | |
| Perimeter shear strength, kN | 34 | PASS |
| Backing plate thickness, mm | 2 | PASS |
| Backing plate perimeter, mm | 180 | |
| Perimeter shear strength, kN | 34 | PASS |



| Main Hoop Bracing Attachments | | |
|---------------------------------|-----|------|
| Fastener dia., mm | 10 | PASS |
| No. of fasteners | 1 | PASS |
| Bracket to hoop weld length, mm | 95 | PASS |
| Bracket thickness, mm | 2 | PASS |
| Bracket perimeter, mm | 188 | |
| Skin thickness, mm | 1,4 | |
| Skin shear strength, MPa | 136 | |
| Perimeter shear strength, kN | 34 | PASS |
| Backing plate thickness, mm | 2 | PASS |
| Backing plate perimeter, mm | 188 | |
| Perimeter shear strength, kN | 34 | PASS |



Suspension and other components attachments

Besides the FEM results on the entire monocoque under the dynamic loadcases stated before, a further calculation of all the interfaces to the monocoque apart of those verified by the Safety equivalence spreadsheet were verified with the same formulae using the experimental data obtained by the perimeter shear strength and the interlaminar shear stresses obtained from the material's datasheet.

| Laminate zone | Skin Thickness [mm] | Sigma_shear [Mpa] | ISS [Mpa] |
|------------------|---------------------|-------------------|-----------|
| Zone 1 (SI) | 1 | 130 | 50 |
| Zone 2 (FBS,TSS) | 1,25 | 130 | 50 |

Front Suspension Inserts

| Suspension Point | Case 1 - Max Lateral Acc | | | Case 2 - Max Longitudinal Acc | | | Case 3 - Max combined Acc | | |
|-------------------------|--------------------------|-------------|--------|-------------------------------|---------|---------|---------------------------|---------|---------|
| | Fx [N] | Fy [N] | Fz [N] | Fx [N] | Fy [N] | Fz [N] | Fx [N] | Fy [N] | Fz [N] |
| Lower control arm front | -29,4 | -3306 | -23,3 | -169 | -2738,4 | 1146,1 | -143,4 | 5356,8 | -1680,8 |
| Lower control arm rear | -28,8 | - 3249,2 | -23,3 | -96,1 | 1799,6 | -1181,6 | 40,5 | -1565,8 | -1679,4 |
| Upper control arm front | - 134,7 | - 1467,5 | -37 | -1,25 | -8,4 | 9 | -173,4 | -2801,3 | 773,3 |
| Upper control arm rear | 145,1 | - 1638,7 | -37 | -2,2 | -45,8 | 9 | -2,2 | 259,4 | -789,5 |
| Rocker to body | - 531,5 | 622 | -314,5 | -489,7 | 498,2 | -364,3 | -472,6 | 424,4 | -239,1 |

After determining the loads, those that represent the in-plane forces and the out of plane forces where used to calculate each insert. A minimum area and perimeter insert was calculated with this data then the actual geometry of the designed insert is presented with its actual safety factor

| Suspension Point | Finplane | FOOP | Zone | SF | Required Insert Geometry | | Actual Geometry | | SF min |
|-------------------------|----------|---------|------|------|--------------------------|--------------|-----------------|-----------|--------|
| | | | | | MinPerimeter [mm] | MinArea [mm] | Perimeter [mm] | Area [mm] | |
| Lower control arm front | 1686,91 | 5356,80 | 2 | 1,50 | 61,81 | 25,30 | 144,00 | 1152,00 | 2,33 |
| Lower control arm rear | 1679,89 | 3249,20 | 2 | 1,50 | 37,49 | 25,20 | 144,00 | 1152,00 | 3,84 |
| Upper control arm front | 792,50 | 2801,30 | 2 | 1,50 | 32,32 | 11,89 | 174,00 | 1872,00 | 5,38 |
| Upper control arm rear | 789,50 | 1638,70 | 2 | 1,50 | 18,91 | 11,84 | 174,00 | 1872,00 | 9,20 |
| Rocker to body | 617,58 | 622,00 | 2 | 1,50 | 7,18 | 9,26 | 188,50 | 1413,72 | 26,26 |

The same process was followed to define the geometry of the rear suspension inserts.

| Suspension Point | Finplane | FOOP | Zone | SF | Required Insert Geometry | | Actual Geometry | | SF min |
|-------------------------|----------|--------|------|-----|--------------------------|----------------------------|-----------------|-----------|--------|
| | | | | | MinPerimeter [mm] | MinArea [mm ²] | Perimeter [mm] | Area [mm] | |
| Lower control arm front | 2275,1 | 5315,9 | 2,0 | 1,5 | 49,1 | 34,1 | 144,0 | 1152,0 | 2,9 |
| Lower control arm rear | 2270,3 | 5377,0 | 2,0 | 1,5 | 49,6 | 34,1 | 144,0 | 1152,0 | 2,9 |
| Upper control arm front | 979,5 | 2056,4 | 2,0 | 1,5 | 19,0 | 14,7 | 174,0 | 1872,0 | 9,2 |
| Upper control arm rear | 983,3 | 2427,9 | 2,0 | 1,5 | 22,4 | 14,8 | 174,0 | 1872,0 | 7,8 |
| Tierod to body | 24,1 | 134,2 | 2,0 | 1,5 | 1,2 | 0,4 | 147,4 | 1320,1 | 119,0 |
| Rocker to body | 528,7 | 314,7 | 2,0 | 1,5 | 2,9 | 7,9 | 188,5 | 1413,7 | 64,9 |



Figure 38. Image of the manufactured inserts

The inserts were made of pure carbon fiber. Usually aluminum is used due to its lower cost, but making the inserts of CFRP corresponds to a reduction of the insert's weight of 50%.

5.11- ENSAT Pullout Test

The inserts were machined and filleted to allow an ENSAT to fit in, these components were used to avoid the wear that will be caused by its life service.



In order to verify the resistance of this process another test was performed to certify that the ENSAT sustains the loads. The entire process was well documented in order to develop a standard process that will be used on each insert.

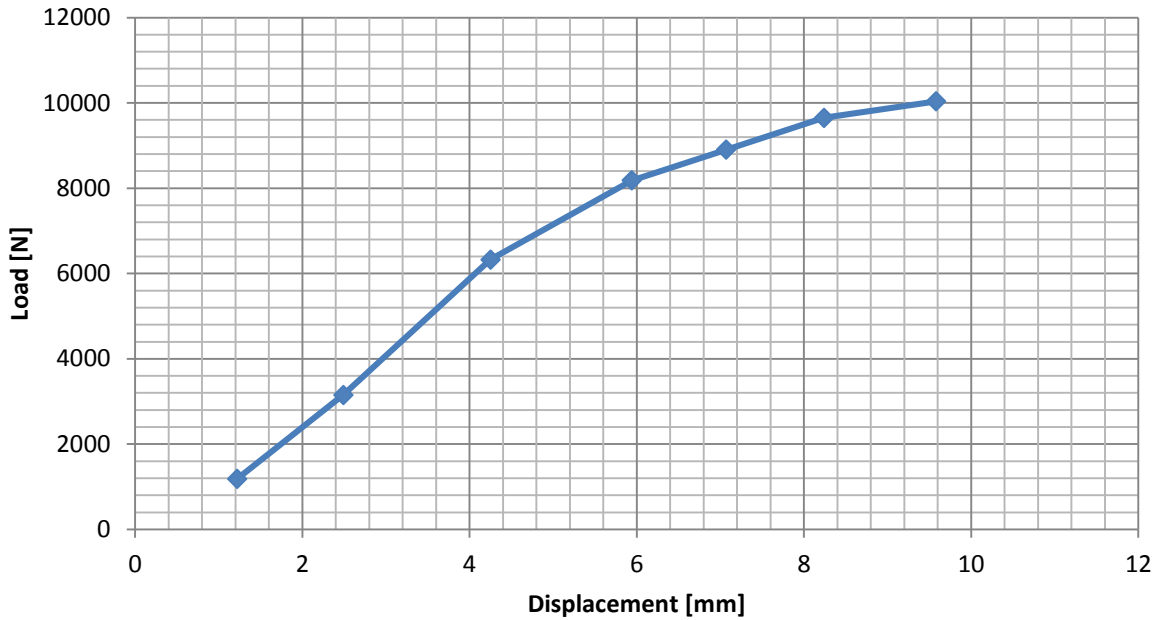


Figure 39- pullout test of an ensat insert

The pullout test verified that the ENSAT insert was more than enough, due to the fact that the failure was presented on the rod. Therefore, the maximum load that the ENSAT can withstand was not reached.

5.12 - Safety Harness Attachments Pullout Tests

Before the monocoque can be built, a final test should be performed to ensure that the safety harnesses used on the monocoque withstand the minimum loads presented by the rules.

- T3.41.1 The monocoque attachment points for the shoulder and lap belts must support a load of 13 kN (~3000 pounds) before failure.
- T3.41.2 The monocoque attachment points for the anti-submarine belts must support a load of 6.5 kN (~1500 pounds) before failure.
- T3.41.3 If the lap belts and anti-submarine belts are attached to the same attachment point, then this point must support a load of 19.5 kN (~4500 pounds) before failure.
- T3.41.4 The strength of lap belt attachment and shoulder belt attachment must be proven by physical test where the required load is applied to a representative attachment point where the proposed layup and attachment bracket is used.

The shoulder belts will be attached to the main roll hoop therefore no verification its needed, the lap belts and the anti-submarine belts remaining attachments of the 6 point harness should be

integrated to the monocoque. The insert dimension was determined as on the previous chapters, using the maximum perimeter shear strength and interlaminar shear strength of the used layups.

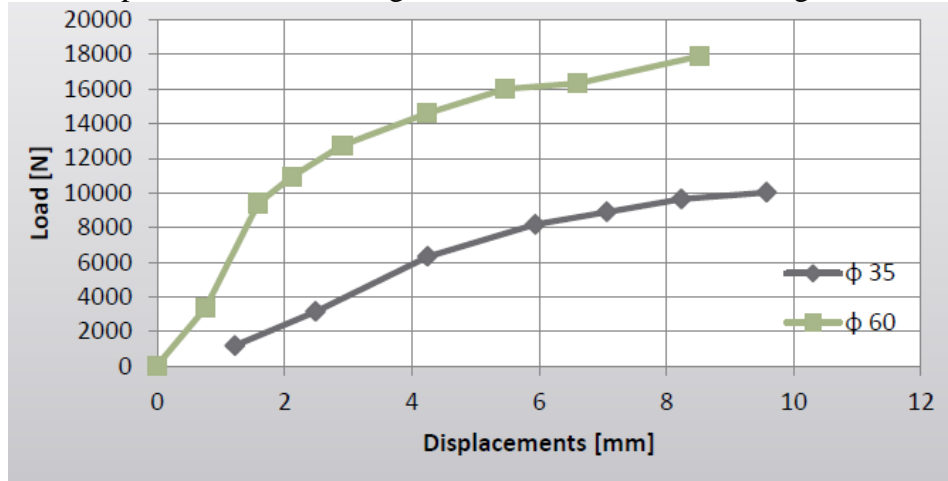


Figure 40 - Load vs displacement of the belt attachment inserts of 35 and 60 mm OD



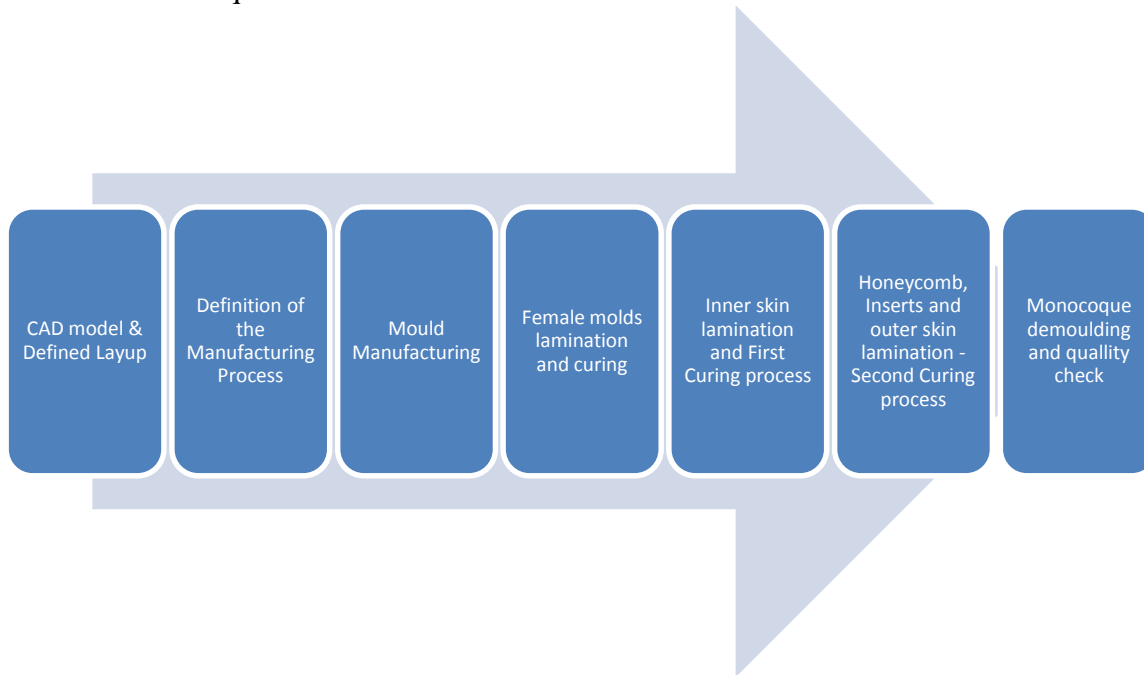
Figure 41- Pullout test of the safety harness attachments

The insert of 35 mm OD reached the minimum load required for the anti-submarine belts, as well as, the insert of 60mm OD achieved a maximum load above the minimum required for the lap belt attachments.

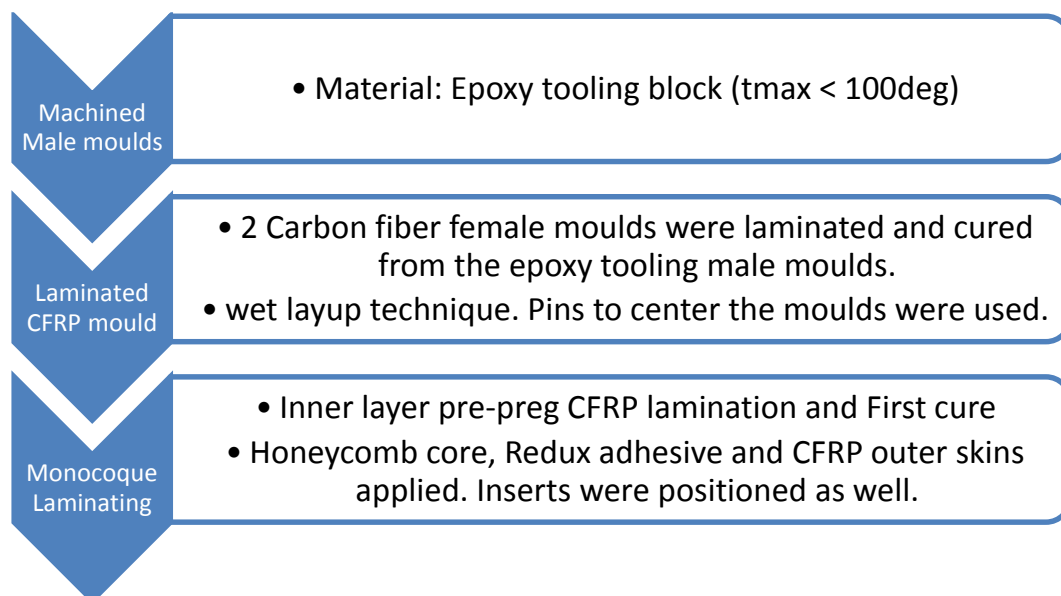
Chapter 6 – Manufacturing

6.1 - Manufacturing Process

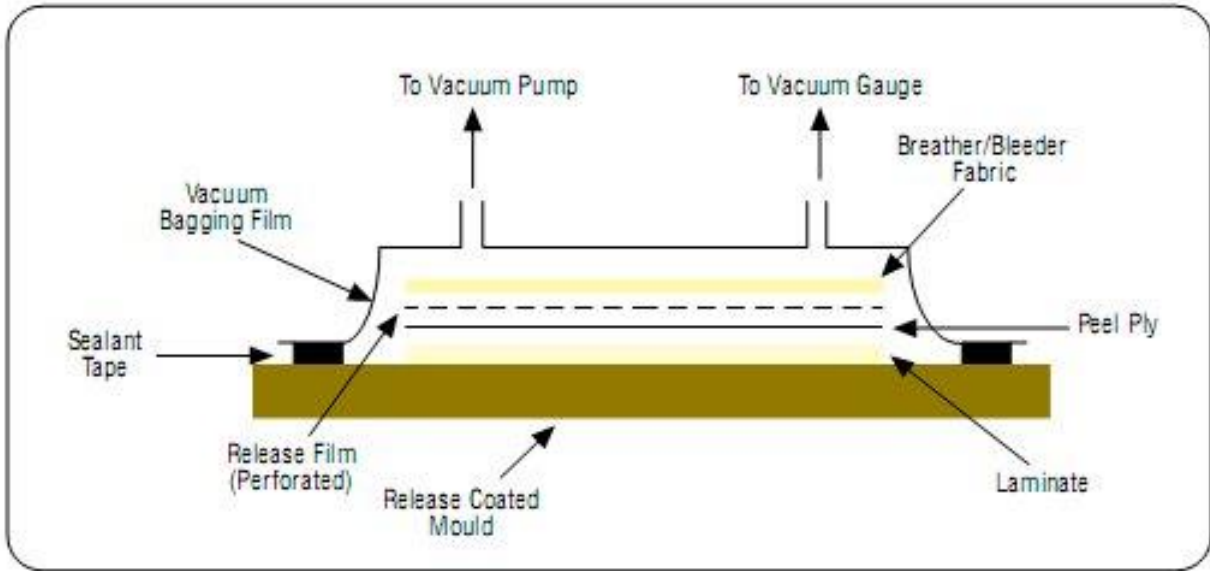
The calculations and the experimental results of the sandwich panels and inserts showed that the monocoque was feasible. On this chapter we will present the process followed to manufacture the SCR monocoque.



The manufacturing process chosen to build the monocoque was to vacuum curing on an autoclave. The team also decided to build a unique demountable mold to make a monocoque on one piece, even if the monocoque production will be more difficult due to the lack of space (only one person at the time) but it will not require to make 2 half's of the monocoque and then bond them together.



Vacuum bagging curing process



6.2 - Carbon Fiber and honeycomb core draping analysis and plybook generation

In order to be able to generate the exploded plies defined by each zone that will allow the CFRP and the Honeycomb core to be cut from its flat configuration and then be laminated by hand Laminate Tools was used to generate these shapes and the plybook as well.

Finished “real” thicknesses model generated with laminate tools superposing all the plies needed for the lamination

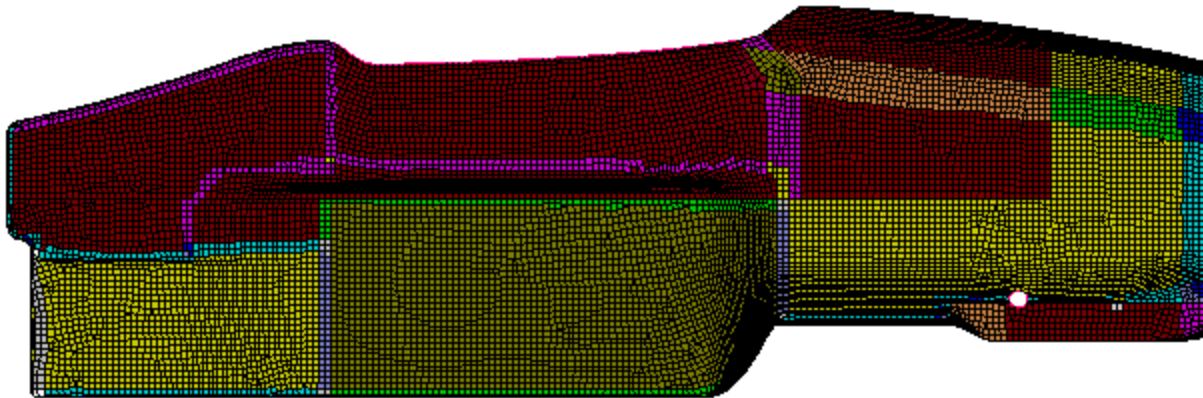


Figure 42 - SCR monocoque thickness distribution from the generated plies

In order to generate the model that contains all the plies needed to fully comply with the layup derived from the simulations the following process was performed until the goal was achieved:

The plies were generated by selecting “areas” from which a certain ply should be generated and cutting it where it becomes unfeasible from a lamination point of view”

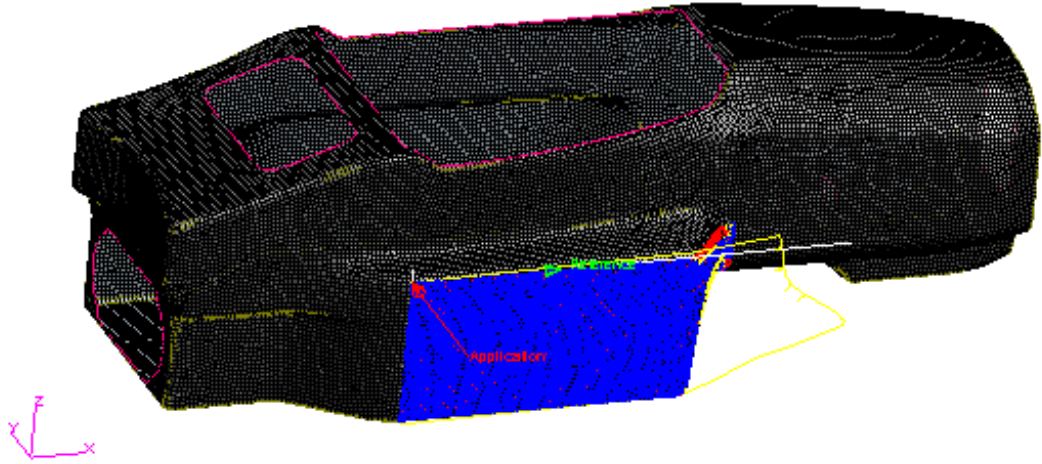


Figure 43- Draping simulation of the SI zone ply (red) unfeasible area

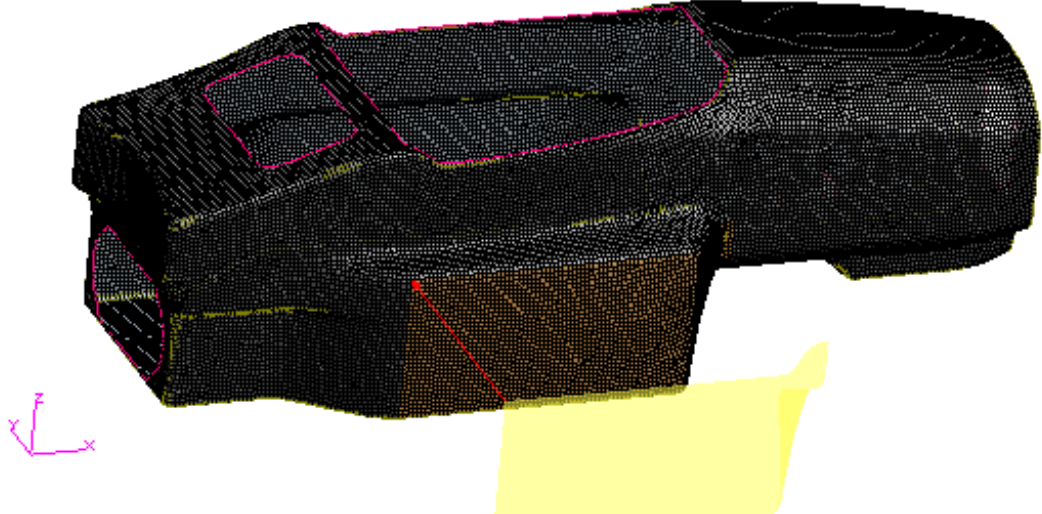


Figure 44 - Plybook illustrating image of a SI zone ply

After the draping simulation was done, the flattened shape of the ply was generated and it was ready to be cut from the CFRP sheets.

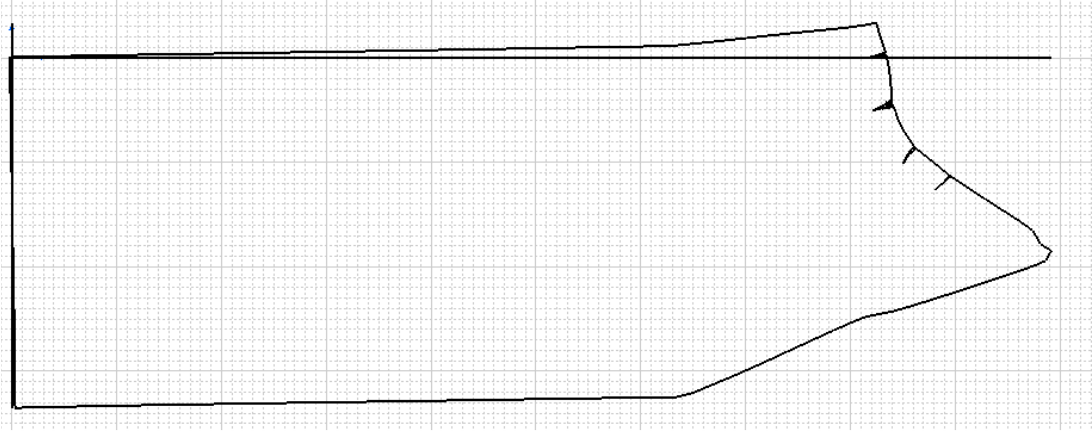


Figure 45 - Generated Ply for the SI zone, a line shows the reference line

After doing this process for each ply, the plybook was generated containing images of the position, shape and angles of each ply. The entire plybook can be found at the appendix



Figure 46- Plybook sample view

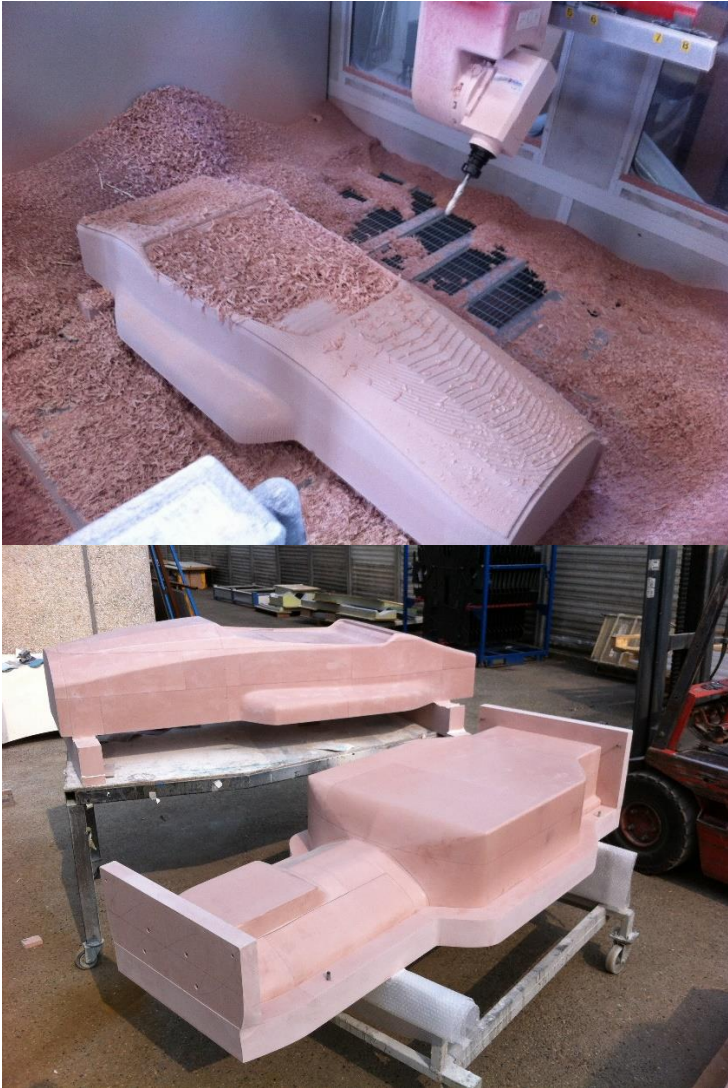
The final process before the manufacturing process starts was the nesting of each ply to optimize the material's use. Even if several commercial tools are available to perform this task, due to the lack of time and resources the nesting process was performed manually.



Figure 47- Section of the nested plies to be cutted

6.3 - Manufacturing Images

Male molds from Epoxy Tooling Blocks



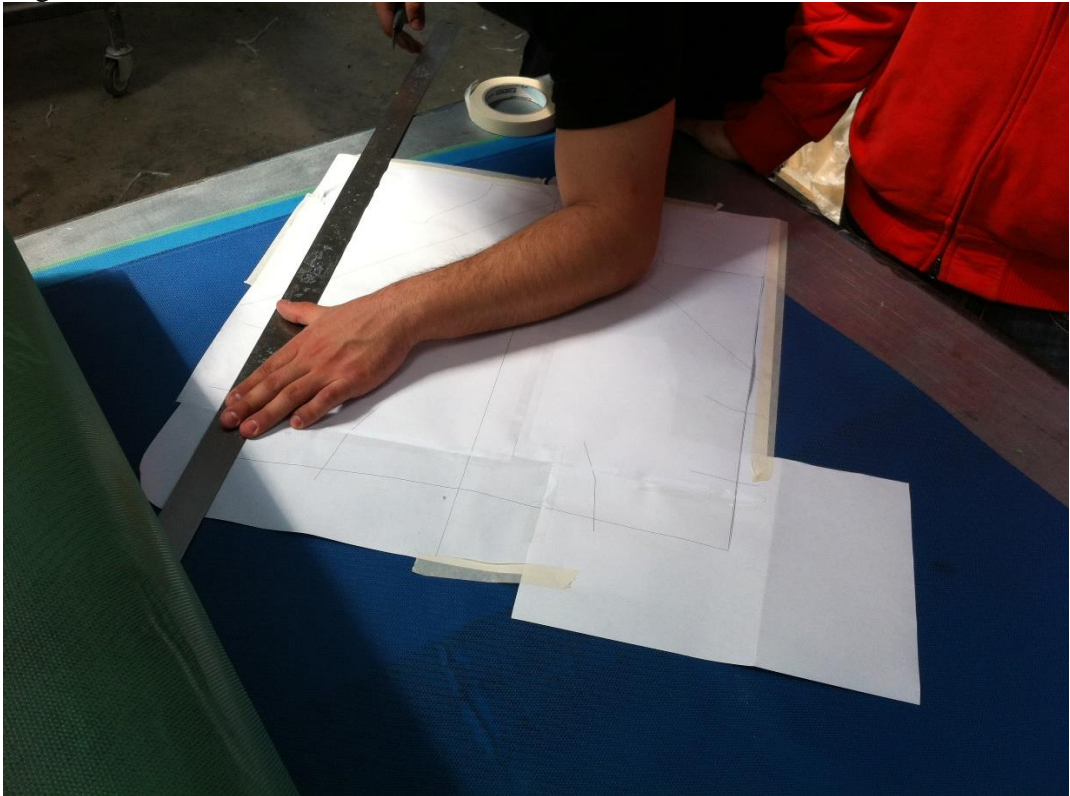
Female CFRP – Glassfiber Molds



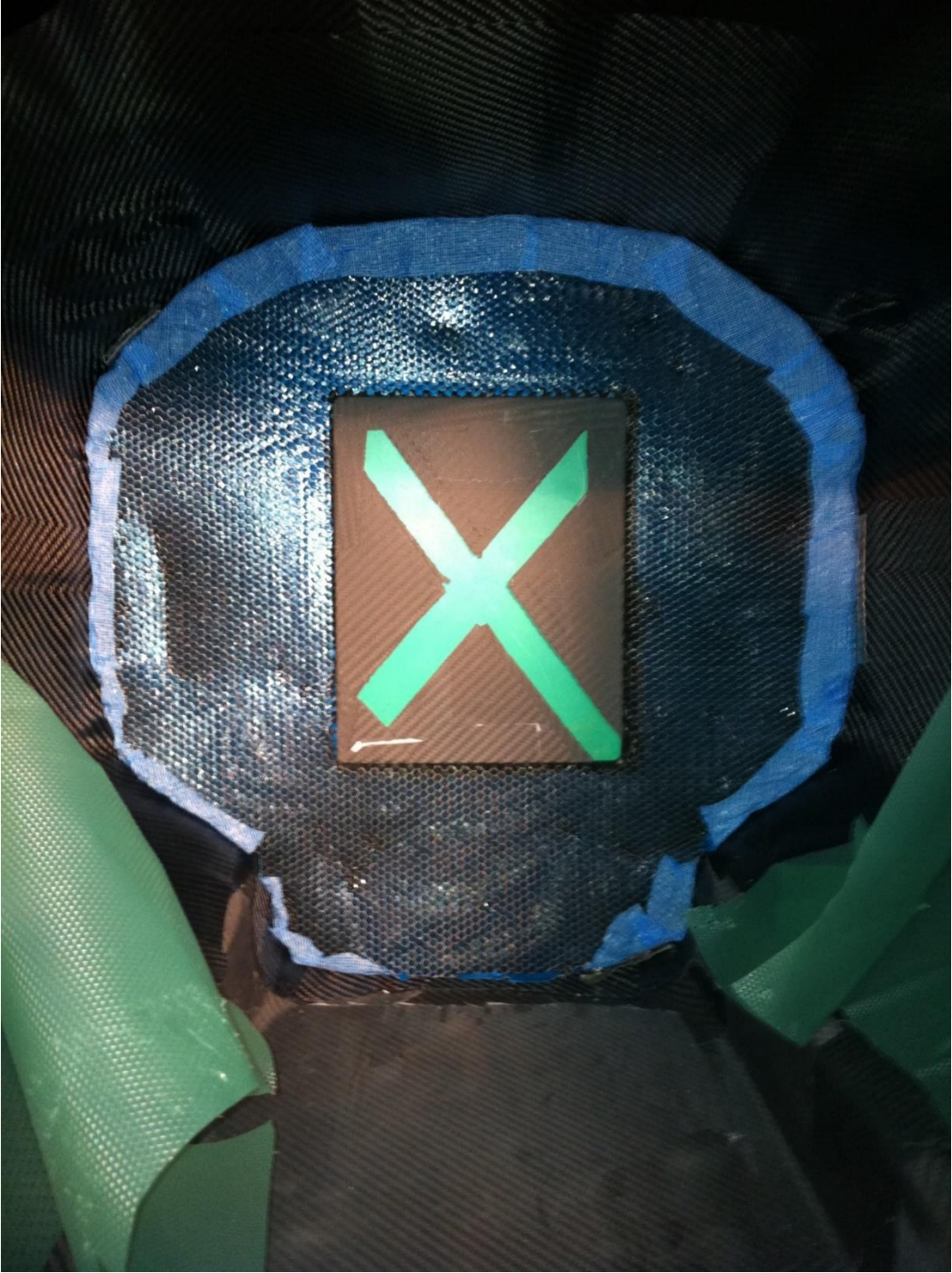
Assembled Female molds ready for lamination



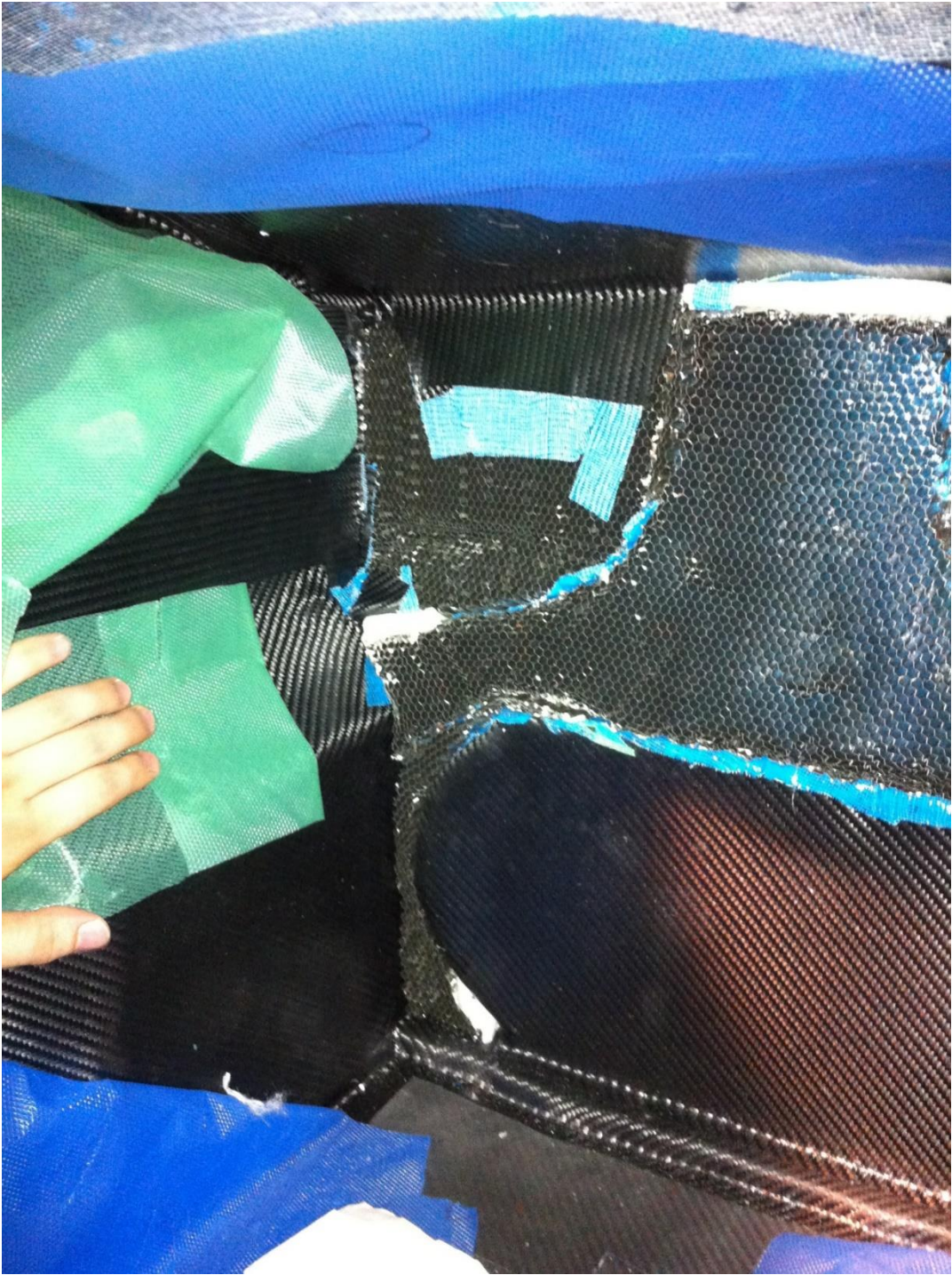
Ply cutting and lamination



Laminated Inner skin and Front Bulkhead core



Laminated Core of the rear tractive system support zone



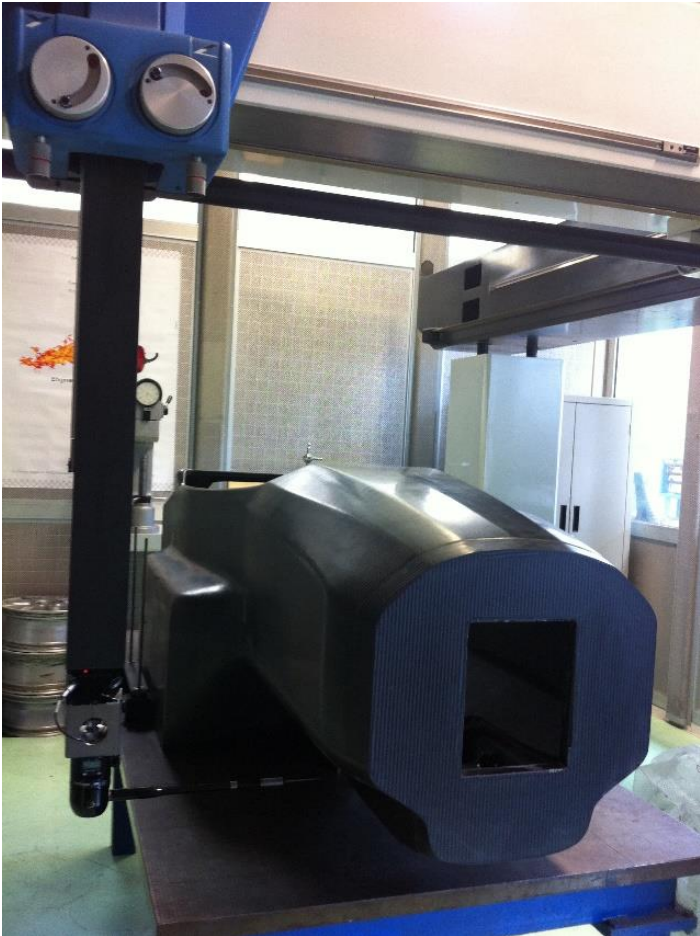
Laminated Inner skin with vacuum bag ready for the autoclave



Finished Monocoque After the final curing process



Dimensional check of the monocoque with a Coordinate Measuring Machine



Painted and polished monocoque model



Chapter 7 – Testing

7.1 – Torsional stiffness test bench

In order to correlate the manufactured monocoque with the FEA results a torsional stiffness tests bench was designed and a test to correlate the results was performed. The results here presented can be further investigated on the thesis project of Gabriele Celi, “studio ed ottimizzazione di una monoscocca per competizioni di formula student”.

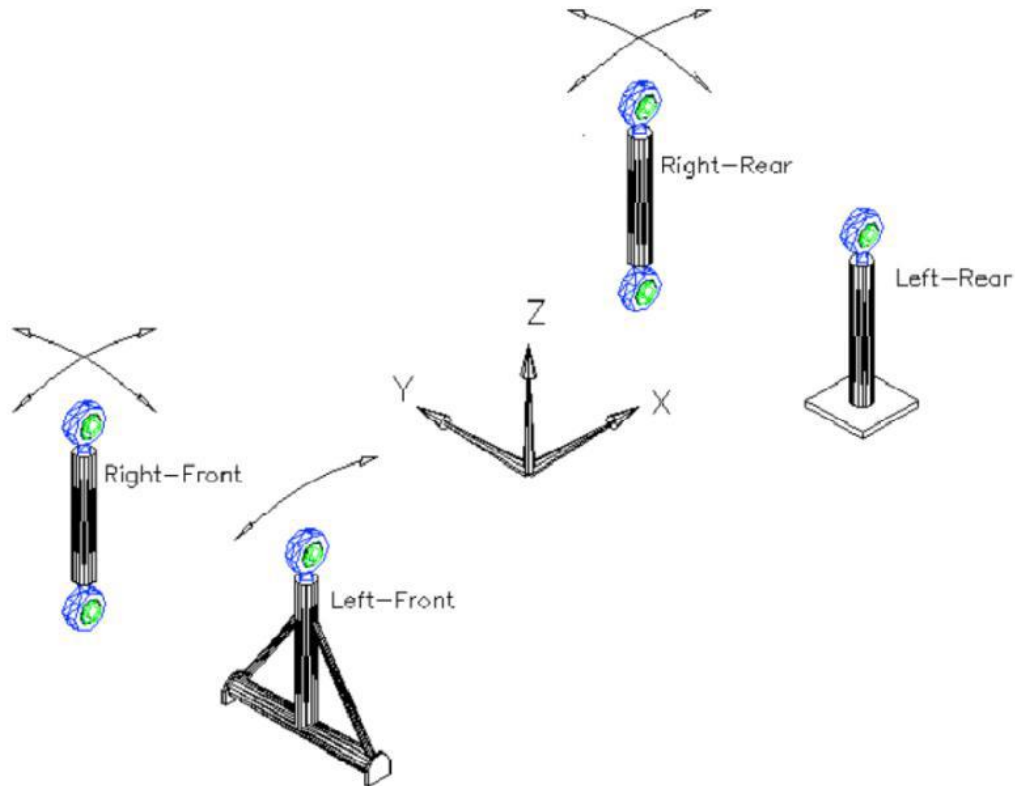


Figure 48- Torsional test rig

The literature suggest to adopt a test rig as the one shown in the picture above. In correspondence of the front corners on such a rig are placed the actuators which provide 2 counteracting force in z direction which constitutes the torque applied to the overall frame.

Images of the Torsional test being performed



7.2 - Torsional Stiffness Test Results and comparison

The torsional stiffness was measured by applying vertical loads to a wheel and measuring the deformation on the other. The following tables illustrates the results of this test.

| pesi[g] | deformazione[0,01mm] | Ktor[N*m/rad] | Ktor[N*m/deg] |
|---------|----------------------|---------------|---------------|
| 1876 | 34 | 92979.11778 | 1622.929609 |
| 3750 | 78 | 81015.51873 | 1414.619597 |
| 5232 | 104 | 84774.64778 | 1480.772181 |
| 8502 | 176 | 81402.96559 | 1423.978453 |
| 9768 | 204 | 80687.70837 | 1412.563096 |
| 12818 | 254 | 85039.10308 | 1491.223593 |
| 15992 | 328 | 82160.19789 | 1445.233628 |

| | | |
|------------|------------|-------------|
| Ktor media | 84008.4656 | 1470.188594 |
|------------|------------|-------------|

The comparison between the FEA results and the experimental results are presented on the following table

| | SCR FEA | SCR experimental | Relative error |
|--------------|-------------|------------------|----------------|
| Kt [N*m/rad] | 116320,7663 | 84008 | -28% |

The relative error between the FEA and the experimental results are considerable but within the expected range due to the 40% stiffness target increased for the FEA model to take into account defects on the manufacturing processes and modelling errors. If we compare the experimental result with the objective set at the beginning of the project we have:

| | SC12e | SCR experimental | delta % |
|----------------------------------------|-------------|------------------|---------|
| Kt [N*m/rad] | 72404,3683 | 84008 | 16% |
| Weight [kg] | 37 | 25 | -32% |
| Stiffness to weight ratio [N*m/rad]/kg | 1956,874819 | 3360,32 | 72% |

Finally, as can be observed on the previous table, the SCR monocoque achieved a weight reduction of 32% with respect the SC12e Tubular steel chassis without taking into account the further reduction due to the lack of bodywork. The stiffness increased of a 16% and finally the total stiffness to weight ratio with respect the SC12e increased 72%.

7.3 - Track Testing



During testing the monocoque did not present any insert failure neither any incorrect behavior was noticed.

As for the performance expected from the vehicle, the telemetry system was not available during testing therefore we cannot determine the actual dynamic conditions on the track with respect those defined during the simulations, we can only assume that the loads present during testing are in the range of those expected.

7.4 - Presentation of the SCR at the “Museo Nazionale dell'Automobile di Torino” the 16th of July 2013



7.5 - Crash Event

During the development the suspension was redesigned to break in case of accident to avoid unrepairable damage to the monocoque and therefore the fail of the racing season. The safety factors taken into account to design this suspension were 25% smaller with respect to safety factor of the suspension inserts.

During testing the powertrain system failed, forcing the pilot to drive full throttle without touching the pedals, after a hard brake the race car finished into a wall causing severe damage at the front of the monocoque where the impact attenuator is supported but the pilot resulted unharmed. At the sides the suspension arms broke as they were designed preventing visible damage at the sides, nevertheless, further study should be performed to check the integrity of the structure.



Figure 49- Suspension breakage during crash

Chapter 8: Conclusions

A full new monocoque for the squadracorse politico race team was designed, manufactured and tested.

The final specifications of the monocoque are compliant with the following project objectives:

- Compliant with the Formula SAE 2013 Rules
- Torsional stiffness higher or equal than 72404 [N*m/rad]
- Suspension angles variation < 0.1 deg under loads
- Weight less than < 25kg

The only objective that was not satisfied by this project was the manufacturing time

- Manufacturing time < 1 month

Due to the lack of experience this factor was too conservative when the choices for the production were made. The know-how from ERRETI composite that had years of experience producing CFRP parts was not enough to predict several issues that delayed the production from 1 month to 3 months.

The following factors were the most time delaying:

- Delays on the autoclave use due to the production of the company components
- During the lamination process the carbon fiber where no “sticking” enough to the polished surface of the mold, making the laminating process VERY difficult for the outer laminated skin. At the end of the process, the CFRP supplier gave us an epoxy glue that is used when these problems arise, therefore it should be used in the future.
- The lamination of the entire monocoque made from a single piece allowed only one person to laminate at the time, therefore in the future, a split bonded monocoque should be the correct solution to reduce production time, but special care and more simulations should be made to glue correctly the sides.

Finally, during testing the monocoque showed no structural problems. And after an accident, the entire structure did not fail, the front bullhead supported the loads coming from the impact attenuator, and the suspension links broke to avoid unrepairable damage of the monocoque, the pilot remained unharmed therefore the passive safety of the vehicle worked.

Bibliography

- [1] Formula SAE. About formula sae series. <http://students.sae.org>.
- [2] Squadra Corse Polito. Chi siamo. <http://squadracorse-polito.com/WP/>.
- [3] 2013 Formula SAE Rules. <http://students.sae.org/cds/formulaseries/rules/2013fsaerules.pdf>
- [4] L. D. L. A. A. P. B. G. Sala, Tecnologie e materiale aerospaziali.
- [5] Petras, Sutcliffe. “Failure mode maps for honeycomb sandwich panels”, ELSEVIER, 1999
- [6] Hexweb Honeycomb sandwich design technology. Hexcel. Source: http://www.hexcel.com/Resources/DataSheets/Brochure-Data-Sheets/Honeycomb_Sandwich_Design_Technology.pdf , 2014
- [7] Marco Cairola. “Analisi Strutturale di un Telaio in Materiale Sandwich di Una Vettura da Competizione Formula SAE”
- [8] Gabriele Celi, “studio ed ottimizzazione di una monoscocca per competizioni di formula student”.